Clinical Applications of Diffusion

2

Reza Forghani and Pamela W. Schaefer

Introduction

Diffusion-weighted magnetic resonance imaging (DWI) is a technique based on diffusion of water molecules in tissues with clinical applications to a wide array of pathological conditions. In vitro measurements of diffusion coefficients for liquids based on their nuclear magnetic resonance signal using the pulse field gradient method were originally described in the 1960s [1] and improved in the early 1970s [2]. These were followed by in vivo measurements of molecular diffusion of water and applications to various pathologic states in human and animal studies, including cerebral ischemia and neoplasms in the mid-1980s and early 1990s [3–14]. However, because of significant technical requirements of DWI, there has only been widespread clinical application of this technique in the last decade. Currently, DWI is the most reliable method for detection of early and small ischemic infarcts in the brain. However, applications of DWI extend far beyond the work-up of acute ischemia. DWI is increasingly used for the evaluation of a large variety of neoplastic and nonneoplastic conditions affecting the brain, head, and neck. This chapter begins with a description of the basic mechanisms underlying DWI changes on magnetic resonance imaging (MRI) scans, focusing on the extensive work using experimental models of brain ischemia. This is followed by a discussion of currently established and experimental clinical applications of DWI, starting with the use of DWI for imaging acute ischemic stroke. The physics of DWI is reviewed in a separate chapter and is not discussed here.

R. Forghani (✉)
Department of Radiology, Sir Mortimer B. Davis Jewish General Hospital, Montreal, QC, Canada

McGill University, 3755 Cote Ste-Catherine Road, Room C-210.2, H3T 1E2, Montreal, QC, Canada
e-mail: rforghani@jgh.mcgill.ca

Basic Mechanisms Underlying Diffusion Changes in Pathologic States

Much of our understanding of the mechanisms underlying DWI changes in pathologic states is based on in vitro and in vivo experimental models of cerebral ischemia in animals. Cerebral ischemia results in diminished diffusion of water molecules within the infarct territory with a rapid decline in apparent diffusion coefficient (ADC) values. Based on current data, the decline in the ADC seen during acute ischemia can be attributed to a combination of complex biophysical factors resulting from disruption of normal cellular metabolism (Table 2.1). Disruption of normal cellular metabolism and depletion of adenosine triphosphate (ATP) stores result in failure of Na^+/K^+ ATPase and other ionic pumps with loss of ionic gradients across cellular membranes. This in turn leads to a net shift of water from the extracellular (EC) to the intracellular (IC) compartment with a change in the relative volume of these compartments as well as alterations in the IC and EC microenvironments. These alterations ultimately result in the restricted diffusion seen on MR imaging. Although there is some controversy regarding the biophysical determinants of diffusion changes seen on MRI, three major mechanisms are believed to account for the restricted diffusion seen during acute ischemia; they are (1) changes in relative volumes of the intracellular and extracellular spaces, (2) increased extracellular space tortuosity resulting in increased impedance to diffusion of water, and (3) diminished energy-dependent cytoplasmic circulation/microstreaming in the intracellular compartment. Some of the key investigations and controversies pertaining to mechanisms of DWI changes are summarized in the paragraphs that follow.

One widely proposed mechanism for the diffusion changes during cerebral ischemia is that disruption of energy metabolism results in failure of the Na^+/K^+ ATPase pump. This in turn leads to a net shift of water from the EC compartment, where the diffusion of water is relatively unimpeded, to the IC compartment where the diffusion of water is postulated to be

S.H. Faro et al. (eds.), *Functional Neuroradiology: Principles and Clinical Applications*,
DOI 10.1007/978-1-4419-0345-7_2, © Springer Science+Business Media, LLC 2011

Table 2.1 Theories for decreased diffusion in acute stroke

Failure of Na^+/K^+ ATPase and other ionic pumps with loss of ionic gradients across membranes, net shift of water from the extracellular to the intracellular space, and changes in the relative volumes of intracellular and extracellular space
Decrease in the size of the extracellular space due to fluid shifts and cell swelling with a resultant increase in extracellular space tortuosity
Diminished energy-dependent intracellular cytoplasmic circulation/microstreaming
Increased intracellular viscosity and intracellular space tortuosity secondary to breakdown of organelles and the cytoskeleton
Increased cell membrane permeability
Temperature decrease

relatively restricted [15]. This model is supported by animal studies demonstrating that ischemic infarction is associated with a reduction of the Na^+/K^+ ATPase pump activity [16], that pharmacologic inhibition of the Na^+/K^+ ATPase pump with ouabain in the *absence* of ischemia results in decreased ADC values [17, 18], and that nonischemic cytotoxic edema secondary to acute hyponatremia is associated with decreased ADC values [19]. However, the concept of relatively impeded diffusion of water in the IC compared to the EC compartment in not universally accepted, with some experiments supporting the theory [15] and others disputing it [20, 21].

Multiple investigations have demonstrated that alterations in the EC compartment can result in changes in diffusion seen on MRI [20–24]. Early DWI changes following transient ischemia in vivo correlate with shrinkage and reexpansion of the extracellular space [22]. In addition, based on observations on osmotically driven changes in compartment volume in ex vivo rat optic nerve preparations, it has been argued that assuming the IC and EC water constitute approximately 80% and 20% of total water in the brain, respectively, moderate fractional changes in cell volume can result in large changes in the contribution of the EC to the ADC [23]. Using these assumptions, it has been postulated that changes in the extracellular fraction are the main factor accounting for the ADC changes observed during ischemia [23]. Changes in relative compartment volume and associated cellular swelling may result in diffusion changes by increasing the tortuosity of the EC space, which in turn results in greater impedance to diffusion of water and the decreased ADC seen on MRI [20, 24].

Additional experiments suggest that changes in the intracellular microenvironment also contribute to the decreased ADC associated with acute ischemia. In experiments in which 2-[^{19}F]luoro-2-deoxyglucose-6-phosphate was used as a compartment-specific marker for the IC and EC compartments by manipulation of routes of administration, the ADC in both compartments were similar at baseline and both were similarly reduced following cerebral ischemia [20]. In addition, experiments using diffusion-weighted MR spectroscopy evaluating predominantly intracellular metabolites such as *N*-acetyl-aspartate and phosphocreatine (Cre) [25] or the potassium analog Cesium (Cs) [26] have also demonstrated a decrease in the ADC of the IC compartment following ischemia. In light of investigations suggesting that the diffusion in the IC and EC spaces may not be significantly different, it has been proposed that the changes in IC ADC are secondary to disruption of the energy-dependent cytoplasmic motion of molecules or *microstreaming* [20].

Increased cytoplasmic viscosity, such as from breakdown of intracellular organelles or cytoskeleton, is an alternate potential mechanism for changes in IC ADC. However, the increased IC water and cellular swelling in isolation would be expected to facilitate diffusion [27], and dissociation of the cytoskeleton likewise appears to facilitate diffusion of water in experimental models [27, 28], making this hypothesis less attractive. A number of other potential mechanisms of ADC change during acute ischemia have been discussed in the literature including changes in tissue temperature and membrane permeability. Although theoretically valid, they probably play a minor and insignificant role under typical circumstances in vivo during an acute stroke [20, 29].

Basic Principles of Diffusion-Weighted Imaging Map Interpretation

All DWI images (linearly T2 weighted and exponentially diffusion weighted) should be processed at the MR console with generation of ADC maps (linearly diffusion weighted, without a T2 component) and exponential images (exponentially diffusion weighted, without a T2 component) (Fig. 2.1). The use of the ADC map is essential for proper interpretation of DWI images since both areas of diminished and increased diffusion can appear bright on DWI images. In lesions with restricted diffusion such as acute ischemic strokes, the T2 and diffusion effects both cause increased signal on DWI, and the DWI images consequently have the highest contrast-to-noise ratio (Fig. 2.2). Areas of restricted diffusion also appear hyperintense on exponential images, although less bright, compared to the DWI image because of absence of the T2 effect (Fig. 2.2). Lesions with restricted diffusion appear dark on the ADC map (Fig. 2.2). Areas of increased diffusion, on the contrary, may appear hyperintense, isointense, or hypointense to normal brain parenchyma on DWI images depending on the strength of the T2 and diffusion components, but are hyperintense on the ADC map (Figs. 2.3 and 2.4). When a lesion is hyperintense on both the DWI image and the ADC map and hypointense on the exponential image, the phenomenon is referred to as T2 shine-through and may be seen with late subacute infarcts or chronic ischemic lesions (Fig. 2.4). Lesions with T2 shine-through may be misinterpreted as an acute infarct if findings on the ADC map or exponential image are not taken into account.

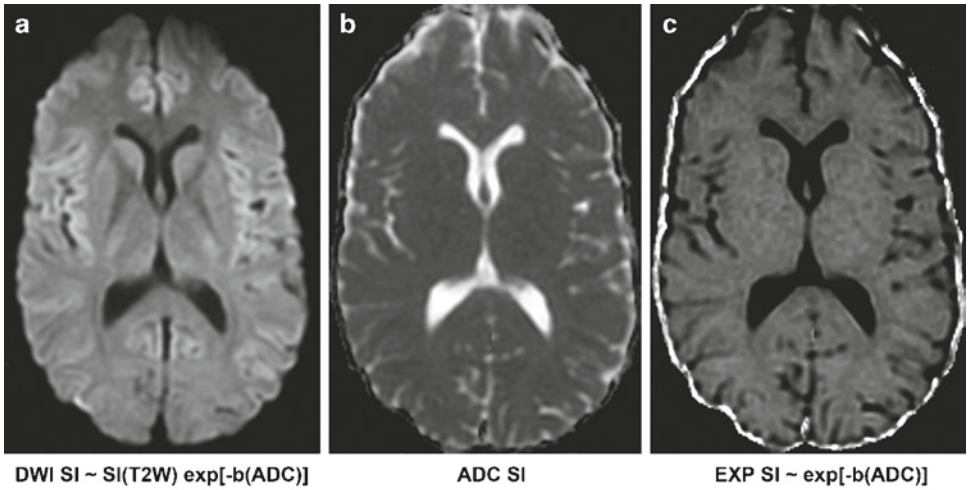

Fig. 2.1 Normal diffusion MR maps. (**a**) Axial DWI, (**b**) ADC, and (**c**) exponential images demonstrate normal diffusion MR maps from a 24-year-old man ($b = 1{,}000$ s/mm^2; TR, 5,000 ms; minimum echo time; matrix, 128 × 128; field of view, 22 × 22 cm; section thickness, 5 mm with 1 mm gap). DWI are linearly T2-weighted and exponentially diffusion-weighted, whereas exponential maps are linearly diffusion-weighted without a T2 component. Note how the normal cerebral cortex and deep gray nuclei have mildly increased intensity on DWI compared to adjacent white matter. Normal CSF spaces appear *dark* on DWI and exponential maps and *bright* on the ADC map given the lack of physical barriers to free motion of water. Abbreviations: *SI* Signal intensity, *SI(T2W)* Signal intensity on T2-weighted images

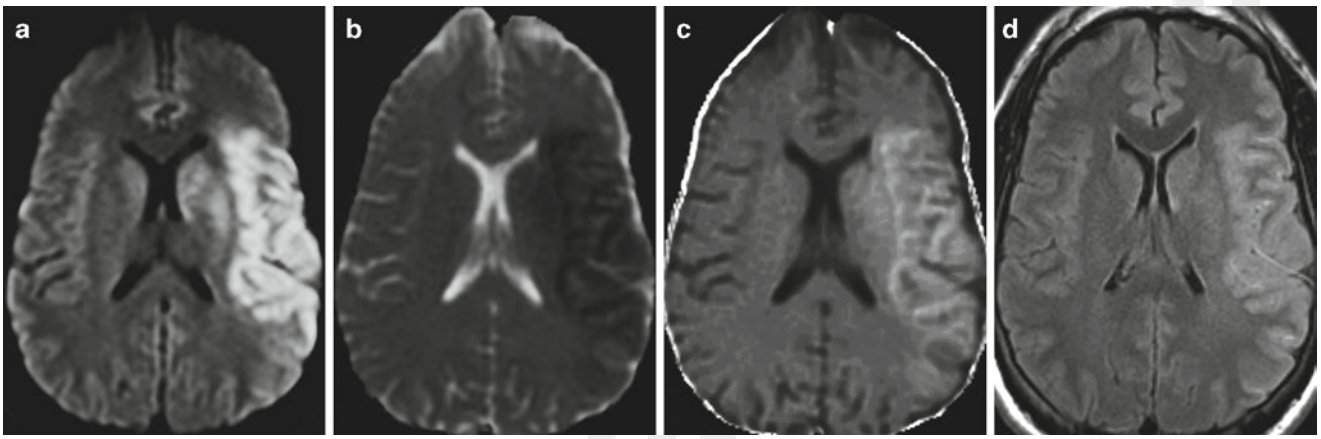

Fig. 2.2 Acute infarction. Diffusion MR maps from a 31-year-old man with embolic occlusion of the left M1 segment, imaged 3 h after developing aphasia and right hemiparesis, demonstrate a large area of signal abnormality in the left MCA territory that is (**a**) hyperintense on DWI, (**b**) hypointense on the ADC map, and (**c**) hyperintense on the exponential map consistent with restricted diffusion secondary to an acute infarction. (**d**) There is mild corresponding hyperintensity on the FLAIR image, although the infarct is more conspicuous on the DWI image

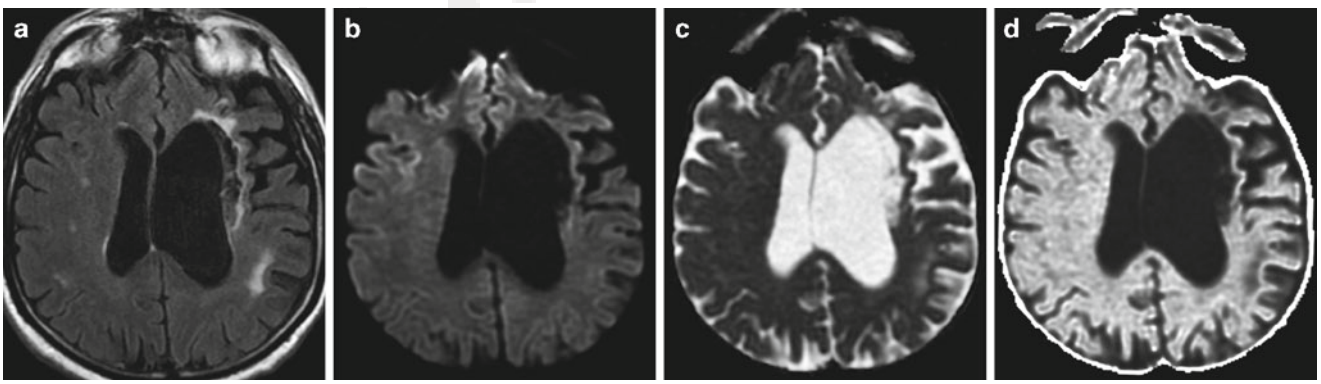

Fig. 2.3 Chronic infarction on DWI. Axial MR images of a chronic left MCA territory infarction demonstrate (**a**) an area of heterogenous signal abnormality within the left MCA territory with local volume loss and associated ex-vacuo dilation of the left lateral ventricle on the FLAIR image. There is corresponding signal abnormality on the diffusion maps that is heterogenous, but (**b**) predominantly hypointense on DWI, (**c**) hyperintense on the ADC map, and (**d**) hypointense on the exponential image consistent with elevated diffusion

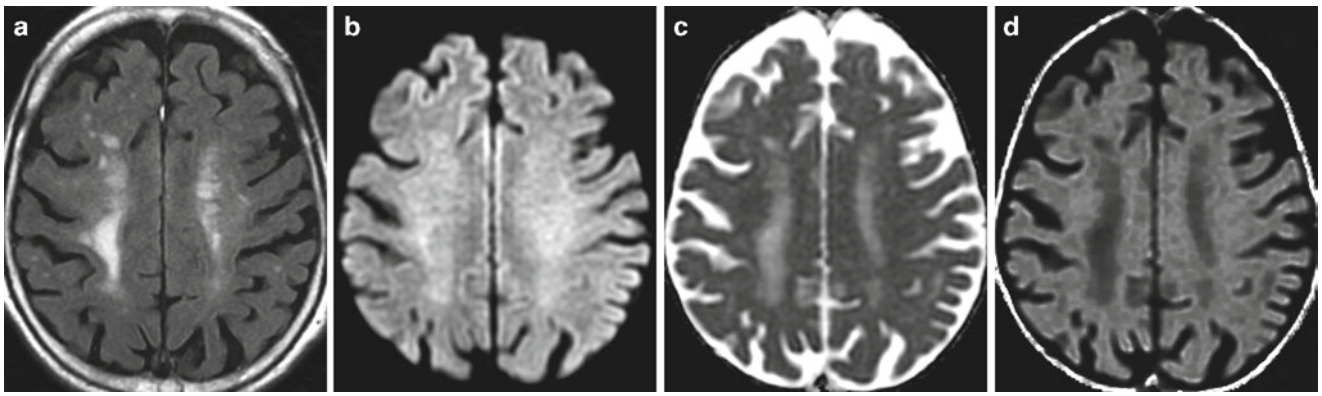

Fig. 2.4 T2 shine-through. (**a**) Axial FLAIR image demonstrates nonspecific periventricular FLAIR hyperintense lesions. (**b**) On DWI, mildly increased signal raises the possibility of acute ischemia. However, the lesions are (**c**) hyperintense on the ADC map and (**d**) hypointense on the exponential map, consistent with elevated diffusion secondary to chronic ischemic changes

Diffusion-Weighted Imaging of Ischemic Arterial Infarcts

Diffusion Characteristics of Ischemic Lesions at Different Stages

DWI is highly sensitive (81–100%) and specific (86–100%) for detection of acute ischemia within the first 12 h after stroke onset [30–34], with sensitivities and specificities approaching 100% at specialized high volume stroke centers (Tables 2.2 and 2.4, Figs. 2.2 and 2.5). DWI may demonstrate infarcts as early as 11 min after symptom onset [35] and is superior to conventional MRI or computed tomography (CT) in the first 3–6 h, at which time there is frequently insufficient accumulation of tissue water for reliable detection of hypoattenuation on CT and hyperintensity on T2 weighted and fluid-attenuated inversion recovery (FLAIR) MR images [30, 31, 34] (Fig. 2.5). In a recent prospective evaluation, MRI with DWI had a sensitivity of 73% and specificity of 92% for identification of ischemic infarcts within 3 h of symptom onset compared to a sensitivity of 12% and specificity of 100% for CT [30]. In another study, DWI had a sensitivity of 97% and specificity of 100% for identification of acute ischemia within 6 h of stroke symptom onset compared to 58% and 100%, respectively, for conventional MRI sequences and 40% and 92%, respectively, for CT [34]. Although most useful in the first 6–8 h when infarcts are frequently not identifiable on T2 or FLAIR images, DWI can also be valuable at later time points because of its higher contrast-to-noise ratio compared with CT and conventional MRI images. DWI has superior sensitivity for identification of small infarcts that may be overlooked on FLAIR or T2 images by increasing their conspicuity and enables distinction of small recent white matter infarcts from nonspecific T2 hyperintense white matter lesions [36, 37] (Fig. 2.6).

Following the onset of acute ischemia, there is a rapid decrease in water diffusion that is markedly hyperintense on DWI and hypointense on the ADC map and is generally postulated to represent cytotoxic edema (Table 2.2, Figs. 2.2, 2.5, and 2.7). After the initial period of decreased ADC values, there is a gradual increase in the ADC values secondary to cell lysis and increasing vasogenic edema, with a transient return to baseline known as pseudonormalization, a period during which the ADC of the nonviable ischemic tissue is similar to normal brain ADC (Fig. 2.7). In animal models of stroke, ADC values are reduced for a very short period of time and return to baseline between approximately 24–48 h [38, 39]. In humans, the peak signal reduction on ADC occurs between 1 and 4 days, with a return to baseline at approximately 4–10 days following the ictus [40–44]. The DWI at this stage is typically hyperintense secondary to T2 effects, although less intense than during the acute phase, while on ADC and exponential images the infarct is isointense to normal brain parenchyma. Subsequently, as the infarct progresses to a more chronic stage, there is a progressive increase in the ADC of an ischemic lesion. This is secondary to increased water content as well as emerging gliosis and cavitation, which result in breakdown of the normal tissue structure and barriers to free diffusion of water molecules. During the chronic stage, an infarct can be mildly hyperintense, isointense, or hypointense to normal brain parenchyma on DWI depending on the strength of the T2 effects and diffusion, but should be hyperintense on ADC and hypointense on exponential images (Figs. 2.3 and 2.7).

Although separation of infarct stages into hyperacute, acute, subacute, and chronic (Table 2.2) provides a useful general framework for dating an infarct on MRI, there is variability in the time course of the DWI and ADC signal changes of evolving infarcts. A number of factors including infarct type, patient age, and reperfusion status affect the evolution of signal changes observed on MRI. In one study,

Table 2.2 Diffusion MRI findings during different stages[a] of human stroke

Pulse sequence	Hyperacute (0–6 h)	Acute (6–24 h)	Early subacute (2–7 days)	Late subacute (8–21 days)	Chronic weeks – months
DWI	Hyperintense	Hyperintense	Hyperintense Gyral hypointensity from petechial hemorrhage	Hyperintense (secondary to T2 component)	Isointense to hypointense
ADC	Hypointense	Hypointense	Hypointense to isointense[b]	Hypointense to hyperintense[b]	Hyperintense
Exponential	Hyperintense	Hyperintense	Hyperintense to isointense[b]	Hyperintense to hypointense[b]	Hypointense
Histopathologic changes	Cytotoxic edema	Cytotoxic edema	Cytotoxic edema with a small amount of vasogenic edema	Cytotoxic and vasogenic edema	Resolving vasogenic edema followed by gliosis and tissue loss

[a] The provided timelines are approximate and can vary between patients and depending on infarct type
[b] Pseudonormalization, a period during which the ADC of nonviable ischemic tissue is similar to normal brain ADC, most commonly occurs between 4 and 10 days post ictus in humans, and can overlap the early and late subacute stages

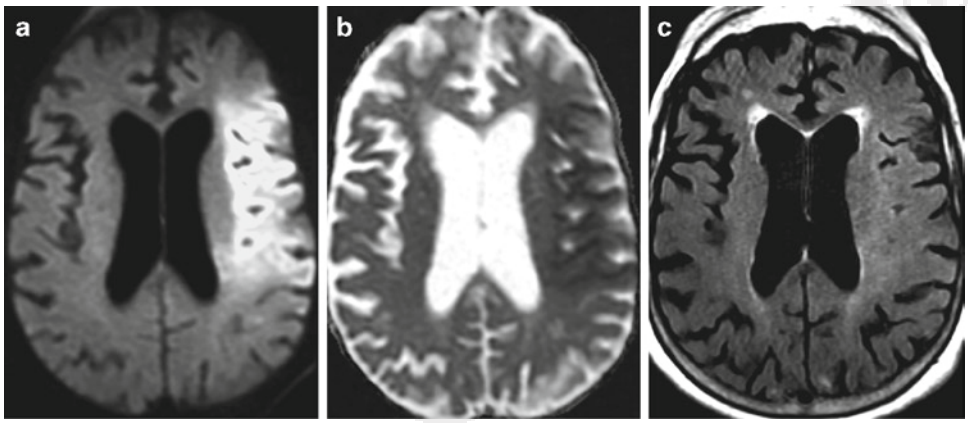

Fig. 2.5 Superiority of DWI imaging for detection of early ischemic change compared to FLAIR images. (**a**) Axial DWI and (**b**) ADC images from an 89-year-old man with a history of acute aphasia and right hemiparesis of 4-h duration demonstrate a large area of restricted diffusion, (**c**) without any significant corresponding signal abnormality on the FLAIR image

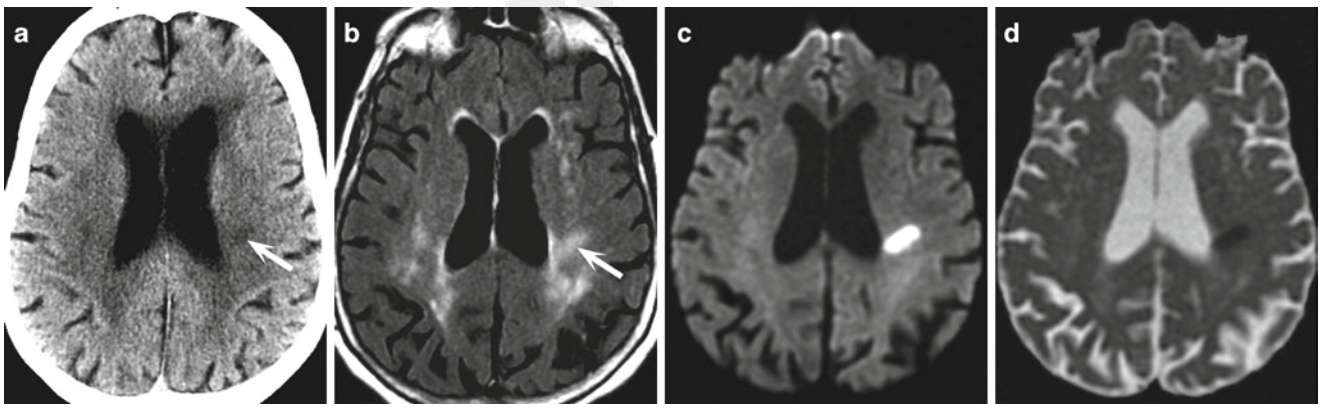

Fig. 2.6 Distinction of acute white matter infarctions from chronic white matter change based on diffusion characteristics. (**a**) There is a focus of hypoattenuation in the left corona radiata on computed tomography (CT) with (**b**) corresponding hyperintensity on the FLAIR image that is age indeterminate and indistinguishable from the remainder of white matter abnormalities. However, (**c**) the DWI and (**d**) ADC images clearly distinguish this acute infarct from nonspecific white matter changes by demonstrating restricted diffusion in the acute infarction and elevated diffusion in the nonspecific white matter changes

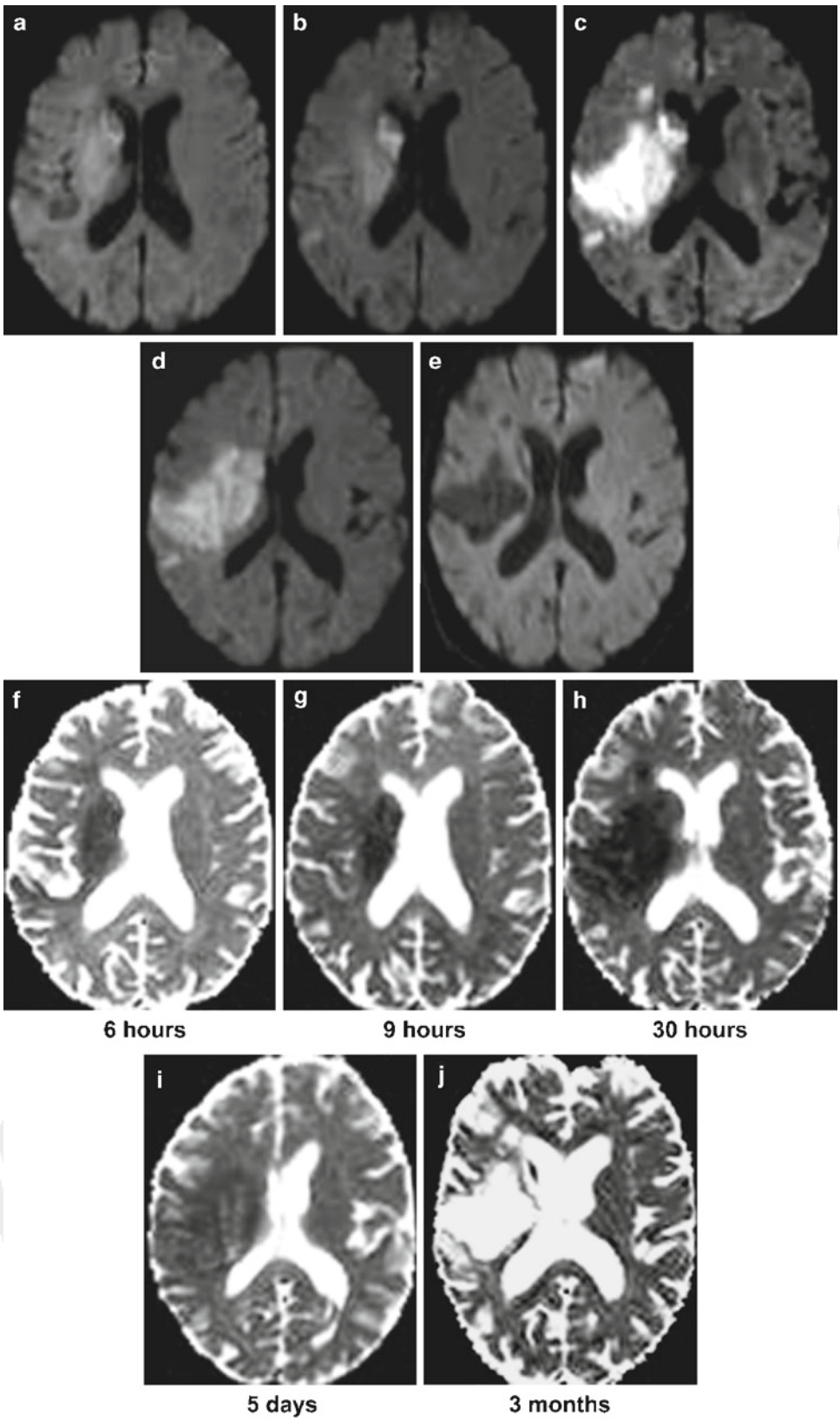

Fig. 2.7 Temporal evolution of infarction on diffusion maps. (**a**–**e**) Axial DWI images and (**f**–**j**) ADC maps demonstrate the appearance of different infarct stages on diffusion maps. At 6 h, the right middle cerebral artery (MCA) territory infarction is mildly hyperintense on DWI images and hypointense on ADC maps secondary to early cytotoxic edema. By 30 h, the DWI hyperintensity and ADC hypointensity are pronounced secondary to increased cytotoxic edema. This is the ADC nadir. By 5 days, the ADC hypointensity is mild and the ADC has nearly pseudonormalized due to cell lysis and the development of vasogenic edema. The lesion remains hyperintense on the DWI images because the T2 and diffusion components are combined. At 3 months, the infarction is hypointense on DWI and hyperintense on ADC maps due to increased diffusion secondary to the development of gliosis and tissue cavitation

the transition from decreasing to increasing ADC values occurred earlier in nonlacunar infarcts than lacunar infarcts [45]. The same study also found a trend toward earlier transition to increasing ADCs of nonlacunar infarcts in patients older than a median age of 66 [45]. In another study, there was slightly faster recovery (increase) in ADC values of infarcted gray matter compared to white matter [43]. Early reperfusion, as seen after treatment with thrombolytic therapy, also changes the evolution of diffusion abnormalities and is discussed later in the section on DWI reversibility.

Reliability and Pitfalls of Diffusion-Weighted Imaging in Identification of Acute Ischemic Lesions

Despite its exquisite sensitivity for detection of acute ischemic lesions, DWI is not infallible. Although false-negative DWI results have been described in many cerebral arterial territories and for different lesion sizes, small punctate infarcts and infarcts located within the brainstem, especially those imaged at less than 12 h from symptom onset, have the highest likelihood of a false-negative DWI study [36, 46–53]. Among brainstem infarcts, medullary infarcts appear to be the most difficult to detect. Proximity to skull base structures resulting in susceptibility artifact and differences in anatomic composition and organization of the normal fiber tracts in this region are likely contributing factors [46].

In cases of clinically suspected strokes, where no infarct is identified on the initial axial DWI scan, obtaining images with a higher resolution and/or in the coronal plane may reveal an infarct (Fig. 2.8). Another approach for increasing sensitivity is acquisition of DWI at a *b*-value of 2,000 s/mm^2 or higher. Some studies have demonstrated mildly increased sensitivity and increased conspicuity of ischemic lesions at higher *b*-values, but this comes at the expense of decreased signal-to-noise ratio and increased imaging time and a clear diagnostic benefit remains to be proven [54–57]. In addition, in one study of patients with transient ischemic attacks (TIA), the use of thinner DWI sections increased the sensitivity for detection of small ischemic lesions [58]. However, the increased acquisition time and associated propensity for motion degradation in this patient population may preclude widespread application of this technique in the evaluation of acute stroke. In any case, a short-term follow-up MRI scan within 24 h should identify most small infarcts not visible on the initial study. A team approach is essential since correlation with clinical signs and symptoms may bring into attention regions of potential abnormality that would otherwise be dismissed as artifact.

Recently, 3 Tesla (T) magnets have been used to evaluate acute ischemic stroke. In a prospective study comparing 1.5 and 3T acquisitions in 25 patients with clinical symptoms of acute (7/25) or subacute ischemia (18/25), there was increased contrast-to-noise ratio on 3T and a greater number of small ischemic lesions were identified on 3T compared to 1.5T, although all patients with infarcts on 3T had at least one identifiable infarct on their 1.5T images [59]. Six of 25 patients had no DWI abnormality on either 3T or 1.5T images and were diagnosed with a TIA. There was increased image distortion at 3T compared to 1.5T, although this may be overcome in the future with advances in image acquisition.

False-positive DWI findings may occur secondary to T2 shine-through, as discussed earlier, and can be readily distinguished from true restricted diffusion if the DWI images are interpreted in conjunction with the ADC or exponential maps. In addition, a variety of nonischemic lesions may have diminished diffusion and could potentially be mistaken for infarcts (Table 2.3), as discussed in the following sections. Most are readily distinguishable from acute infarcts when the DWI findings are considered in conjunction

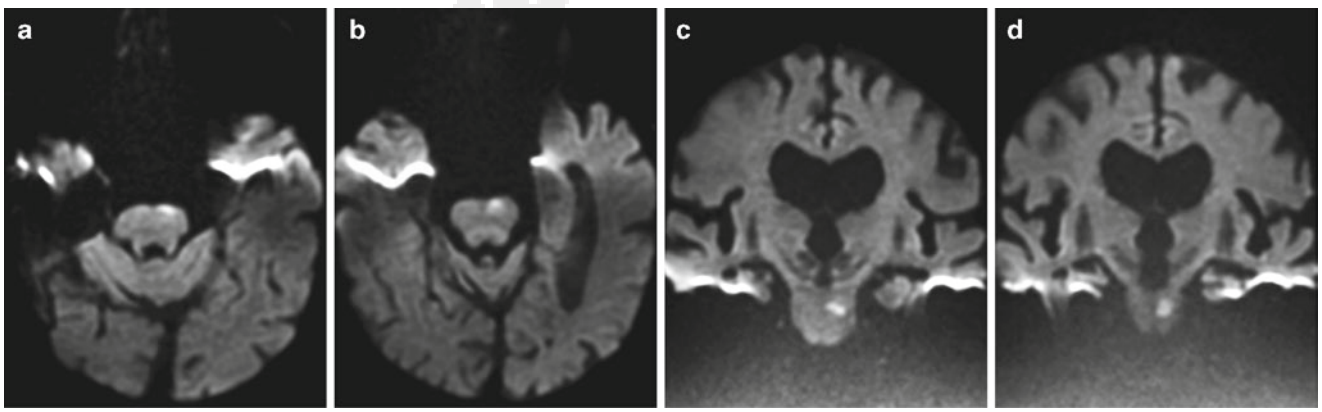

Fig. 2.8 Acute pontine infarct. Axial DWI images demonstrate mild hyperintensity in the ventral left pontine tegmentum that could represent (**a**) artifact, but (**b**) has an appearance suggestive of a true focus of restricted diffusion on one image. (**c**, **d**) Coronal DWI images unequivocally demonstrate restricted diffusion from a small perforator infarction

with findings on conventional MR sequences such as T2, FLAIR, and pre- and postgadolinium T1-weighted images. However, hypoglycemia and acute demyelinating disease can present with acute neurologic deficits and a single non-enhancing FLAIR hyperintense lesion with restricted diffusion, and are at times misdiagnosed as acute strokes.

Table 2.3 Nonischemic lesions that may have restricted diffusion on DWI

Entity	Proposed cause of restricted diffusion
Cerebral abscess	Increased viscosity
Neoplasms such as lymphoma and high-grade glial neoplasms	Dense cell packing
Venous infarcts	Cytotoxic edema
Acute demyelinating lesions	Cytotoxic edema and/or inflammatory cell infiltrates? myelin vacuolization
Encephalitides – Herpes simplex virus	Cytotoxic edema
Hemorrhage – oxyhemoglobin, extracellular methemoglobin	? Intracellular for oxyhemoglobin and ? increased viscosity for both
Diffuse axonal injury	Cytotoxic edema, axonal retraction balls
Hypoglycemia	Cytotoxic edema
Hemiplegic migraine	Cytotoxic edema, ? spreading depression
Seizures	Cytotoxic edema
Transient global amnesia	Cytotoxic edema, ? spreading depression
Heroin-induced leukoencephalopathy	? Myelin vacuolization
Metronidazole toxicity	? Cytotoxic edema
Cretzfeldt Jakob disease	Spongiform change
Osmotic myelinolysis	? Cytotoxic edema, ? myelin vacuolization
Carbon monoxide poisoning	Cytotoxic edema

Reversibility of DWI Positive Lesions in Ischemic Stroke and the Use of DWI for Determination of Infarct Core

It is generally accepted that diffusion-weighted imaging is the best method for identifying infarct core or tissue that will progress to infarction (Table 2.4). In the absence of early reperfusion in the setting of intravenous thrombolytic therapy or intra-arterial recanalization procedures, reversibility of restricted diffusion (defined as DWI abnormality on the initial scan without any corresponding abnormality on follow-up FLAIR or T2-weighted MRI scans) is very rare. In fact, frequently, the final infarct volume not only includes the initial area of diffusion abnormality but also extends to involve surrounding tissues [60–62].

Significantly higher rates of partial diffusion reversal have been reported after early reperfusion secondary to thrombolytic therapy [63–65] (Fig. 2.9). In one retrospective study of patients treated with intra-arterial thrombolysis, 19% had some reversal of DWI hyperintense regions on follow-up imaging [65]. In another study, 18 patients treated with intra-arterial or combined intravenous and intra-arterial thrombolytic therapy resulting in recanalization were evaluated with MRI before treatment, early after treatment, and on day 7 post-treatment [64]. The authors reported partial or complete normalization of diffusion abnormalities in 8/18 (44%) of patients on the early posttreatment scan, although in 5/8 patients (63%) there was partial or complete reappearance of the lesion on the MRI performed on day 7. The authors referred to this as late secondary injury, although the transient reversal may have represented a pseudonormalization-like phenomenon in which the MRI findings transiently resolved despite tissue injury, similar to observations in animal experiments in which transient reversal of MRI findings may be seen despite histopathologic evidence of tissue injury [66]. Persistent normalization of all reversed tissue was seen in 3/8 (38%, or 17% of all patients) on the scan performed on day 7. A voxel-by-voxel analysis of the regions of DWI abnormality

Table 2.4 DWI use for imaging of acute stroke: Key concepts

DWI is the gold standard for identifying infarct core in acute ischemic stroke
DWI has sensitivity and specificity over 95% in high volume stroke centers with experienced neuroradiologists. Scanning with higher resolution DWI sequences, a *b*-value of 2,000 s/mm^2 or higher, and/or on a 3T scanner may increase sensitivity
The rare acute infarcts not detected on DWI are usually punctate infarcts in the brainstem or deep gray nuclei
Single lesions with restricted diffusion confused with acute stroke are frequently due to hypoglycemia or demyelinating disease
DWI reversibility (abnormal on initial DWI but normal on follow-up T2 or FLAIR at 1 week or later) is rare. Greater reversibility of DWI positive lesions has been demonstrated after recanalization following intravenous or intra-arterial thrombolysis. DWI reversibility is overestimated in some studies due to tissue loss at follow-up imaging at 30–90 days. Threshold ADC values for DWI reversibility have not reliably been established
DWI lesion volume correlates with clinical outcome scales and is an independent predictor of outcome in multiple studies. The correlation depends on lesion location. DWI lesion volume greater than one-third of the expected MCA territory or 100 mL is associated with poor outcome regardless of reperfusion therapy. It is used by some as an exclusion criterion for thrombolytic therapy
DWI lesion greater than 100 mL is associated with an increased risk of hemorrhagic transformation. Mean ADC of less than 300×10^{-6}mm^2/s in the DWI positive lesion is predictive of *symptomatic* HT

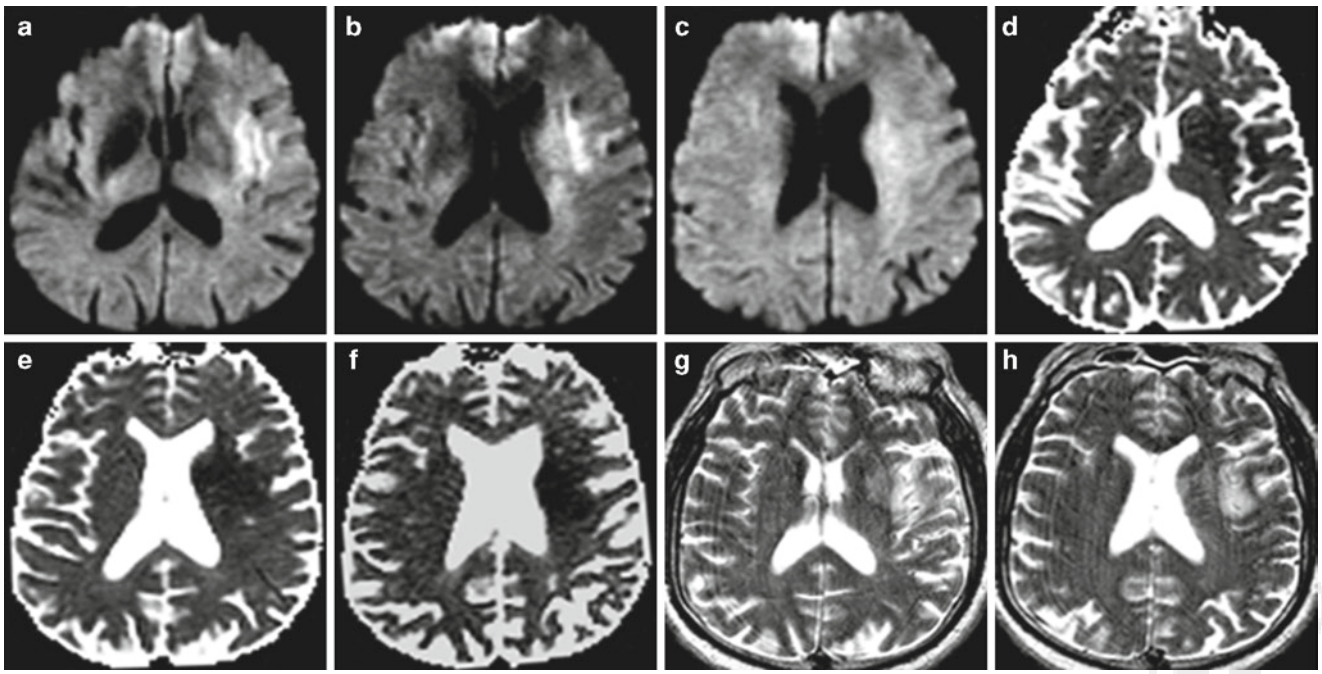

Fig. 2.9 DWI reversibility. A 69-year-old man presenting with acute dysarthria and right-sided weakness who was treated with intra-arterial thrombolysis with successful recanalization of a left M1 clot 6 h after symptom onset. (**a**–**c**) DWI and (**d**–**f**) ADC images obtained prior to therapy demonstrate restricted diffusion consistent with acute ischemia involving the left insula, basal ganglia, corona radiata, and frontal subcortical white matter. (**g**, **h**) On follow-up T2 weighted images there is T2 hyperintensity, consistent with infarction, in the left insula, basal ganglia, and frontal subcortical white matter. However, the residual corona radiata infarction appears smaller than on the initial diffusion maps

in all patients combined was also performed and demonstrated a sustained reversal of 33% in addition to a late reversal of 8% (i.e., persistent diffusion abnormality on the early posttreatment scan but normal DWI/T2W characteristics on the day 7 scan). In a more recent analysis of 32 patients from a prospective multicenter trial of treatment with IV thrombolysis within 3–6 h of stroke onset (DEFUSE trial: *D*iffusion and perfusion imaging *E*valuation *F*or *U*nderstanding *S*troke *E*volution), the authors reported a median reversal rate of 43% by comparing final infarct volumes on FLAIR images obtained at 30 days post-ictus with the total baseline DWI lesion volume [67]. The DWI reversal rate was greater in regions with normal baseline perfusion, in patients with early recanalization, and among cases with a favorable clinical outcome.

While there is evidence to support some degree of DWI reversibility after early reperfusion, the determination of the percentage of DWI reversibility is not straightforward. In animal studies, exposure to short periods of ischemia can result in a transient decline in ADC with normalization after cessation of the ischemic insult. However, despite complete normalization on imaging, there can be selective neuronal injury on histopathology that is below the threshold of the imaging technique [66]. Another technical factor that may result in an overestimation of DWI reversibility on follow-up imaging is volume loss and tissue retraction during the chronic stage that may result in an underestimation of final infarct volume.

In general, tissues with a higher absolute ADC value tend to have a higher likelihood of reversibility [68–72]. Based on this premise, some have tried to determine an ADC threshold for tissue infarction [64, 65, 70]. However, there is significant variation in the reported ADC values of irreversibly damaged ischemic tissue and of DWI reversible tissue and there is much overlap between the two [68–73]. Furthermore, it has been demonstrated that even tissues with severely diminished ADC may recover. Apart from the ADC value, the duration and severity of ischemia and tissue perfusion status have been shown to represent important determinants of final infarct volume in animal and human studies [64, 66, 68, 71, 73, 74]. Therefore, although tissues with severely reduced ADC have a higher likelihood of progressing to an irreversible infarct, it is likely that ADC values alone are insufficient for absolute determination of tissue viability.

Use of DWI for Predicting Hemorrhagic Transformation of Ischemic Infarcts

Hemorrhagic transformation (HT) of brain infarcts represents secondary bleeding into ischemic tissue that occurs after the initial ictus. The reported incidence of HT across different studies varies widely because of differences in the definitions, modalities, and time frames used to evaluate for hemorrhage. However, the incidence of HT is clearly

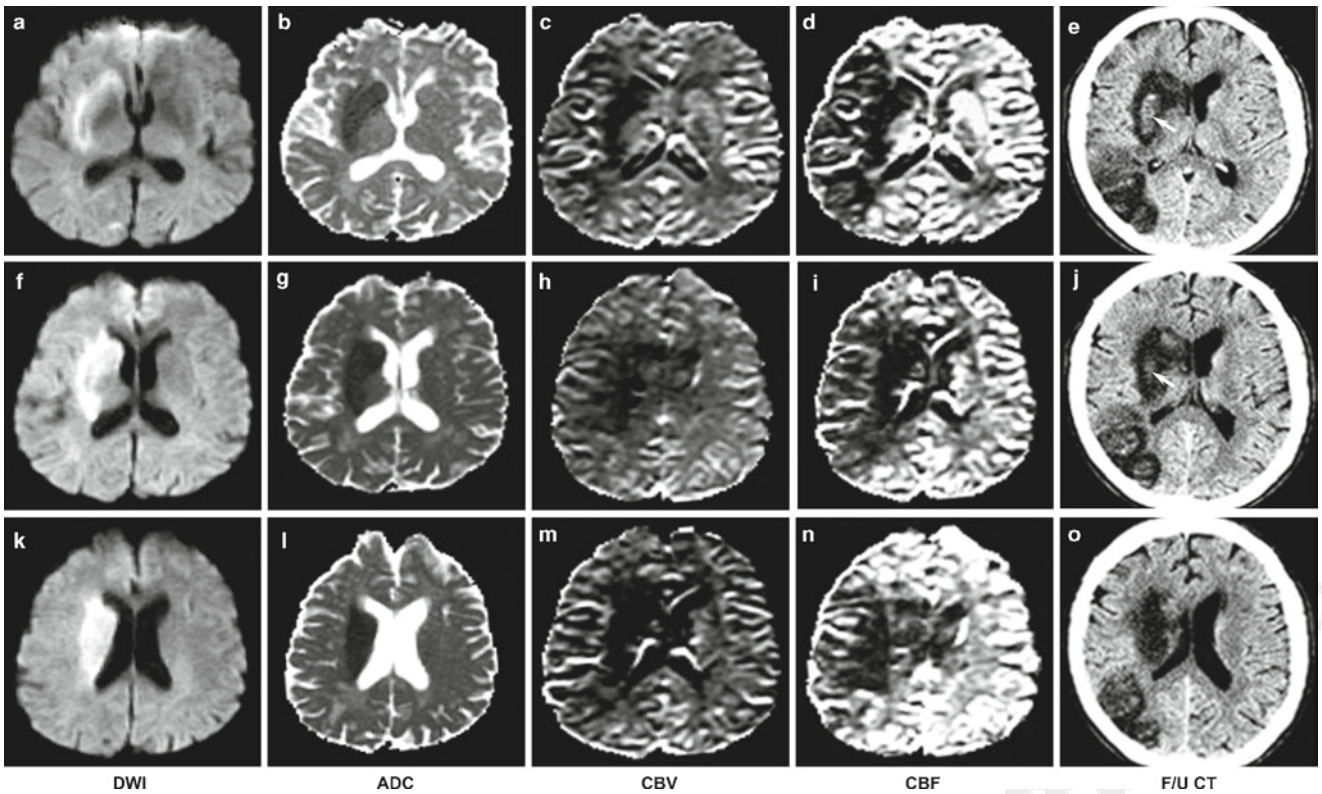

Fig. 2.10 (**a**–**o**) Hemorrhagic transformation of an acute ischemic stroke in a 76-year-old man treated with intra-arterial tPA. DWI and ADC maps demonstrate restricted diffusion in the right basal ganglia and deep white matter, consistent with an acute right middle cerebral artery (MCA) territory infarction. There is marked reduction of the ADC, cerebral blood volume (CBV), and cerebral blood flow (CBF) within the infarction. On follow-up CT, there is hemorrhagic transformation (*arrow* in (**e**) and (**j**)) within the infarct bed. There is also extension of the infarction into the right parietal region

increased after thrombolytic therapy and ranges from 6% up to 44% if susceptibility-sensitive MR sequences such as gradient echo sequence are used, although the incidence of *symptomatic* HT is significantly lower [75–83].

Given that ADC values are believed to represent the severity and extent of ischemia, a number of investigators have assessed the value of ADC in predicting HT. In a retrospective analysis of 27 patients with acute stroke who underwent DWI and perfusion-weighted MRI, the investigators demonstrated that the mean ADC of ischemic regions that underwent HT ($510 \pm 140 \times 10^{-6}$ mm^2/s) was significantly lower than the overall mean ADC of all ischemic areas analyzed ($623 \pm 113 \times 10^{-6}$ mm^2/s) [84] (Fig. 2.10). The authors also noted that a persistent perfusion deficit within the infarct bed on the MRI performed 3–6 h after the baseline scan was associated with a higher risk of HT within that area. Another investigation of 29 patients treated with intravenous thrombolytic therapy demonstrated that the absolute number (or volume) of voxels with ADC $\leq 550 \times 10^{-6}$ mm^2/s correlated with HT [85]. In a third study, using a monovariate model, the authors concluded that a mean ADC of less than 300×10^{-6} mm^2/s in the infarct core was predictive of *symptomatic* HT [86]. However, despite these studies, other investigations have not found a statistically significant difference in the ADC of infarcts that subsequently underwent HT [83]. Thus, the clinical utility of ADC values in determining HT and its use for exclusion of patients from thrombolytic therapy remains unproven and requires further investigation.

The utility of initial DWI volume has also been evaluated as a potential predictor of HT. In a study of 645 patients with anterior circulation strokes treated with intravenous or intra-arterial thrombolysis, increasing DWI lesion size was associated with an increase in symptomatic HT. DWI lesion size was also found to be an independent risk factor when including National Institutes of Health Stroke Scale (NIHSS), age, time to thrombolysis, and leukoariosis using logistic regression analysis [87]. The highest risk for symptomatic HT was 16.1% and was observed in the subgroup with a large DWI abnormality, defined as >100 mL.

More recent work suggests that MR cerebral blood volume values may predict hemorrhagic transformation of acute ischemic stroke better than ADC values or initial DWI volume. In an analysis of 91 patients from the Echoplanar Imaging Thrombolytic Evaluation Trial (EPITHET), very

low cerebral blood volume (VLCBV2.5) (defined as MR cerebral blood volume at or below the 2.5th percentile) was found to predict *all* (i.e., not just symptomatic) HT better than DWI lesion volume and thresholded ($<550\times10^{-6}$ mm^2/s) ADC lesion volume both in receiver operating characteristic analysis and logistic regression, although all three parameters were found to be significant in univariate analysis [88]. In another study of 184 patients, a large area with a severe perfusion deficit, defined as a T_{max} of >8 s, along with aggressive therapy (defined as endovascular treatment with or without intravenous tissue plasminogen activator administration) were found to correlate with radiological HT whereas DWI volume did not [89]. A number of other imaging parameters are associated with an increased risk of hemorrhagic transformation and include increased permeability on dynamic contrast-enhanced T1 MRI [90] and early parenchymal enhancement [91]. A detailed discussion of these techniques is beyond the scope this chapter.

Extrapolating from studies using CT scans in which hypoattenuation involving greater than one-third of the middle cerebral artery (MCA) territory was associated with an increased risk of hemorrhagic transformation and poor outcomes following the administration of IV tissue plasminogen activator (tPA) [92], some clinicians consider a DWI lesion volume greater than one-third of the expected MCA territory a contraindication to the use of IV thrombolytic therapy and/or intra-arterial recanalization procedures. However, there remains lack of a widely accepted consensus on the use of DWI and other MR parameters for determination of risk of HT (Table 2.4).

Correlation of DWI Lesion Volume with Clinical Outcome

Initial DWI and ADC lesion volumes correlate with clinical outcome measured by various acute and chronic neurological assessment tests including the NIHSS, the Glasgow Outcome Scale, the Barthel Index, and the Rankin or Modified Rankin Scale [42, 61, 62, 93–96]. Reported correlations range from $r=0.56$ to 0.73 and in some studies are stronger for cortical strokes than for penetrator artery strokes [42]. The variation in correlation of lesion size with the clinical score is not surprising. Given that many of the commonly used clinical scoring systems are weighted toward motor symptoms and the left hemisphere, lesion location [42, 93] can result in a significant discrepancy between total burden of disease and clinical score. For example, a small brainstem lesion affecting a compact motor fiber tract may result in high clinical scores, whereas a similarly sized lesion in the frontal lobe may not have a detectable associated abnormality on standard clinical scoring systems. This would also explain why some studies have failed to find a correlation between DWI volume and clinical outcome in infratentorial strokes [36].

Regardless of these variations, there is emerging evidence that patients with a DWI lesion volume of greater than approximately 70 mL do poorly regardless of treatment and recanalization status [97–100]. For example, Yoo et al. [99] demonstrated that in 54 patients treated mainly with IV TPA or heparin, all patients with a DWI lesion volume of greater than 72 mL had a poor outcome (modified Rankin Score = 3–6). Furthermore, in a retrospective analysis of 34 patients with anterior circulation strokes who underwent intra-arterial reperfusion therapy with or without IV thrombolysis, the same authors found that all patients (6/34) with an initial DWI lesion volume of >70 cm^3 had poor outcome, in spite of a 50% recanalization rate [100]. In another study analyzing 98 patients from the EPITHET trial, Parsons et al. [98] found that while patients with an initial DWI lesion volume of 18 mL had substantially improved chances of a good outcome if treated with IV tPA, the odds of a benefit dropped rapidly at larger volumes and there was little treatment benefit with a DWI lesion volume > 25 mL. Similar to the observations by Yoo et al., the authors from this study found that a large initial DWI lesion volume of >65 mL was strongly associated with a poor outcome.

Transient Ischemic Attacks

TIAs have been classically defined as any sudden focal neurologic deficit of presumed vascular origin with symptoms lasting less than 24 h [101, 102]. The classic definition of a TIA is based on studies from the 1950s and 1960s, at which time noninvasive diagnostic techniques were not available to evaluate for tissue injury [102]. This definition has been demonstrated to be outdated and unreliable, given that a substantial percentage of clinically defined TIAs have evidence of tissue injury on DWI consistent with small infarcts [101–105]. Furthermore, in addition to being outdated, the classic definition of a TIA can be potentially misleading, giving a false impression of a benign process rather than a potentially serious and urgent condition that requires prompt investigation. It has been shown that 21–48% of patients presenting with a "classic" TIA have DWI hyperintense lesions consistent with infarcts. These patients are at a higher risk for future vascular events (compared to those with "classic" TIA who do not have DWI hyperintense lesions) [103–107]. In one study, 19.4% of patients presenting with transient neurologic symptoms and evidence of infarction on DWI had in-hospital recurrent ischemic stroke and TIAs compared to 1.3% of patients with ischemic stroke (i.e., not a clinical TIA/transient neurologic symptoms) [108].

Table 2.5 Transient ischemic attacks (TIAs)

Approximately 50% of patients with "classic" transient ischemic attacks (TIAs) have punctate infarctions on DWI. Patients with lesions on DWI have an increased risk of a subsequent stroke
American Heart Association statement in 2009 endorses a revised definition of a TIA as a "transient episode of neurological dysfunction caused by focal brain, spinal cord, or retinal ischemia, *without* acute infarction"

After many years of discussion in the literature, a scientific statement published in 2009 by the American Heart Association/American Stroke Association Stroke Council endorsed a tissue-based definition of a TIA as "a transient episode of neurological dysfunction caused by focal brain, spinal cord, or retinal ischemia, without acute infarction" [101]. Regardless of the definition used, it is well established that patients presenting with a TIA are at a high risk for subsequent stroke and require urgent work-up with a MRI, if available, as well as vascular imaging with CTA, ultrasound (US), or magnetic resonance angiography to identify potentially treatable causes of stroke (Table 2.5).

Venous Infarctions and Other Vascular Vasogenic Edema Syndromes

Vasogenic edema syndromes presenting with acute neurologic deficits can mimic acute ischemic stroke clinically. Furthermore, conventional MR sequences such as T2 and FLAIR cannot distinguish cytotoxic from vasogenic edema because both produce hyperintensity and can involve gray and/or white mater. However, DWI can be used to differentiate the two types of edema. Depending on the contributions from T2 effects, vasogenic edema may appear hypointense, isointense, or hyperintense on DWI. However, while cytotoxic edema is hypointense on the ADC map, vasogenic edema is hyperintense.

Venous Infarctions

Cerebral venous thrombosis (CVT) is an often underdiagnosed condition with a nonspecific clinical presentation and a large variety of underlying etiologic factors. The diagnosis of CVT requires a high index of clinical suspicion and a combination of conventional MRI and vascular imaging. Both nonhemorrhagic and hemorrhagic intraparenchymal lesions can be seen on conventional MRI. Nonhemorrhagic lesions consist of areas of T2 prolongation that typically do not conform to the major arterial territories [109]. These regions may have elevated diffusion, restricted diffusion, or both [109–112] (Fig. 2.11, Table 2.6) [111, 112]. The foci of elevated diffusion representing vasogenic edema are thought to result from increased vascular pressure and leaky vessels and usually resolve on follow-up [109, 110]. Foci of restricted diffusion representing cytotoxic edema may progress to permanent tissue damage or be reversible. In one study, reversible areas of restricted diffusion were seen only in patients with seizures [109]. Hemorrhagic lesions can have a variable appearance on DWI. Both oxyhemoglobin (seen in the first few hours) and extracellular methemoglobin (seen at a few weeks to a few months) are characterized by decreased diffusion (Fig. 2.12). Other products of hemorrhage (deoxyhemoglobin, intracellular methemoglobin, and hemosiderin) have decreased signal due to susceptibility effects on DWI, and a diffusion coefficient cannot be calculated.

Posterior Reversible Encephalopathy Syndrome

Posterior reversible encephalopathy syndrome (PRES) can occur in association with a wide variety of clinical entities including acute hypertension, various hematologic disorders, treatment with immunosuppressive agents, and treatment with chemotherapeutic agents. The pathophysiology of PRES is controversial but believed to be secondary to endothelial dysfunction and failure of cerebral autoregulation with capillary leakage. On MRI, PRES is characterized by relatively symmetric patchy or confluent areas of bilateral T2 prolongation involving the subcortical white matter and overlying cortex. There is frequent involvement of the parieto-occipital areas, posterior temporal lobes, and posterior fossa structures such as the cerebellum and brainstem [113–116] (Fig. 2.13, Table 2.6). However, anterior circulation lesions are not uncommon and are frequently located in a border zone distribution between the anterior, middle, and posterior cerebral arteries [114–118]. Rare variants of PRES with a unilateral distribution or involving only the medulla oblongata have also been described [114, 119]. Most frequently, areas of T2 prolongation in PRES are secondary to vasogenic edema and appear slightly hypointense, isointense, or mildly hyperintense on DWI images with increased signal on the ADC map [113–117, 120] (Fig. 2.13). This is helpful since posterior distribution lesions can mimic basilar tip occlusion with arterial infarctions and border zone lesions can mimic watershed infarctions both clinically and on T2-weighted sequences. However, acute arterial and watershed infarctions can be distinguished using DWI since they have restricted diffusion. The clinical deficits and MR abnormalities in PRES are typically reversible [114, 118]. Occasionally, some

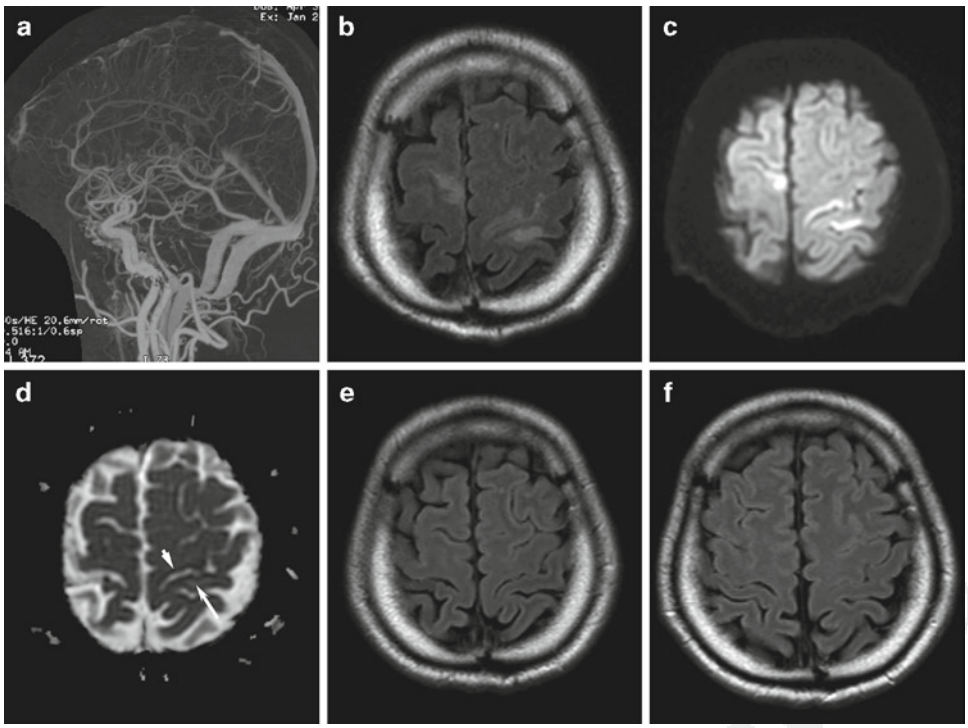

Fig. 2.11 Transient diffusion changes in cerebral venous sinus thrombosis. (**a**) A 3-D reformatted image from a CT venogram demonstrates no opacification of the anterior two-thirds of the superior sagittal sinus (SSS) consistent with thrombosis. (**b**) There is bilateral cortical and subcortical FLAIR hyperintensity, consistent with edema. (**c**) Some areas are hyperintense on DWI and (**d**) hypointense on ADC (*short arrow*) consistent with diminished diffusion due to cytotoxic edema. (**d**) Other areas are hyperintense on ADC (*long arrow*), consistent with vasogenic edema. The patient was successfully anticoagulated with partial recanalization of the SSS and no detectable residual parenchymal abnormality on (**e**, **f**) follow-up FLAIR images performed 1 month later

Table 2.6 MR findings of venous sinus thrombosis and other vascular vasogenic edema syndromes that can mimic acute stroke

Venous sinus thrombosis
Hemorrhagic and nonhemorrhagic lesions typically not corresponding to major arterial territories
Nonhemorrhagic lesions present as areas of T2 prolongation. These lesions may have elevated diffusion, restricted diffusion, or both. Lesions with elevated diffusion likely represent vasogenic edema and resolve. Lesions with decreased diffusion likely represent cytotoxic edema and may resolve (especially if associated with seizures) or progress to permanent injury
Posterior reversible encephalopathy syndrome (PRES)
Conventional MR findings include patchy bilateral areas of cortical and subcortical T2 prolongation in a predominantly posterior distribution and/or the border zones between the ACAs, MCAs, and PCAs. Both patterns can mimic acute stroke
Unlike acute stroke, lesions typically represent vasogenic edema, are usually isointense or mildly hyperintense on DWI, have elevated ADC values, and usually resolve
Occasionally, lesions may have transiently restricted diffusion or progress to infarction
Hyperperfusion syndrome (HS) post carotid endarterectomy
Typical MR findings consist of areas of T2 prolongation within the ipsilateral anterior circulation territory that mimic acute ischemia
Lesions are isointense to mildly hyperintense on DWI but have elevated ADC consistent with vasogenic edema, and resolve

lesions may display transiently restricted diffusion and rarely small areas of restricted diffusion or tissue initially characterized by elevated or normal diffusion may progress to infarction [114, 115, 118]. One study reports greater reversibility of cortical and subcortical lesions compared to deep white matter or brainstem lesions [120].

Hyperperfusion Syndrome Following Carotid Endarterectomy

Hyperperfusion syndrome (HS) is a relatively uncommon complication of carotid endarterectomy that is believed to occur as a result of post-revascularization changes in cerebral hemodynamics and impairment of cerebral autoregulation. It is thought that similar to PRES, increased pressure damages endothelial tight junctions, leading to a capillary leak syndrome. Patients with HS typically present with a unilateral headache, face and eye pain, and seizures, but may also have focal neurologic deficits [121]. In addition to areas of parenchymal hemorrhage, T2 and FLAIR images demonstrate hyperintense areas within the ipsilateral anterior circulation territory that can mimic arterial infarction but typically have elevated diffusion consistent with vasogenic edema [122–125] (Fig. 2.14, Table 2.6). Small embolic infarcts presenting as tiny foci of restricted diffusion can occur after CEA [124, 125] and should not be confused with or attributed to HS. Some studies describe transient cytotoxic edema in HS based on hyperintensity on DWI images, although the findings on the ADC map are not always clearly described making it difficult to exclude T2 shine-through with certainty

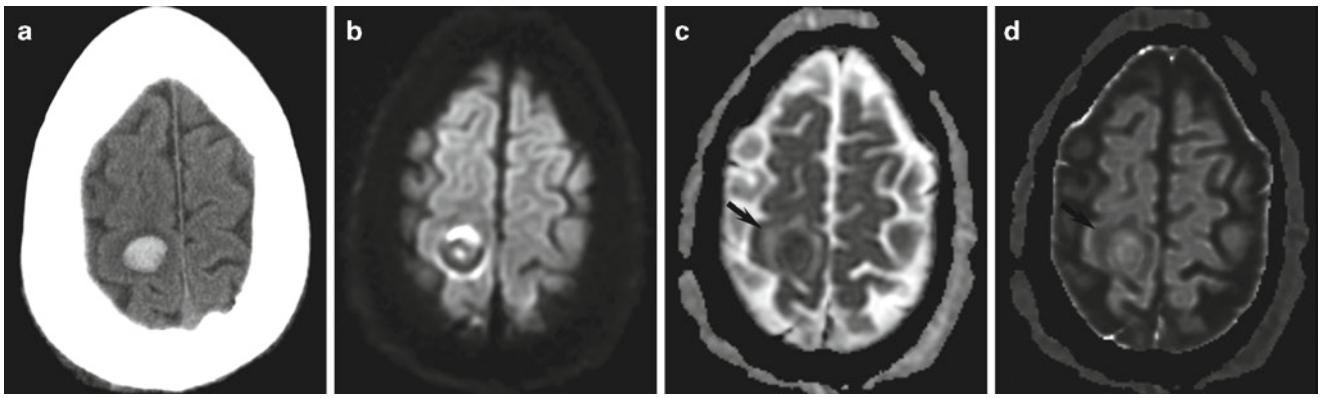

Fig. 2.12 Diffusion abnormalities associated with acute hemorrhage. (**a**) Axial unenhanced CT demonstrates an acute right superior frontal subcortical hematoma. (**b**) Axial DWI, (**c**) ADC, and (**d**) exponential MR images demonstrate predominantly restricted diffusion, consistent with oxyhemoglobin. Note the elevated diffusion within the vasogenic edema surrounding the hematoma, best seen on the ADC and exponential maps (*arrows* in (**c**) and (**d**))

[126, 127]. Since patients with HS can present with seizures, this represents an additional potential etiology of transiently restricted diffusion on MRI.

Transient Global Amnesia

Transient global amnesia (TGA) is characterized by sudden onset of profound memory impairment resulting in both retrograde and antegrade amnesia [128] (Table 2.7). The amnestic syndrome typically resolves spontaneously within 24 h, although some impairment of cognitive function may persist beyond that time period [128, 129]. The etiology of TGA is controversial; some articles propose ischemia as an etiologic factor, while others propose spreading depression, among other theories. Regardless of the mechanism, punctate DWI hyperintense foci have been reported in 41–100% of TGA cases imaged within the first 3 days after the event, depending on the time lag for imaging and use of specialized sequences (described later). These lesions typically measure 1–3 mm in diameter and involve the lateral aspect of the hippocampus [129–133] (Fig. 2.15). Lesions are most frequently unilateral, but may involve the hippocampal formations bilaterally or present as multiple (2 to 3) lesions on the same side [130, 132–136]. In a small percentage of cases, lesions have also been reported in the splenium of the corpus callosum, cerebellum, or temporal lobe not involving the hippocampus [130, 133, 136, 137]. Frequently, no corresponding abnormality is detectable on follow-up MRI (either because of complete resolution or because the residual lesion is below the threshold of detection on T2 or FLAIR images), although occasionally the initial DWI abnormality may evolve into a T2/FLAIR hyperintense lesion consistent with a small infarct [130, 135].

Multiple studies have demonstrated that the timeline of imaging after symptom onset has a significant impact on lesion detection. In one study performing serial MRIs for 3 days, only 2/31 (6%) had detectable lesions when imaged within 2–8 h, but 23/31 (74%) and 26/31 (84%) had a DWI hyperintense lesion if imaged after 24 h or after 48 h from symptom onset, respectively [129]. At least two other studies demonstrate increased sensitivity when imaging is performed within 12–72 h [130] or at 3 days [133], compared to imaging within the first 12 h or first 24 h, respectively. However, one study reported a 100% sensitivity (20/20 patients) when patients were imaged in the first 24 h, although this study employed specialized DWI sequences including thinner section and coronal acquisitions that may explain the increased sensitivity for lesion detection [132]. In general, sensitivity for lesion detection is greatest 24–72 h after symptom onset [129, 130, 133]. The use of thinner sections (3 mm compared to 5 mm), a higher *b*-value (2,000 or 3,000 s/mm^2), or a 3T scanner may also increase sensitivity for lesion detection [132, 133, 138].

Hemiplegic Migraine

Hemiplegic migraine is a rare subtype of migraine characterized by some degree of transient hemiparesis in addition to visual, somatosensory, or dysphasic symptoms, although some patients may have progressive cerebellar dysfunction as well. Usually, no abnormality is detected on MRI, but occasionally patients with prolonged hemiplegic migraine may have FLAIR and DWI hyperintensity involving the cortex and subcortical white matter, with or without corresponding hypointensity on the ADC map [139–145], which can be confused with an acute infarct (Fig. 2.16). A number of factors

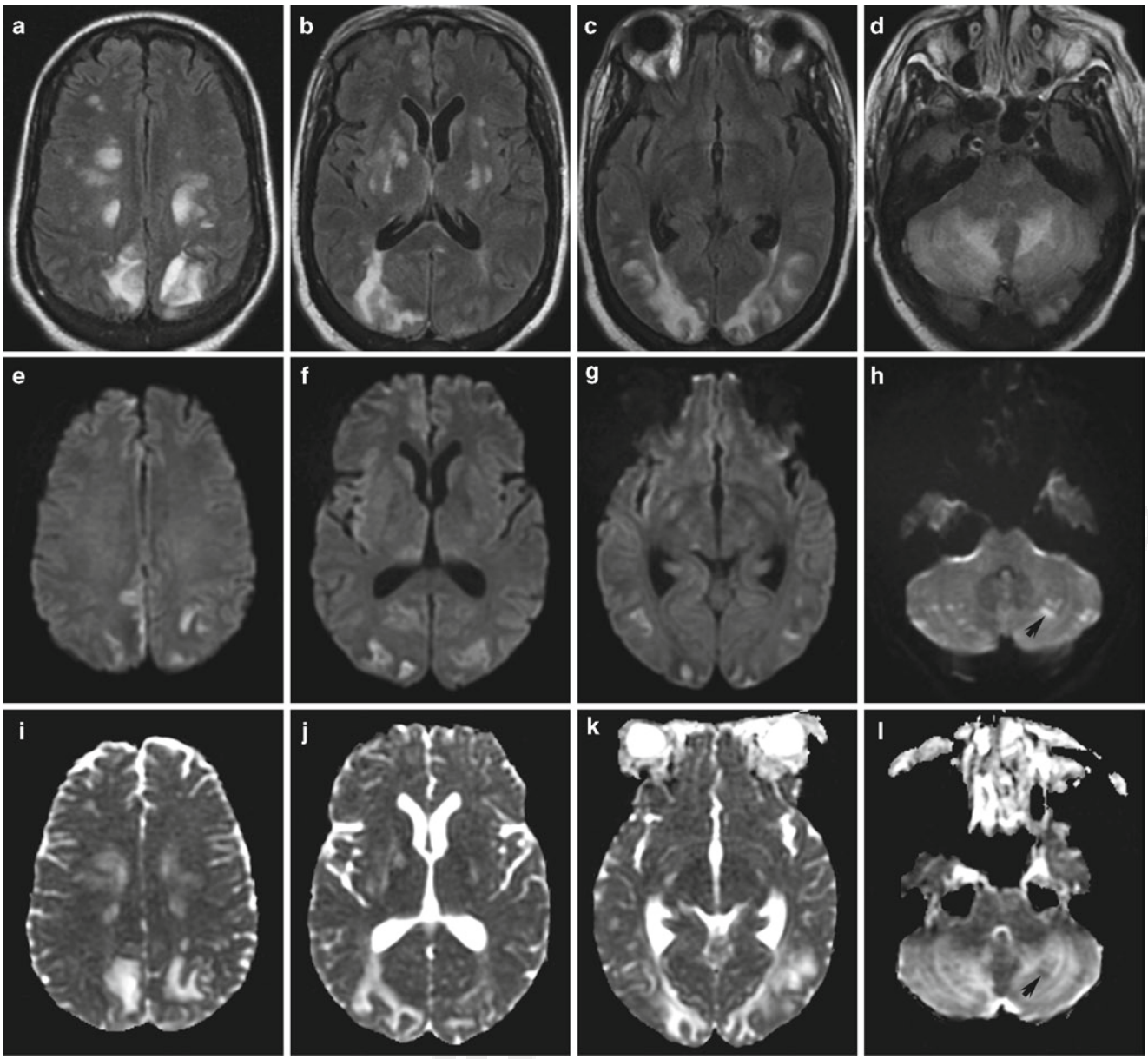

Fig. 2.13 PRES. (**a**–**d**) Axial FLAIR images demonstrate extensive patchy FLAIR hyperintensity involving the supratentorial cortex and-subcortical white matter, deep gray and white matter, and the cerebellum. Many of the lesions are in a border zone distribution and are indistinguishable from subacute infarctions on FLAIR images. (**e**–**h**) The lesions are of mixed intensity on DWI, but (**i**–**l**) predominantly hyperintense on the ADC maps, consistent with elevated diffusion secondary to vasogenic edema. However, there are small punctate DWI hyperintense foci that are hypointense on the ADC map consistent with diminished diffusion due to cytotoxic edema (e.g., *arrow* in (**h**) and (**l**)). Although lesions in PRES most commonly have elevated diffusion, occasionally lesions with restricted diffusion can be seen

can distinguish these lesions from acute stroke: (1) the patients usually have a strong history of migraines; (2) the lesions may cover multiple arterial territories [145]; (3) perfusion is usually normal or elevated [142–144, 146]; (4) angiography may demonstrate transient vessel dilation [146], be normal, or show vasospasm [147], but vessel cut-offs are not identified; and (5) the lesions and clinical deficits are usually reversible (Table 2.8). Other abnormalities that may be seen on MRI in patients with hemiplegic migraine include cerebral atrophy contralateral to the side with restricted diffusion in patients with hemiparetic auras of alternating sides [139] or cerebellar atrophy with increased ADC values [148].

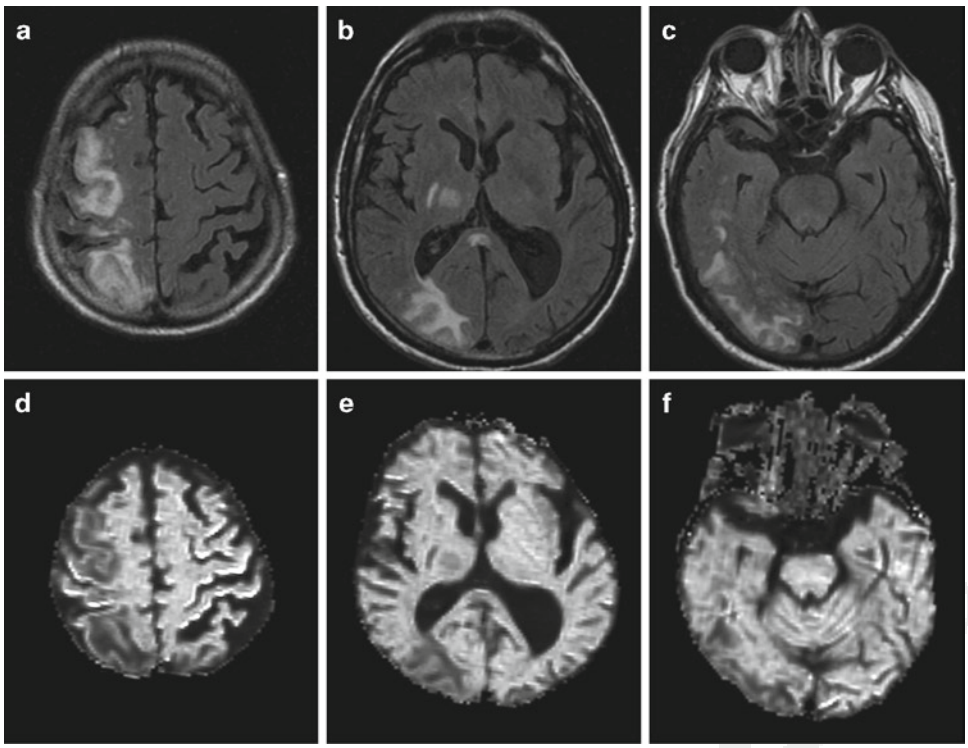

Fig. 2.14 Hyperperfusion syndrome following carotid endarterectomy. (**a**–**c**) Axial FLAIR images demonstrate patchy hyperintense areas with local mass effect in a border-zone distribution in the right cerebral hemisphere, ipsilateral to the carotid endarterectomy. These lesions are indistinguishable from subacute infarctions on FLAIR images. (**d**–**f**) However, these areas are hypointense on the exponential images consistent with elevated diffusion from vasogenic edema

Table 2.7 Transient global amnesia

Clinical syndrome characterized by sudden onset of profound memory impairment resulting in both retrograde and antegrade amnesia that typically resolves within 24 h
Punctate DWI hyperintense lesion(s) are seen in 41–100% of cases. Punctate lesions are typically located in the lateral aspect of the hippocampus with less frequent involvement of other structures such as the splenium of the corpus callosum, other parts of the temporal lobe, and the cerebellum

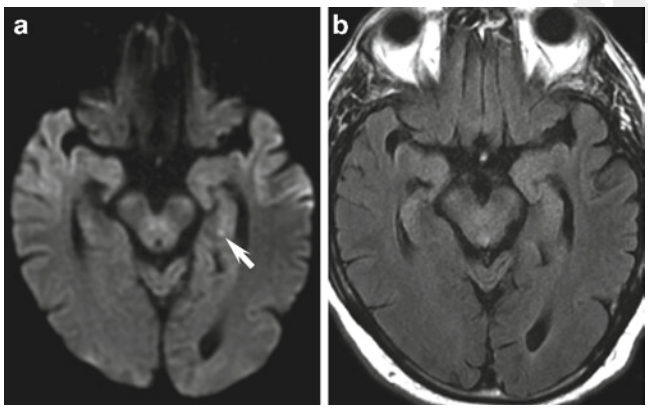

Fig. 2.15 Transient global amnesia (TGA). (**a**) Axial DWI image from a 64-year-old man presenting with transient memory loss lasting several hours without a focal neurological deficit demonstrates a punctate DWI hyperintense focus in the left hippocampus, an appearance and location typical for TGA (*arrow*). (**b**) No abnormality is seen on the FLAIR image. DWI has superior sensitivity to T2 and FLAIR images for detection of the subtle lesions in TGA

Seizures

Seizures can result in transiently decreased diffusion in animals and humans, likely secondary to transient cytotoxic edema [149–156] (Figs. 2.17 and 2.18, Table 2.9). A number of factors can help distinguish restricted diffusion due to seizure activity from that seen during an acute ischemic stroke: (1) The area of abnormality may not correspond to a typical vascular distribution; (2) there is frequently associated sulcal effacement and mass effect, earlier than would be expected with an acute stroke; (3) the abnormalities are usually reversible; (4) there is usually normal or increased perfusion; (5) there may be gyral or leptomeningeal enhancement on postcontrast images earlier than would be expected for an acute infarct; and (6) some reports of DWI changes in status epilepticus describe mixed diffusion findings with restricted diffusion in the cortex and elevated diffusion in the subcortical white matter, a pattern that would be unusual for acute ischemic stroke [151, 153, 157]. Occasionally, areas of chronic infarction may serve as seizure foci and present with DWI hyperintensity around the infarct area [152] that may be difficult to distinguish from an acute or chronic infarction in the absence of prior and follow-up imaging. In addition, a few reports describe transiently decreased diffusion in the corpus callosum in patients with a recent seizure, particularly involving the splenium [158, 159]. However, it should be noted that treatment with certain antiseizure medications

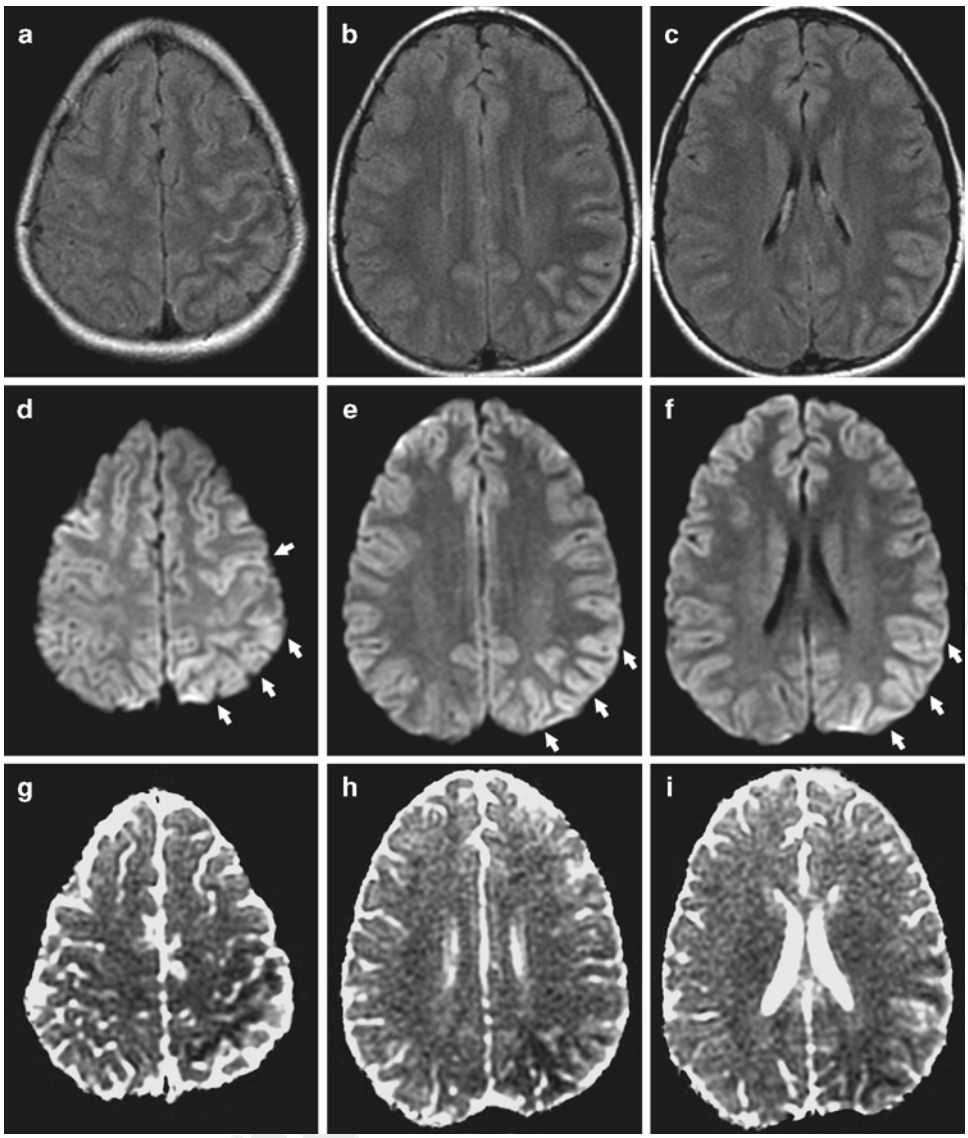

Fig. 2.16 Diffusion changes in a patient with hemiplegic migraine. (**a**–**c**) Axial FLAIR images demonstrate mild gyral FLAIR hyperintensity in the left parietal and posterior frontal lobes. (**d**–**f**) On diffusion maps, there is mild cortical and subcortical DWI hyperintensity (*arrows* in (**d**–**f**)), with (**g**–**i**) corresponding hypointensity on the ADC maps consistent with restricted diffusion. The diffusion changes resolved on a follow-up scan performed 3 days later although the FLAIR hyperintensity persisted (*not shown*)

Table 2.8 Hemiplegic migraine

Rare migraine subtype characterized by transient hemiparesis
Occasionally, patients with prolonged hemiplegic migraine have FLAIR hyperintensity, DWI hyperintensity, and restricted diffusion
Factors that help distinguish hemiplegic migraine from an acute arterial infarct
Strong history of migraines
Lesions may cover multiple arterial territories
Perfusion is normal or elevated
Absence of vascular occlusion
Lesions and clinical deficits are usually reversible

and withdrawal from these medications can also be associated with a transient splenial abnormality in patients without seizures (discussed later). Restricted diffusion in the cerebellar hemisphere contralateral to an area of supratentorial restricted diffusion in a crossed-cerebellar diaschisis pattern has also been described [154, 160].

Areas of diminished diffusion after seizures frequently resolve on follow-up. However, occasionally they can evolve into areas with increased ADC and T2 prolongation consistent with tissue damage, particularly in the hippocampus (Fig. 2.18) [149, 154, 155, 157, 161, 162]. Furthermore, initial MRI scans of patients with temporal lobe epilepsy can also have elevated ADC in the hippocampi [163], and hippocampal sclerosis has been associated with increased ADC and a lower anisotropy index [164]. Some investigators have found increased ADC in *ipsilateral* and *contralateral* hippocampi (compared to control subjects) on interictal scans of patients with temporal lobe epilepsy *without* evidence of hippocampal sclerosis on conventional imaging, although the ADC alone did not appear to provide any lateralizing information [165, 166]. Diffusion tensor imaging (DTI) is a

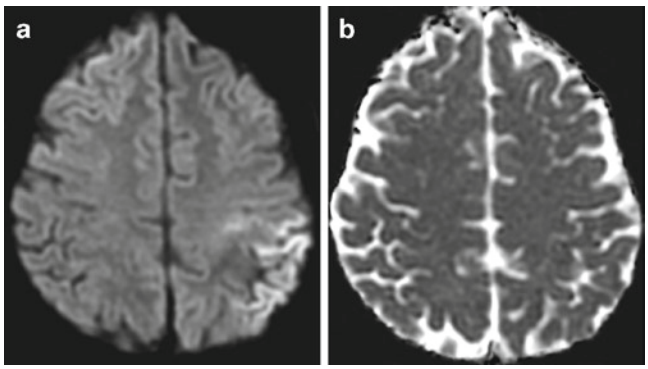

Fig. 2.17 Diffusion changes associated with seizures. (**a**) Axial DWI and (**b**) ADC maps demonstrate cortical and subcortical DWI hyperintensity in the left parietal and posterior frontal lobes with minimal corresponding hyperintensity on the ADC map. The findings resolved on follow-up imaging (*not shown*)

promising tool for evaluation of microstructural changes in epileptic patients and white matter tracts involved in the epileptic network [167, 168]. DTI is discussed in a separate chapter.

Metabolic, Toxic, and Drug-Induced Encephalopathies

A wide variety of metabolic, toxic, and drug-induced encephalopathies can present with areas of T2 prolongation and diffusion abnormality on brain MRI. Their imaging appearance in isolation is typically not pathognomonic for a particular cause, but one clue to the presence of a more generalized metabolic or toxic etiology rather than an ischemic infarct is the presence of relatively symmetric bilateral patchy abnormalities not

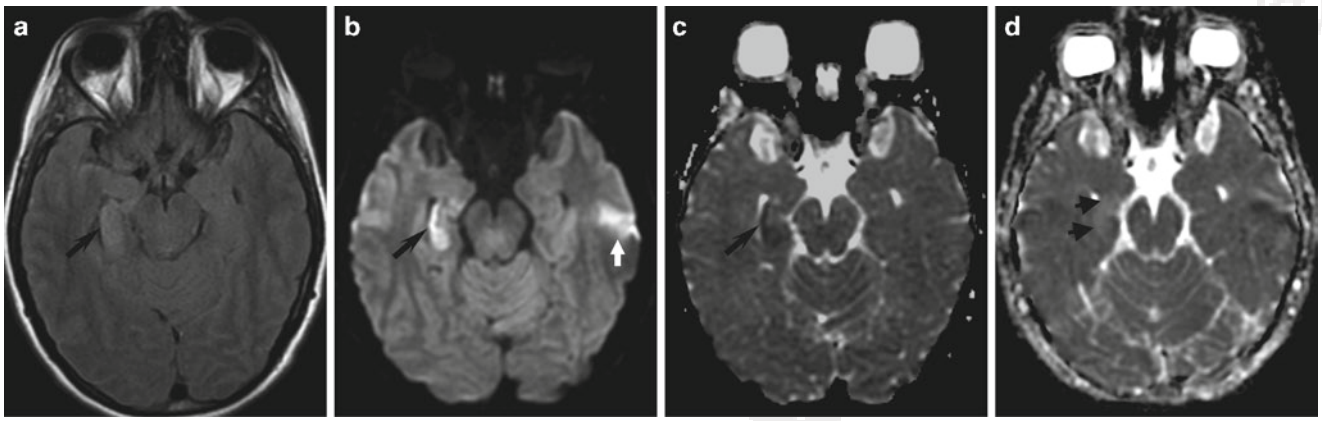

Fig. 2.18 Diffusion changes associated with seizures. (**a**) Axial FLAIR, (**b**) DWI, and (**c**) ADC images demonstrate FLAIR hyperintensity with restricted diffusion in the right hippocampal formation (*black arrow* in **a**–**c**). (**d**) On follow-up exam performed 2 months later, the right hippocampal formation is hyperintense on the ADC map consistent with elevated diffusion secondary to alterations in tissue microstructure (*short wide arrows*). There was progression to a mesial temporal sclerosis pattern of volume loss and T2 prolongation on conventional MR images (*not shown*). The DWI hyperintensity in the left temporal lobe represents susceptibility artifact from the adjacent petrous temporal bone (*white arrow* in (**b**))

Table 2.9 Diffusion changes associated with seizures

Transiently restricted diffusion typically involving the cortex and subcortical white matter, the hippocampus, and the splenium of the corpus callosum
Diffusion changes may evolve into an area of T2 prolongation secondary to gliosis, particularly in the hippocampus
Patients with temporal lobe epilepsy can have elevated ADC values and loss of anisotropy in their hippocampi compared to control subjects, sometimes before the presence of a detectable abnormality on T2 or FLAIR images
Factors that help distinguish restricted diffusion due to seizure activity from an acute arterial infarct
Lesions may cover multiple arterial vascular territories
Mass effect earlier than would be expected for an acute stroke
Perfusion is normal or elevated
Absence of vascular occlusion
Gyral and leptomeningeal enhancement earlier than would be expected for an acute stroke
Lesions may be reversible
Presence of mixed diffusion with restricted diffusion in the cortex and elevated diffusion in the subcortical white matter, a pattern that would be unusual for an acute ischemic infarct

confined to a particular arterial distribution. Involvement of the splenium of the corpus callosum has also been described in toxic and metabolic encephalopathies (Table 2.10), either in isolation or in combination with other lesions. Although this is not specific for any one disorder, the splenium is an unusual site for an acute infarct secondary to arterial occlusion and its presence should alert the radiologist to the possibility of a nonischemic process. Similar to other entities that may mimic an acute stroke, the absence of significant stenosis on vascular imaging and normal or increased perfusion are also helpful in distinguishing toxic and metabolic encephalopathies from an acute stroke. This section provides a brief overview of the diffusion changes seen in these disorders.

Table 2.10 Causes of a splenial lesion[a] on T2-weighted and DWI images

Antiepileptic drug treatment or withdrawal
Seizures[b]
Hypoglycemia
Trauma
Marchiafava–Bignami disease
Wernicke's encephalopathy
Viral encephalitis
Radiation therapy
Hypernatremia and osmotic myelinolysis
Hemolytic uremic syndrome
Altitude sickness
Sympathomimetic-induced kaleidoscopic visual illusion

[a] The splenial lesion may be isolated or part of a more widespread lesion pattern

[b] Because seizure patients with splenial abnormalities typically either were on antiepileptic medications or had been recently taken off such medications, it is difficult to attribute the changes to seizures rather than the medications with certainty

Hypoglycemia

Severe hypoglycemia can have a variety of clinical presentations ranging from a focal neurologic deficit mimicking an acute stroke to hypoglycemic coma. On MRI, severe hypoglycemia can be associated with bilateral and widespread areas of T2 prolongation with restricted diffusion that can involve the splenium of corpus callosum, cortex, and subcortical white matter (with a predilection for the occipital lobes and hippocampi), basal ganglia, internal capsules, brainstem, and middle cerebellar peduncles [169–175] (Fig. 2.19, Table 2.11). Depending on the severity and duration of hypoglycemia, the lesions can be reversible or evolve into areas of permanent T2 prolongation secondary to tissue

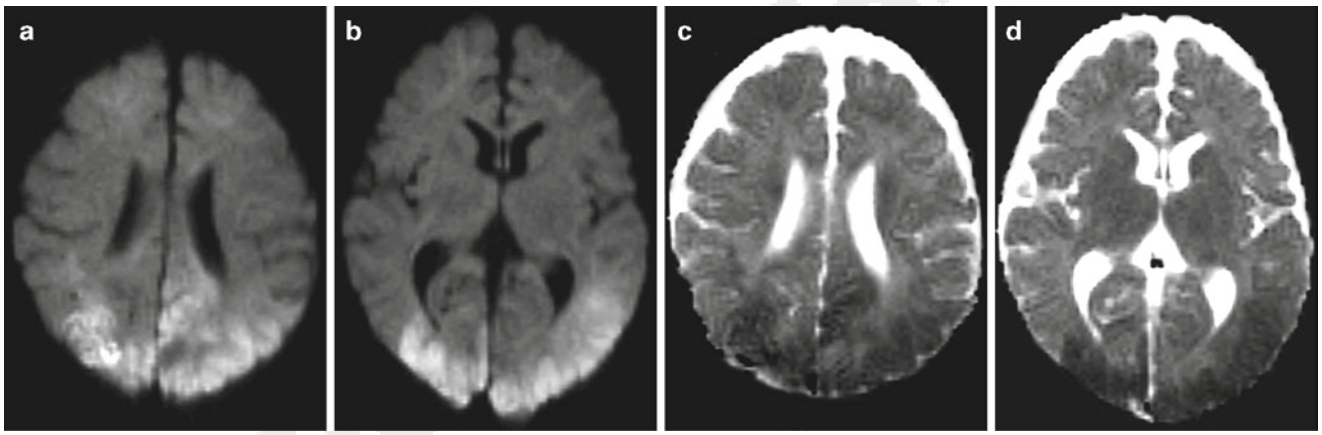

Fig. 2.19 Hypoglycemic encephalopathy. (**a**, **b**) Axial DWI and (**c**, **d**) ADC images from a 3-month-old boy with severe hypoglycemia demonstrate markedly restricted diffusion in the occipital and parietal lobes bilaterally

Table 2.11 DWI findings in metabolic, toxic, and drug-induced encephalopathies

Severe hypoglycemia
Bilateral areas of T2 prolongation and restricted diffusion that can involve the splenium of the corpus callosum, cortex and subcortical white matter, hippocampi, basal ganglia, internal capsules, and posterior fossa structures
Predilection for the occipital lobes and splenium
Cause of restricted diffusion – cytotoxic edema

(continued)

Table 2.11 (continued)

Heroin inhalation leukoencephalopathy
Symmetric areas of white matter T2 prolongation with a predilection for the posterior cerebral hemispheres, cerebellum, and posterior limb of the internal capsules
May also involve the splenium of the corpus callosum
Lesions are usually hyperintense on DWI images with restricted diffusion. Cases with elevated diffusion have also been reported, probably related to the time from injury
Cause of restricted diffusion – ? myelin vacuolization
Metronidazole-induced encephalopathy
Rare complication of Metronidazole use
Bilateral and symmetric T2 hyperintense lesions involving the dentate nuclei
Less frequent involvement of other brainstem structures, subcortical white matter, and corpus callosum
Lesions are hyperintense on DWI with a variable appearance on the ADC map
Cause of restricted diffusion – ? cytotoxic edema
Carbon monoxide poisoning
T2 prolongation and restricted diffusion predominantly involving the deep gray nuclei and the deep white matter and cortex, especially the hippocampus
Mild cases can involve only the globus pallidi
A delayed encephalopathy syndrome with extensive white matter T2 prolongation and restricted diffusion may also occur
Cause of restricted diffusion – cytotoxic edema
Osmotic myelinolysis syndromes
Severe damage of the myelin sheath due to rapid correction of hyponatremia, frequently associated with alcoholism
Central pontine myelinolysis – lesion in central pons
Extrapontine myelinolysis – relatively symmetric lesions in the cerebellum, cerebral peduncles, basal ganglia, internal capsules, and other white matter tracts
Cause of restricted diffusion – ? cytotoxic edema, ? myelin vacuolization
Wernicke's encephalopathy
Inadequate intake or absorption of thiamine
Clinical syndrome – ataxia, ophthalmoplegia, short-term memory impairment, and confusion
T2 prolongation with transient restricted diffusion of the medial thalami, periaqueductal gray, and mamillary bodies
Cause of restricted diffusion – ? cytotoxic edema, ? myelin vacuolization
Marchiafava–Bignami disease
Rare progressive neurologic disease associated with chronic alcoholism.
T2 prolongation and/or restricted diffusion in the corpus callosum, cerebral cortices, internal capsule, and the thalamus
Cause of restricted diffusion – ? cytotoxic edema, ? myelin vacuolization

damage and gliosis [169, 171, 174, 176]. In cases of isolated lesions involving a single vascular territory, distinction from an ischemic infarct may not be possible without additional clinical information or follow-up [170].

Heroin Inhalation Leukoencephalopathy

Inhalation of heroin vapor, sometimes referred to as "chasing the dragon," can result in a rare form of toxic leukoencephalopathy with extensive abnormalities on MRI [177, 178] (Fig. 2.20, Table 2.11). HIL can present as marked symmetric areas of white matter T2 prolongation. In the cerebrum, the occipital lobes are most extensively involved with progressive involvement of the parietal, temporal, and frontal lobes [178]. The splenium of the corpus callosum and cerebellum can also be affected. In addition, there can be symmetric involvement of the corticospinal tracts, medial lemniscus, and tractus solitarius. There are limited descriptions of diffusion changes in the areas of white matter signal abnormality but both restricted diffusion and elevated diffusion have been described, probably depending in part on the time lag between the onset of the encephalopathy and time at which the MRI was performed. Acute lesions can have decreased diffusion.

Metronidazole-Induced Encephalopathy

Metronidazole is a widely used 5-nitroimidazole antibiotic that can be associated with a number of neurologic side effects including peripheral neuropathy, encephalopathy, cerebellar dysfunction, and seizures. Metronidazole-induced encephalopathy is rare. Typically, patients have bilateral and symmetric patchy T2 hyperintense lesions involving the dentate nuclei of the cerebellum, with less frequent involvement

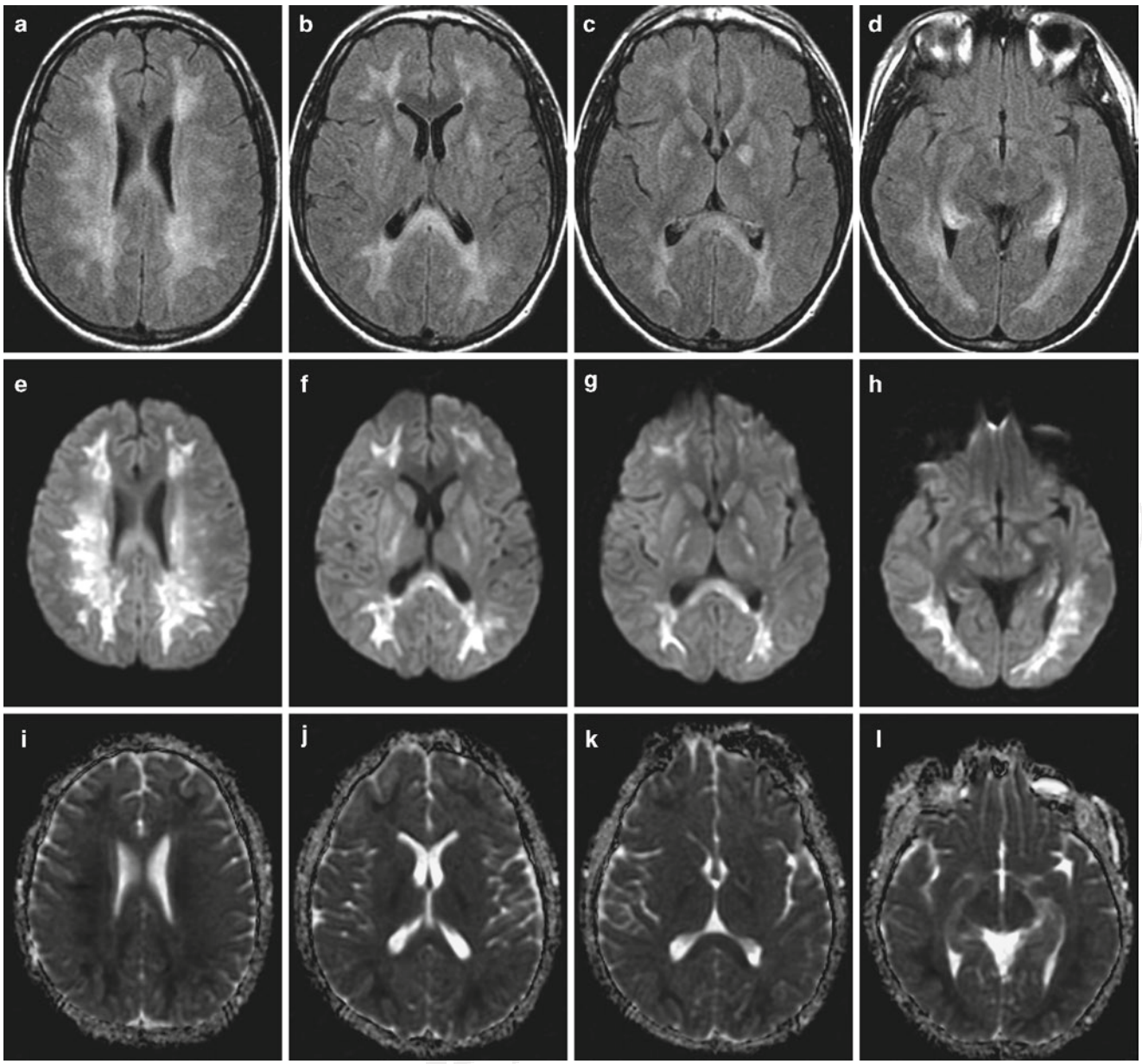

Fig. 2.20 MR images from a 23-year-old man found unresponsive after heroin inhalation. (**a**–**d**) Axial FLAIR images demonstrate extensive hyperintensity in the subcortical white matter, corona radiata, posterior limb of the internal capsule, and corticospinal tracts. (**e**–**h**) The majority of the lesions are hyperintense on DWI and (**i**–**l**) hypointense on ADC maps, consistent with restricted diffusion. This pattern is compatible with severe heroin inhalation injury. Additional foci of signal abnormality in the lentiform nucleus and hippocampal formations are nonspecific but, may represent a component of anoxic brain injury

of subcortical white matter, the corpus callosum, and various other brainstem structures [179–183] (Fig. 2.21, Table 2.11). Lesions are usually hyperintense on DWI but may have restricted diffusion or be isointense or hyperintense on the ADC map [180–183]. The lesions are typically reversible, although there are reports of residual T2 prolongation on short-term follow-up MRI, especially in the corpus callosum [180–183].

Carbon Monoxide Poisoning

Acute carbon monoxide (CO) toxicity can result in multifocal areas of T2 prolongation with restricted diffusion on MRI [184, 185] (Table 2.11). There is a predilection for involvement of the globus pallidus alone in mild cases. In more severe cases, the remainder of the deep gray nuclei and the deep white matter and cortex, especially the hippocampus, can be affected

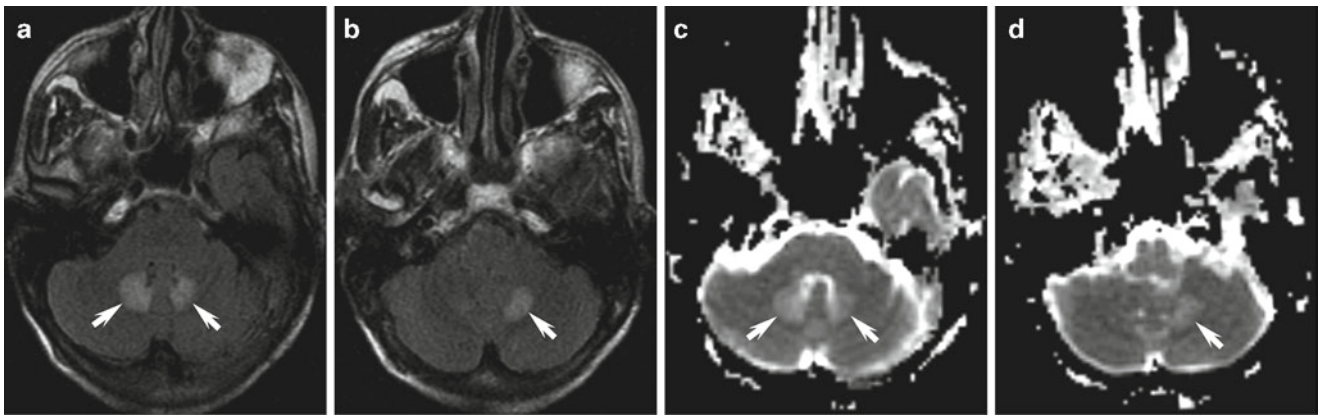

Fig. 2.21 Metronidazole-induced encephalopathy. (**a**, **b**) Axial FLAIR and (**c**, **d**) ADC images demonstrate bilateral symmetric FLAIR hyperintensity involving the cerebellar dentate nuclei. On the ADC map, the lesions are hyperintense consistent with elevated diffusion. The lesions were isointense on DWI (*not shown*). On follow-up after discontinuation of the medication, all abnormalities resolved (*not shown*). Lesions associated with metronidazole toxicity can also have restricted diffusion

[184]. In addition, although less commonly identified on MRI, lesions may also be present in the substantia nigra and when combined with lesions in the globi pallidi, are referred to as a pallidoreticular pattern of injury [184, 186]. In addition to lesions seen after recent CO toxicity, patients with CO poisoning can also present with a delayed encephalopathy consisting of extensive T2 hyperintense white matter lesions that may also at least in part demonstrate decreased diffusion [184, 187].

Osmotic Myelinolysis Syndromes

Osmotic myelinolysis is a neurologic disease caused by severe damage of the myelin sheath due to rapid correction of hyponatremia, frequently associated with alcoholism. Lesions are typically seen in the pons (pontine myelinolysis) but can also be seen in other structures (extrapontine myelinolysis) such as the cerebellum, cerebral peduncles, basal ganglia, internal capsules, and other white matter tracts (Table 2.11). The lesions are T2 hyperintense and relatively symmetric, and may present with either restricted or elevated diffusion, probably depending on the timing of imaging in relation to symptom onset [188–190].

Other Syndromes Associated with Alcoholism

Wernicke's encephalopathy results from inadequate intake or absorption of thiamine and is characterized by ataxia, ophthalmoplegia, confusion, and impairment of short-term memory. On MRI, symmetric T2 prolongation with transient restricted diffusion of the medial thalami, periaqueductal gray, and mamillary bodies has been reported [191]. A case report also describes restricted diffusion in the splenium of corpus callosum [192]. Marchiafava–Bignami disease, a rare progressive neurologic disease associated with chronic alcoholism, can also present with T2 prolongation and/or restricted diffusion in the corpus callosum, cerebral cortices, internal capsule, and the thalamus [193–195]. The callosal lesion typically involves the splenium but may also involve the body of the corpus callosum [193–196].

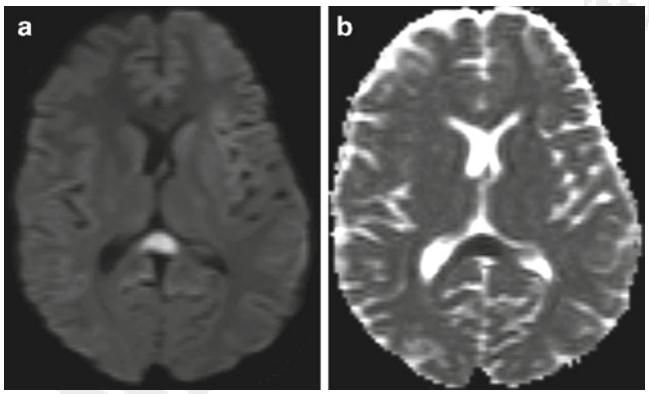

Fig. 2.22 Transient splenial lesion associated with antiepileptic medication (valproic acid) treatment. (**a**) Axial DWI and (**b**) ADC images from a 16-year-old girl treated with antiepileptic medications for psychiatric illness and no history of seizures demonstrate restricted diffusion in the splenium of the corpus callosum. The abnormality resolved on follow-up MRI after discontinuation of the medication (not shown)

Other Drugs and Metabolic Conditions Associated with Restricted Diffusion

In addition to the entities previously discussed, a number of other toxic, metabolic, or drug-related conditions may present with T2 prolongation and restricted diffusion, particularly involving the splenium of the corpus callosum [197]. These include treatment with antiseizure medications [198, 199] (Fig. 2.22), withdrawal of antiseizure medications [200, 201],

sympathomimetic-induced kaleidoscopic visual illusion syndrome [202], hemolytic uremic syndrome, and high altitude brain injury (Table 2.10). There are a few reports of DWI abnormalities in patients with severe hemolytic uremic syndrome. These patients can have restricted diffusion and/or T2 prolongation in the basal ganglia, especially the dorsolateral lentiform nucleus with less frequent involvement of the thalami, cerebellum, and brainstem [203, 204]. Depending on the severity of disease, the lesions may or may not be reversible [203–205]. One case report also describes a focal T2 hyperintense lesion in the splenium of the corpus callosum, but diffusion-weighted images were not performed [205].

Acute high altitude sickness can also be associated with DWI abnormalities. In a simulated study of acute high altitude sickness by exposure to normobaric hypoxia, some patients had decreased ADC values in the splenium of the corpus callosum in addition to mild generalized increase in cerebral volume and edema [206]. One case report describes a T2 hyperintense lesion with elevated ADC in the splenium of the corpus callosum, but the MRI was performed 14 days after symptom onset [207].

Inflammatory Demyelinating Lesions

Numerous investigations have demonstrated diffusion changes in acute and chronic demyelinating lesions [208–213]. Although acute enhancing lesions in MS or acute disseminated encephalomyelitis most frequently have elevated diffusion, they can have transiently restricted diffusion at their periphery or even in their core, usually attributed to cytotoxic edema, fluid shifts between IC and EC compartments, or dense inflammatory cell infiltration [208–210, 212–214] (Fig. 2.23, Table 2.12). Therefore, a demyelinating lesion should always be considered in a patient presenting with an acute neurologic deficit and a small lesion with restricted diffusion in an atypical location, atypical pattern, or an atypical age group for an ischemic stroke. A ring pattern of restricted diffusion has also been described in cases of tumefactive demyelinating lesions (TDL). In one retrospective analysis of 18 cases of TDLs, 11 patients (61%) had lesions with increased ADC

Table 2.12 Demyelinating lesions

Acute demyelinating lesions in multiple sclerosis or acute disseminated encephalomyelitis typically have elevated diffusion
Less commonly, acute lesions have decreased diffusion in both enhancing and nonenhancing lesions
Cause of restricted diffusion: cytotoxic edema, fluid shifts between IC and EC compartments, or dense inflammatory cell infiltration
Tumefactive demyelinating lesions are frequently rim enhancing with restricted diffusion in the rim and elevated diffusion in the center of the lesion
Chronic lesions typically have elevated diffusion with the greatest diffusivity seen in T1 hypointense lesions, which correspond to areas of severe tissue destruction
A single lesion with restricted diffusion can be mistaken for an acute infarction

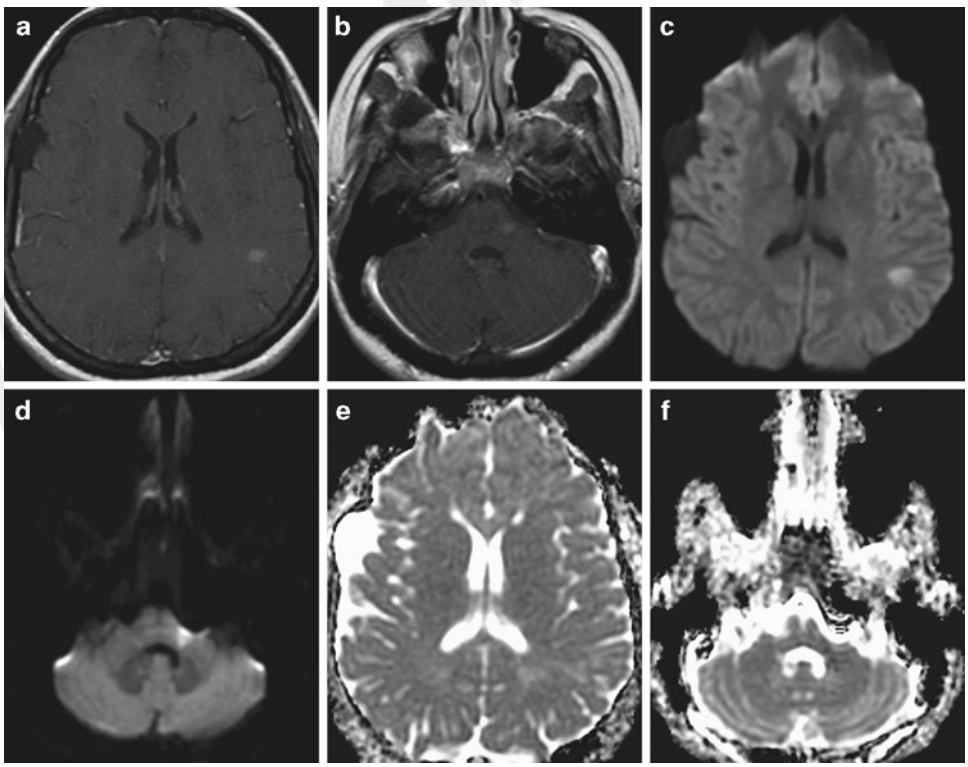

Fig. 2.23 Different appearances of enhancing demyelinating lesions on DWI. (**a**, **b**) Axial contrast-enhanced T1-weighted images from a patient with multiple sclerosis demonstrate two enhancing lesions located in the left temporo-parietal region and at the junction of the left middle cerebellar peduncle and lower pons. (**c**, **d**) Although both lesions are hyperintense on DWI, (**e**, **f**) the supratentorial lesion is mildly hyperintense on ADC whereas the infratentorial lesion is mildly hypointense on ADC. Demyelinating plaques most frequently have normal or elevated diffusion but less commonly have diminished diffusion and can be misdiagnosed as ischemic infarcts. Incidentally, there is a right middle cranial fossa arachnoid cyst

in the center and peripheral restricted diffusion either as a complete or an incomplete ring, 5 had increased ADC without evidence of peripheral diffusion restriction, and 2 had peripheral restriction without increased ADC in the center of the lesion [215]. Therefore, DWI in conjunction with conventional MR sequences and MR spectroscopy may be helpful in distinguishing TDLs from neoplasms. On DWI, chronic T2 hyperintense MS lesions usually demonstrate elevated diffusion with the greatest diffusivity seen in T1 hypointense lesions, which correspond to areas of severe tissue destruction and cavitation [208, 212, 216].

DTI is widely used in MS research. Changes in diffusion anisotropy correlate with demyelination and axonal loss, and DTI can reveal alterations in tissue microstructure that may not be apparent on conventional MR sequences or conventional DWI. Potential applications of DTI that are under investigation include its use for quantification of the severity of degenerative neuronal/axonal change, additional characterization of T2 hyperintense lesions, identification of abnormalities within normal appearing white matter on conventional MR sequences, and mapping structural connectivity among brain regions [211, 217, 218]. A detailed discussion of applications of DTI in demyelinating disease is beyond the scope of this chapter but can be found elsewhere in this book and in review articles on the topic [211, 217–219].

Cerebral Infections

Abscesses

DWI is a very useful adjunctive MR sequence for the evaluation of ring enhancing brain lesions and allows reliable distinction of a pyogenic brain abscess from a necrotic tumor. Pus within the central core of a pyogenic brain abscess restricts diffusion and is typically homogeneously hyperintense on DWI with a low ADC value (Fig. 2.24, Table 2.13). On the contrary, the necrotic or cystic component of a tumor tends to have elevated diffusion with intermediate intensity on DWI and hyperintensity on ADC maps [220–223]. However, it should be noted that treated abscesses tend to have a more heterogenous appearance depending on the stage and response to treatment, and can contain mixed areas of restricted and elevated diffusion [224]. In fact, DWI can be useful for follow-up of pyogenic abscesses. In small studies, decreasing DWI hyperintensity and increasing ADC value within purulent collections, including intraparenchymal

Table 2.13 Cerebral infections

Pyogenic infections
Pyogenic collections have homogeneously restricted diffusion due to increased viscosity of pus
Ring enhancing lesions with homogeneously restricted central diffusion are almost always pyogenic abscesses
Subdural empyemas and subdural effusions appear similar on conventional sequences. Empyemas have homogeneously restricted diffusion, while effusions have elevated diffusion
DWI improves the detection of ventriculitis with intraventricular pus
Nonpyogenic abscesses
These abscesses have a more variable and heterogeneous appearance with areas of diminished diffusion, elevated diffusion, or both
Viral encephalitis
Can have restricted diffusion acutely, especially involving the cortex and subcortical white matter
The lesions may be more conspicuous on DWI compared to T2 weighted or FLAIR images
Regions with restricted diffusion are more likely to lead to irreversible neuronal damage and are associated with poor outcome
HSV 1 lesions have a predilection for the limbic system – the medial temporal lobes, insula, cingulate gyri, and subfrontal regions
Creutzfeldt-Jacob disease
Rapidly progressive dementing illness caused by infection with prion protein
Sporadic CJD – most common appearance – restricted diffusion in the basal ganglia (symmetric) and cortex (symmetric or asymmetric)
Variant CJD – most common appearance – symmetric restricted diffusion in the dorsomedial thalami and pulvinar
DWI is more sensitive than FLAIR or T2 weighted images for lesion detection
Restricted diffusion can persist for a long time in some cases

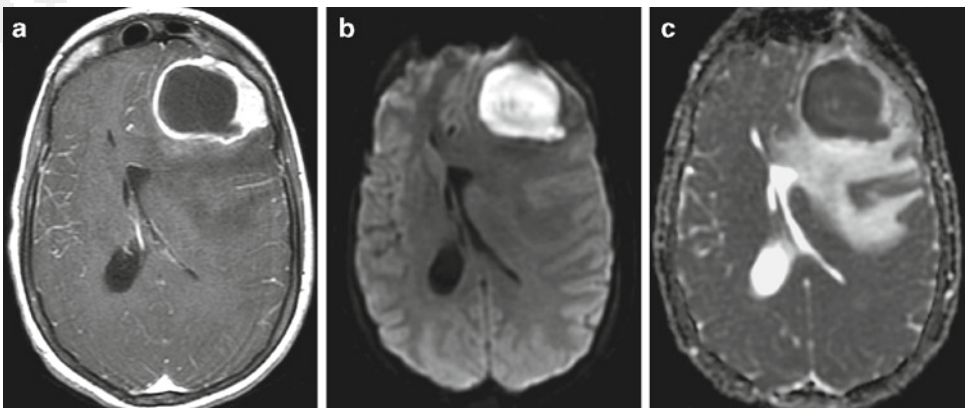

Fig. 2.24 Bacterial abscess. (**a**) Axial contrast-enhanced T1, (**b**) DWI, and (**c**) ADC images demonstrate a large ring enhancing lesion in the left frontal lobe with marked associated vasogenic edema (demonstrating elevated diffusion), mass-effect, and midline shift. There is homogenously restricted diffusion within the lesion, a finding highly suggestive of an abscess

abscesses and extra-axial collections, has been shown to correlate with treatment response clinically [224–227].

Nonpyogenic abscesses have a more variable appearance. Tuberculous abscesses frequently have restricted diffusion in their core and/or wall, similar to pyogenic abscesses [222]. On the contrary, fungal abscesses commonly are heterogeneous with mixed areas of restricted diffusion or with elevated diffusion within the central cavity and restricted diffusion in the abscess wall [222, 228]. Fungal abscesses can also have irregular projections with diminished diffusion corresponding to inflammatory tissue and fungal hyphae [222]. Restricted diffusion within an abscess should not be confused with infarcts secondary to angioinvasive or embolic infections as may occur with aspergillosis or tuberculosis, which are usually distinguishable based on other imaging characteristics.

Toxoplasma abscesses can have a mildly hyperintense core on DWI that is usually isointense or hyperintense to normal brain parenchyma on ADC [229] (Fig. 2.25). Similar to fungal infections, evaluation of the abscess wall may be helpful. In one report of four cases, all had a low ADC value in the abscess wall [229]. In another study of acquired immunodeficiency syndrome (AIDS) patients, toxoplasma abscesses typically had higher ADC values than lymphoma, an important differential consideration in that patient population, and only toxoplasma abscesses had a lesion to normal white matter ADC ratio greater than 1.6 [230]. However, other studies have described greater overlap in lesion ADC values [231], and in many cases a definitive distinction may not be possible.

Meningitis

The diagnosis of meningitis remains primarily a clinical one, but imaging plays an important role in excluding other CNS lesions and may, in addition, demonstrate signs supporting a diagnosis of meningitis. Sulcal restricted diffusion is sometimes seen in cases of bacterial meningitis [227], but DWI is not nearly as sensitive as FLAIR for detection of meningeal abnormalities. However, DWI is excellent for detection of complications of meningitis (Fig. 2.26). For example, DWI is highly sensitive for detection of pyogenic ventriculitis.

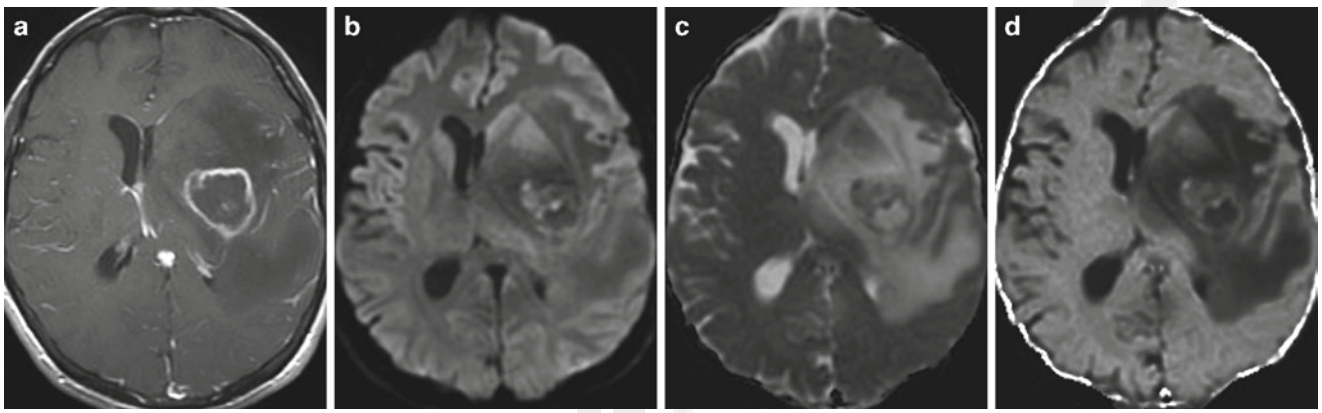

Fig. 2.25 Toxoplasma abscess. (**a**) Axial contrast-enhanced T1, (**b**) DWI, (**c**) ADC, and (**d**) exponential images demonstrate a ring enhancing lesion centered in the posterior putamen with associated vasogenic edema and mass effect. On diffusion maps, the lesion is heterogenous with regions of mildly restricted diffusion and elevated diffusion. There is mildly restricted diffusion in the abscess wall, a feature that may be helpful in characterization of these lesions and has also been described in fungal abscesses

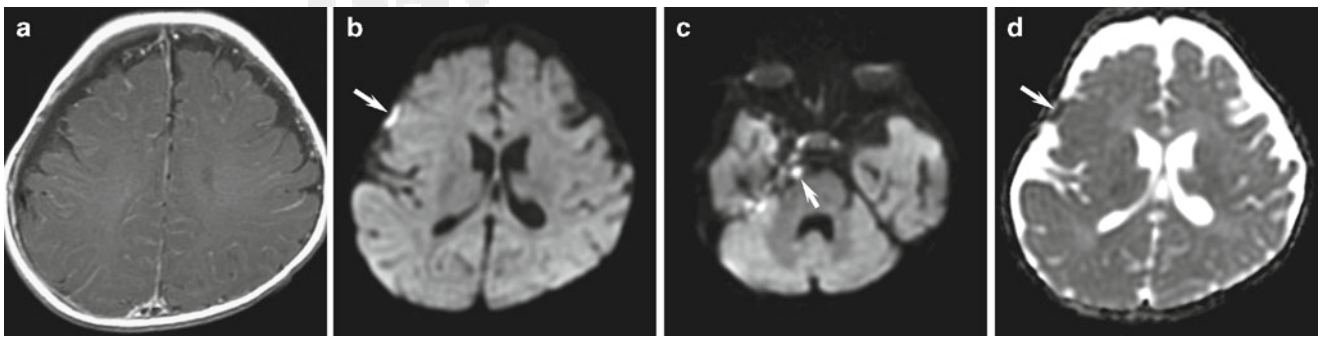

Fig. 2.26 Meningitis and complications. (**a**) Axial contrast-enhanced T1, (**b**, **c**) DWI, and (**d**) ADC images from a 4-month-old girl with *Staphylococcus aureus* meningitis are shown. On the postcontrast T1 image, there is diffuse meningeal enhancement. DWI and ADC maps demonstrate small foci of purulent debris in the right frontal subarachnoid space (*arrow* in (**b**) and (**d**)) and in the prepontine cistern and cerebellopontine angle (*arrow* in **(c)**). In this case, the patient responded to conservative treatment with antimicrobial therapy

Intraventricular pus, similar to pus within an abscess, has restricted diffusion and is markedly hyperintense on DWI. The debris is typically located in a dependent position in the trigones or occipital horns of the lateral ventricles or, less commonly, the fourth ventricle [232–235]. Furthermore, DWI can differentiate subdural empyemas from subdural effusions. Both are T1 hypointense and T2 hyperintense, but empyemas have restricted diffusion while simple effusions have elevated diffusion. Lastly, DWI improves the detection of arterial infarctions due to meningitis-associated vasculitis and of venous infarctions due to associated venous sinus thrombosis.

Encephalitis

Encephalitis is an acute infection of the brain parenchyma characterized clinically by headache, fever, and altered mental status. Viral encephalitis has been associated with more than 100 viruses and its diagnosis requires a combination of clinical findings, serologic and cerebrospinal fluid (CSF) laboratory analysis, and imaging. Although a thorough discussion of the variety of MR patterns seen in viral encephalitis is beyond the scope of this chapter, diffusion findings in a few common encephalitides are discussed to illustrate the adjunctive role of DWI for their characterization. One common feature shared by many viral encephalitides is the presence of restricted diffusion in regions of T2 prolongation during the acute stage (Table 2.13). Occasionally, lesions may be more conspicuous on DWI compared to T2 and FLAIR images [236–240].

Herpes encephalitis is the most common cause of acute fatal sporadic encephalitis in humans [237]. The majority of infections in adults are secondary to herpes simplex type 1 (HSV-1). HSV-1 has a predilection for limbic system structures including the medial temporal lobes, the insula, the subfrontal areas, and the cingulate gyri (Fig. 2.27). Both restricted diffusion from cytotoxic edema and elevated diffusion from vasogenic edema may be seen during the acute phase of herpes simplex encephalitis and the two patterns are frequently present concurrently [236, 237, 241, 242]. In general, areas with restricted diffusion are believed to be more likely to lead to irreversible neuronal damage and are associated with poor clinical outcomes [237, 241]. In some cases, acute lesions may be better visualized on DWI compared to FLAIR or T2-weighted images [236, 237]. Chronically, the lesions tend to demonstrate elevated ADC, similar to parenchymal injury from other causes.

HSV-2 encephalitis is much less common than HSV-1 encephalitis and typically affects neonates. HSV-2 does not have the temporal lobe predilection seen with HSV-1 and may present with patchy areas of T2 hyperintense signal abnormality throughout the cerebral hemispheres and deep gray nuclei. These areas typically have restricted diffusion during the acute phase and progress to cystic encephalomalacia with elevated diffusion in the chronic stage [239].

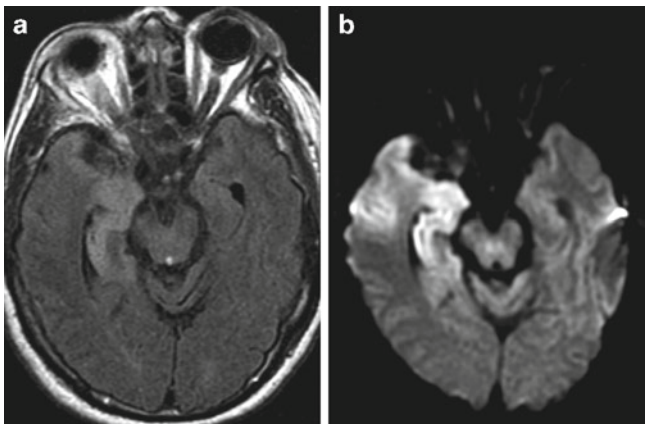

Fig. 2.27 Herpes simplex encephalitis. (**a**) There is FLAIR hyperintensity with (**b**) restricted diffusion in the medial and anterior right temporal lobe. Note that there is overall increased lesion contrast on the DWI image (**b**) compared to the FLAIR image (**a**)

In addition to the human herpes virus family, a large number of nonherpetic viruses can result in meningoencephalitis. These include Japanese encephalitis, a mosquito-borne flaviviral encephalomyelitis, different forms of measles encephalitis, and enteroviral encephalitis, among others [243]. DWI can demonstrate multifocal areas of restricted diffusion involving the cortex, subcortical white matter, and deep gray nuclei during the acute phase of these diseases and is useful for distinguishing areas of cytotoxic edema from vasogenic edema [243]. The specific patterns of T2 prolongation and diffusion change in nonherpetic and other viral encephalitides can be found in primary articles and reviews on the topic [243–246]. Viral encephalitis can also present with, and is on the differential diagnosis for, a reversible splenial lesion [246, 247] (Table 2.10).

Creutzfeldt-Jacob Disease

Creutzfeldt-Jacob disease (CJD) is a rare rapidly progressing and ultimately fatal dementing illness caused by infection from an isoform of the prion protein with an incidence of less than one per million [248, 249]. CJD can be sporadic (from spontaneous mutations), familial (hereditary), or acquired and MRI with DWI is the optimal imaging modality for demonstration of intracranial lesions. In the sporadic form, there are typically symmetric areas of diffusion change with or without T2 prolongation in the basal ganglia, especially the corpus striatum [248–252] (Fig. 2.28, Table 2.13). In addition, symmetric or asymmetric areas of cerebral or cerebellar cortical signal abnormality may be present with or

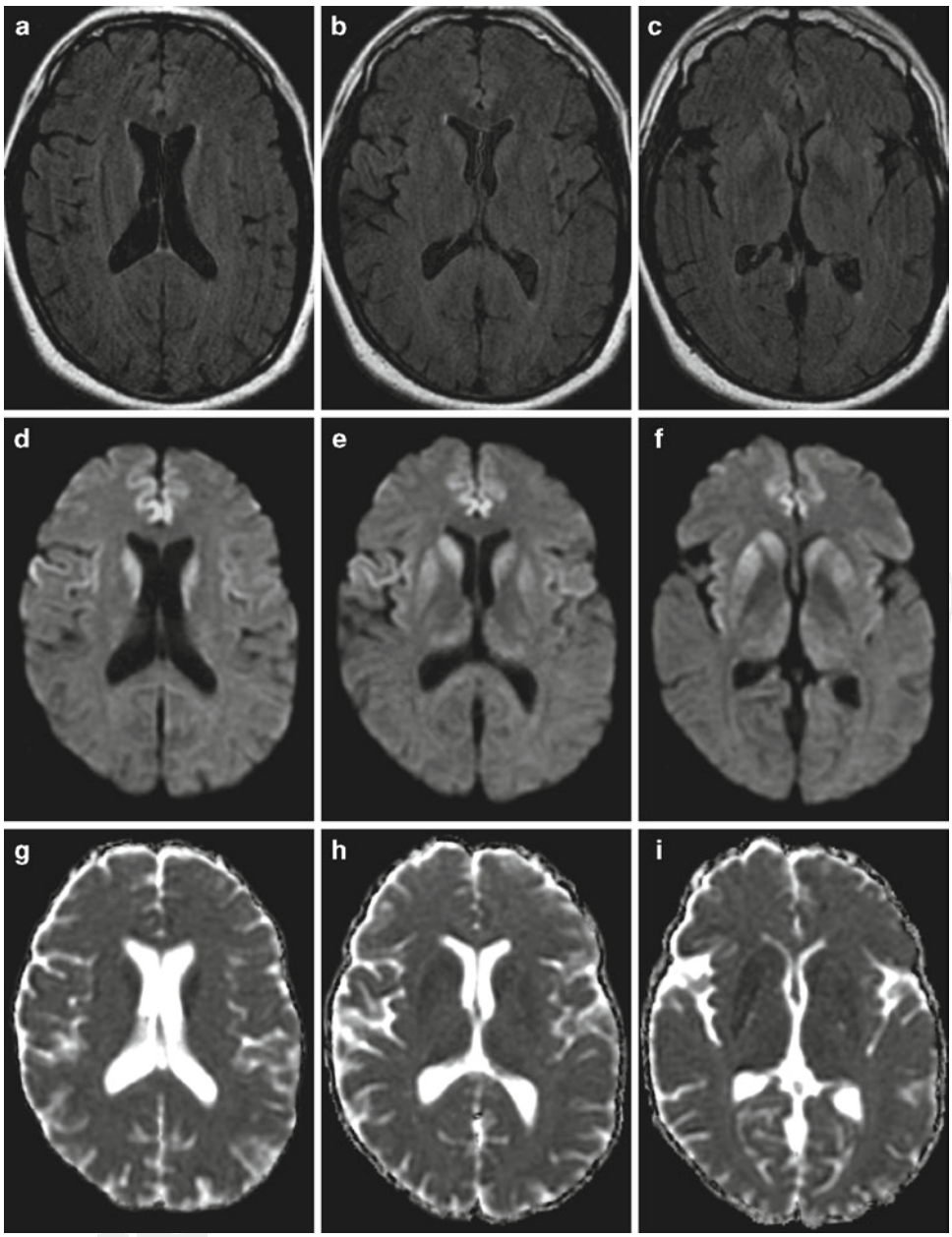

Fig. 2.28 Sporadic Creutzfeldt-Jacob disease (CJD). (**a**–**c**) Axial FLAIR, (**d**–**f**) DWI, and (**g**–**i**) ADC images are shown. On the FLAIR images, there is subtle fairly symmetric hyperintensity involving the corpus striatum, the thalami, the anterior frontal cortex, the cingulate gyri, and the insula. The abnormalities are much better visualized on the DWI images due to increased lesion contrast. The abnormalities are hypointense to isointense on the ADC maps

without striatal involvement. Less common features include involvement of the periaqueductal gray matter, symmetric involvement of the thalami, asymmetric involvement of the corpus striatum, or involvement of the cerebellar cortex. The variant form of CJD shows a different pattern with symmetric involvement of the pulvinar and the dorsomedial thalamus in a high percentage of cases [249, 253]. However, the striatum, periaqueductal gray, and, less commonly, other areas may be affected similar to the sporadic form [249, 254, 255]. Cortical involvement is frequently not seen in the variant form [255].

DWI is more sensitive than conventional MR sequences for identification of lesions in CJD [249, 251, 256–260] and can demonstrate lesions even before development of periodic sharp wave complexes on EEG [261]. Lesions are typically hyperintense on DWI and frequently have low values on the ADC map due to restricted diffusion, although normal or even elevated ADC may occasionally be present, possibly related to the duration of disease and time before imaging [249, 255–258, 261]. Although there is some conflicting data on correlation of MR findings with findings on postmortem pathology, many studies have demonstrated that regions with decreased ADC correlate with spongiform change [251, 259, 260]. On follow-up imaging, there can be persistent, or even an increase in, restricted diffusion over periods lasting weeks to months in some patients, but in others there is an eventual

decrease in DWI intensity and increase in ADC value [252, 256, 261–263]. In addition, different lesions in the *same* patient may evolve differently [261, 262]. In one study, diffusion changes were better visualized on DWI images obtained at a higher *b*-value (3,000 s/mm^2) compared to standard DWI (1,000 s/mm^2), although no new areas of involvement were identified on the high *b*-value images [255]. In addition, the authors found that while the abnormalities in sporadic CJD had predominantly low ADC, including in the thalamus, there was elevated ADC in the pulvinar in variant CJD and this finding may provide an additional useful feature for distinction from sporadic CJD [255].

Neoplasms

DWI is an important adjunctive sequence in the evaluation of both intra-axial and extra-axial brain tumors (Table 2.14). DWI provides important additional information that helps distinguish neoplasms from cerebral abscesses and TDL. In addition, DWI can provide additional information on tumor characteristics such as cellularity. In general, the ADC value is inversely proportional to cellular density of a mass and tumors with high cellularity and densely packed cells tend to exhibit relatively diminished diffusion [264–266]. In certain tumors such as epidermoids, the DWI signature in combination with signal characteristics on conventional sequences is essentially pathognomonic. It should be noted that since the signal intensity of DWI images relies on a number of factors including T2 effects, there can be marked variability in tumor appearance on the DWI image. Therefore, many studies of diffusion characteristics of tumors focus on the ADC map instead.

Primary Glial Neoplasms and Intracranial Metastases

Tumors of glial origin or astrocytomas constitute the most common primary intra-axial neoplasm in adults. Although the ADC of high-grade astrocytomas tends to be lower than low-grade astrocytomas, there is significant variability and overlap between the diffusion characteristics of high- and low-grade neoplasms and the reported accuracy of ADC for prediction of tumor grade [264, 267–271] (Fig. 2.29). Within a tumor, the cystic areas tend to have higher diffusivity/ADC values [268] (Fig. 2.29). Selective analysis of solid tumor areas may help improve accuracy of ADC in predicting tumor cellularity and grade, but even when only the solid portion or darkest area on ADC is used for analysis, there is marked variation in the ADC values [269–272]. For example, when the reported ADC values from three studies that found a difference between high-grade and low-grade malignant tumors are combined, the mean ADC values for high-grade tumors are between 520 to $1{,}130 \times 10^{-6}$ mm^2/s compared to 1,010 to $1{,}350 \times 10^{-6}$ mm^2/s for low-grade tumors, with much greater variation between the ADC of individual cases [269–271]. Furthermore, there are no universally accepted standardized methods for selecting subsites, and the ADC cannot be used to reliably predict tumor grade from a practical clinical perspective. Similar to adult brain tumors, high-grade malignant pediatric brain tumors tend to have diminished diffusion compared to low-grade tumors and some studies have reported high sensitivity and specificity of DWI in this regard [273] that require confirmation in larger studies.

Intracranial metastases typically have elevated diffusion with variable ADC values and cannot be distinguished from malignant gliomas based on diffusion characteristics alone.

Table 2.14 DWI for intracranial neoplasms

Glial neoplasms and intracranial metastases
Solid portions of higher grade tumors tend to have a lower ADC value compared to lower grade tumors
ADC usually increases after successful treatment
Recurrent neoplasms tend to have lower ADC compared to areas of treatment change
Peritumoral "edema" of high-grade glial neoplasms tends to have lower ADC compared to peritumoral "edema" of low-grade glial neoplasms or metastases
DWI characteristics cannot reliably distinguish between high-grade and low-grade tumors or between recurrent tumor compared to treatment change because of significant overlap but can be useful as an adjunctive sequence in combination with conventional MR sequences, MR spectroscopy, and MR perfusion
CNS lymphoma
Lymphomas usually have relatively homogeneously decreased diffusion
Homogeneously enhancing intra-axial lesions with decreased diffusion usually represent lymphomas
Lower pretreatment ADC values are associated with shorter disease-free and overall survival
Extra-axial masses
Epidermoid tumors can be readily distinguished from an arachnoid cyst with DWI. Arachnoid cysts have elevated diffusion, similar to CSF, and are dark on DWI images. Epidermoids have diffusion similar to normal brain tissue and are markedly hyperintense on DWI due to their diffusion and T2 characteristics
Malignant or atypical meningiomas have lower ADC values than typical meningiomas

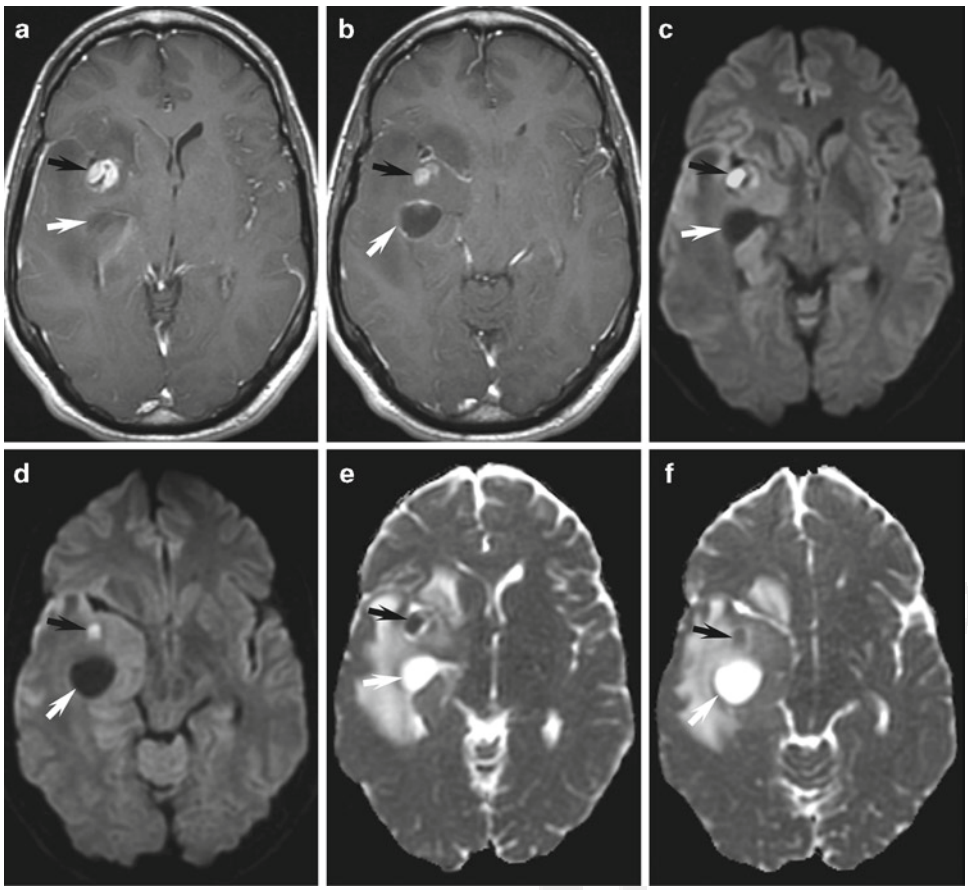

Fig. 2.29 Glioblastoma multiforme. (**a**, **b**) Axial contrast-enhanced T1, (**c**, **d**) DWI, and (**e**, **f**) ADC images demonstrate a heterogeneous tumor involving the right temporal lobe and insular region. There is restricted diffusion in the nodular enhancing focus (*black arrows*) suggesting high cellularity associated with higher grade tumors. There is elevated diffusion in the cystic component (*white arrows*)

Increased cellularity and higher grade of malignant intracranial metastases tend to correlate inversely with the tumor ADC values, but similar to primary brain tumors there is substantial variability and overlap between low-grade and high-grade tumors and between metastases and primary brain tumors [272, 274].

Some studies have found that analysis of ADC of peritumoral "edema" can be helpful for distinguishing different tumor types. For the sake of simplicity, we use the term edema, although we prefer the designation "T2/FLAIR hyperintensity" given the well-known fact that what is called "peritumoral edema" typically has a significant component of neoplastic cells in cases of primary brain neoplasms. In one study, diffusivity was higher in peritumoral "edema" associated with primary neoplasms and metastases compared to normal white matter, but the ADC tended to be lower in areas of T2/FLAIR hyperintensity associated with high-grade astrocytomas compared to metastases [275]. Some, but not all, studies have also found that ADC values are higher in peritumoral "edema" associated with low-grade compared to high-grade gliomas [269, 271, 275]. However, there is overlap in ADC values and diffusion changes in isolation cannot reliably distinguish between peritumoral "edema" associated with high-grade and low-grade primary tumors or metastases.

DWI has also been used to evaluate tumor response to therapy. In both animal studies and humans, an increase in tumor ADC tends to correlate with response to therapy in primary and metastatic CNS neoplasms and a reduction in ADC may be seen with tumor recurrence [266, 276–283]. In addition, changes in ADC may precede the changes in lesion volume on conventional sequences and may provide an early indicator of tumor response to therapy. Image acquisition at higher *b*-values has also been shown to increase sensitivity for detection of diffusion changes following treatment [278]. With continued research and development of more sophisticated computer-aided methods of analysis, DWI has the potential to emerge as an important adjunctive sequence and early biomarker for evaluation of tumor response to therapy [280–282, 284].

In addition to assessing response to therapy, some studies suggest that DWI may be useful for distinguishing tumor recurrence from radiation necrosis and other treatment-related changes. In one retrospective analysis of high-grade gliomas treated with radiation with or without chemotherapy, the mean ADC value of enhancing regions and their ADC ratio compared to normal contralateral white matter was lower in recurrent/progressive tumors compared to the treatment-related change group [283], and other investigators have reported similar observations [285, 286]. However, similar to studies using ADC values for distinguishing

high-grade from low-grade tumors, there is substantial overlap in the ADC values of tumor recurrence and treatment-related change and there are reports of decreased diffusion in pathologically proven radiation necrosis [287, 288]. Even though DWI alone is frequently not sufficient for distinguishing between the two, analysis of ADC changes is helpful when used in combination with other parameters such as perfusion characteristics and MR spectroscopy [285, 287]. A discussion of MR perfusion and spectroscopy is beyond the scope of this chapter but can be found elsewhere in this book.

DWI can also be useful in the evaluation of patients treated with antiangiogenic therapy. In a recent study of patients with high-grade gliomas treated with bevacizumab alone or in combination with other chemotherapeutic agents, the authors found that patients with progressive tumor had a decline in the ADC values of the enhancing as well as non-enhancing components [289]. In this study, there was no significant change in the ADC values of tumors that did not progress, although there was a trend toward increased ADC on follow-up in this group.

DTI is also being investigated for evaluation of radiation change within normal brain parenchyma. Interestingly, there are some contradictory results compared to those with conventional DWI as some have reported an increase in the ADC of the contrast-enhancing component in patients with tumor recurrence [290, 291]. This requires further investigation but may at least in part be related to differences in study design and time from treatment, given that in one DTI study the interval from treatment was much longer, ranging from many months to years after completion of therapy [290].

Lymphoma

CNS lymphoma is typically isointense to hypointense on T1- and T2-weighted images, enhances homogeneously and has homogeneously restricted diffusion due to relatively dense cell packing [230, 292, 293] (Fig. 2.30). This diffusion pattern is unusual for other primary and secondary CNS neoplasms and can be used to suggest the diagnosis. In immunocompromised patients, the diminished diffusion within lymphoma can be helpful for distinction from toxoplasmosis, which tends to have more variable ADC, although some studies have found significant overlap in the DWI appearance of lymphoma and toxoplasmosis [229–231]. DWI may also be important in predicting outcome. Lower pretreatment ADC values within the

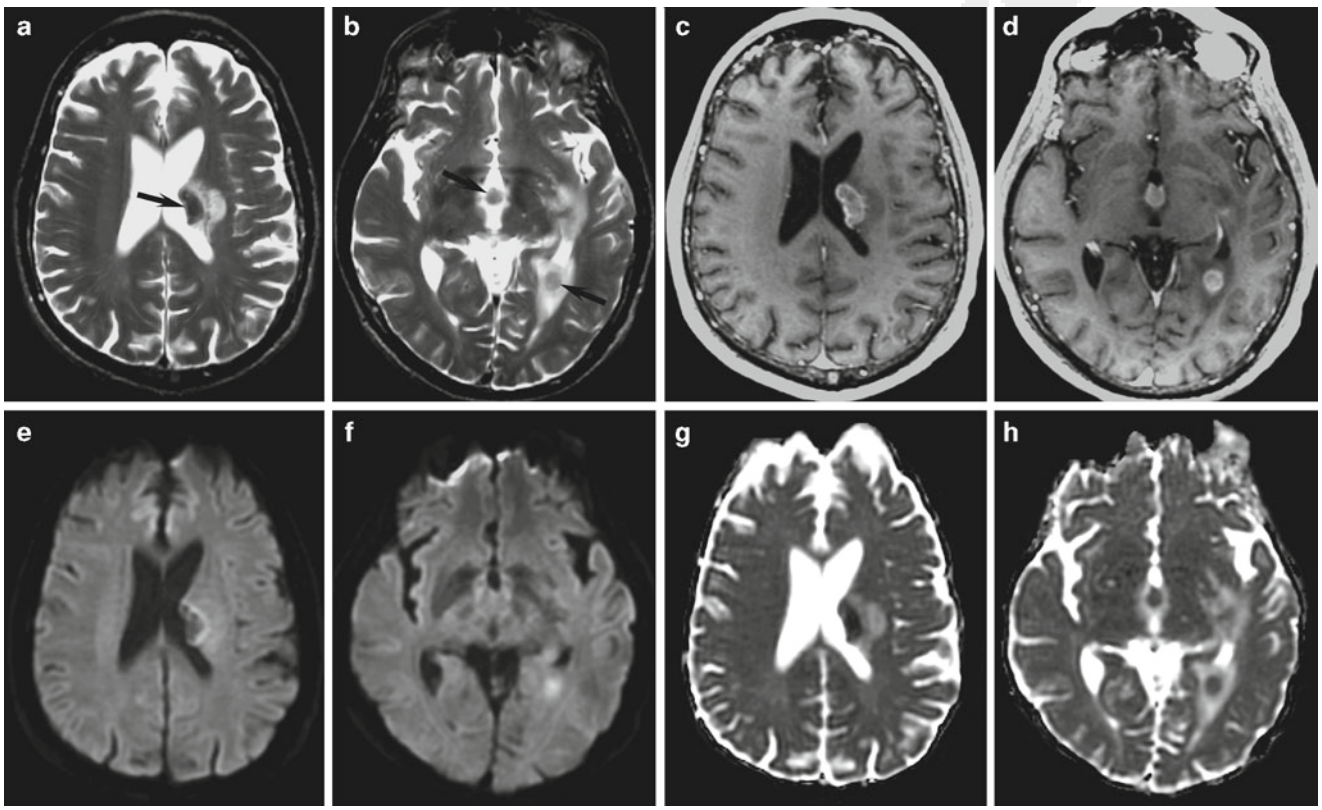

Fig. 2.30 Lymphoma. (**a**, **b**) Axial T2 and (**c**, **d**) postcontrast T1-weighted images demonstrate multiple subependymal enhancing lesions that have relatively low signal on T2 (*arrows* in (**a**) and (**b**)). (**e**, **f**) On DWI, the lesions are heterogenous but partially bright. (**g**, **h**) On ADC, the lesions are hypointense consistent with restricted diffusion secondary to increased cellularity. The more superiorly located lesion had an average ADC value of approximately 600×10^{-6} mm^2/s, whereas the two other lesions have average ADC values ranging between 800 and 850×10^{-6} mm^2/s – all in the expected range for lymphoma

enhancing portion of primary CNS lymphoma have been shown to be associated with shorter disease-free and overall survival [294].

Extra-Axial Masses

The role of DWI in distinction of epidermoid tumors from extra-axial cystic lesions, such as arachnoid cysts, is well established. Both arachnoid cysts and epidermoids have signal characteristics similar to CSF and are indistinguishable on T1- and T2-weighted sequences, although epidermoid cysts do have elevated signal compared to surrounding CSF on FLAIR images. On DWI, arachnoid cysts have diffusion characteristics similar to CSF (markedly hyperintense to brain parenchyma on ADC and hypointense on DWI images), while epidermoids are markedly hypointense to CSF and isointense to brain parenchyma on ADC maps and are markedly hyperintense to CSF and brain parenchyma on DWI images due to T2 components and diffusion characteristics similar to that of normal brain parenchyma [223, 295, 296] (Fig. 2.31).

A number of investigations have also evaluated the use of DWI for differentiation of malignant and atypical meningiomas from benign meningiomas [297–299]. In a recent retrospective study of 25 atypical/malignant and 23 benign meningiomas, the former were found to have significantly lower absolute and normalized ADC values compared to benign meningiomas [298]. Absolute ADC and normalized ADC thresholds of 800×10^{-6} mm^2/s and 0.99, respectively, were found to have high sensitivity and specificity for distinguishing the two, but require validation in larger multicenter studies.

Traumatic Brain Injury

DWI is complementary to conventional MR sequences such as T2/FLAIR and T2* for identification of diffuse axonal injury (DAI) in acute closed-head injury [300, 301] (Fig. 2.32,

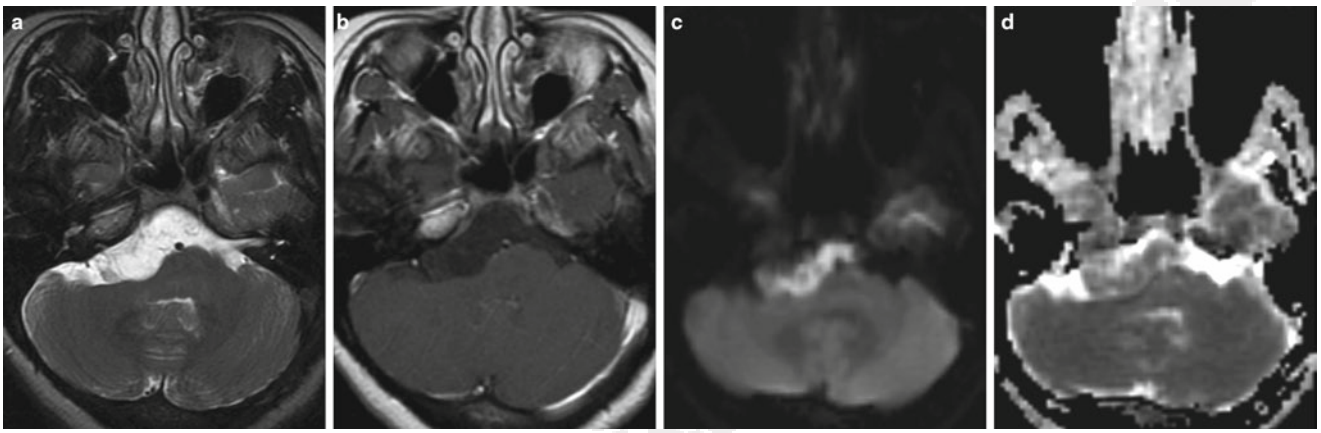

Fig. 2.31 Epidermoid tumor. (**a**) Axial T2, (**b**) contrast-enhanced T1, (**c**) DWI, and (**d**) ADC images demonstrate an insinuating nonenhancing extraaxial lesion anterior to the lower pons and right middle cerebellar peduncle that has signal characteristics similar to CSF on T1- and T2-weighted sequences, but is markedly hyperintense to CSF on DWI images and hypointense to CSF on the ADC map. The lesion has diffusion similar to that of normal brain parenchyma but is hyperintense to brain parenchyma on the DWI images due to the combined diffusion and T2 effects. These findings are essentially pathognomonic for an epidermoid tumor

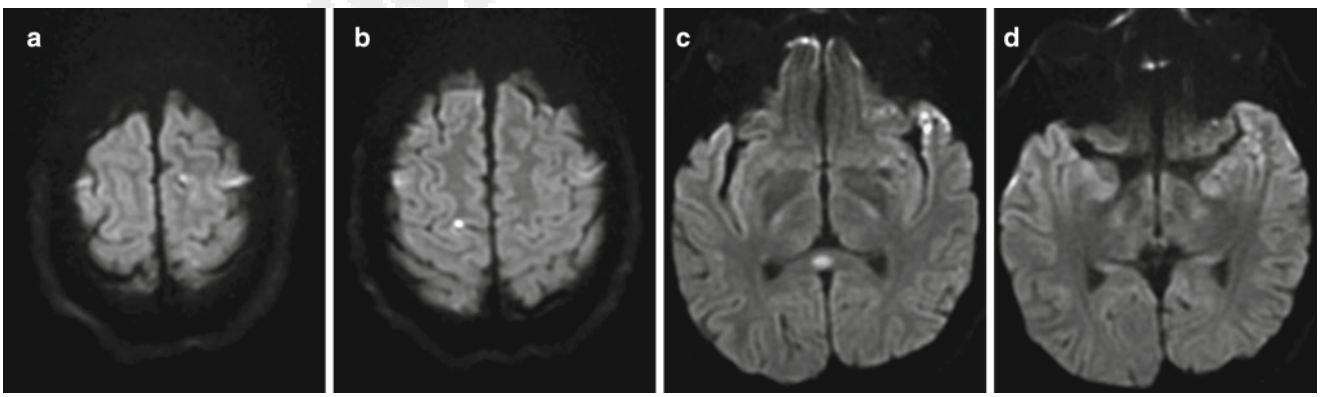

Fig. 2.32 Traumatic brain/shear injury. (**a**–**d**) Axial DWI images demonstrate punctate DWI hyperintense foci at frontal gray white matter junctions bilaterally as well as a lesion in the splenium of corpus callosum in this patient who was evaluated following a closed head injury

Table 2.15). In DAI, the majority of nonhemorrhagic lesions have restricted diffusion, perhaps secondary to ischemia and/or the formation of axonal retraction balls, with a small percentage being isointense or hyperintense on the ADC map, perhaps secondary to increased tissue water [300]. DWI is complementary to other MR sequences because it identifies nonhemorrhagic lesions not visible on T2* images and demonstrates nonhemorrhagic lesions with restricted diffusion better than FLAIR images because of increased lesion contrast [300]. The anatomic distribution of DWI

Table 2.15 DWI for evaluation of acute closed head injury

DWI is complementary to T2* and FLAIR images for evaluation of diffuse axonal injury and can identify additional lesions not detectable on these sequences
The majority of nonhemorrhagic lesions have restricted diffusion, secondary to ischemia and/or the formation of axonal retraction balls. A small percentage is isointense or hyperintense on the ADC map, probably secondary to increased tissue water
In one study, the volume of lesions identified on DWI had a better correlation with the modified Rankin Scale at discharge than volume of lesions on FLAIR, T2, T2* or all images, including DWI, combined
Higher ADC values in normal appearing brain parenchyma are associated with a poor clinical outcome

Table 2.16 Selected articles on diffusion imaging of the brain

Authors	Title	Subjects	Overview
Baird et al. 1997 [60]	Enlargement of human cerebral ischemic lesion volumes measured by diffusion-weighted magnetic resonance imaging. Ann Neurol 1997;41:581–9	Infarcts	Study of progression of infarcts on DWI and perfusion imaging in the absence of thromboytic therapy
Schwamm et al. 1998 [42]	Time course of lesion development in patients with acute stroke: serial diffusion- and hemodynamic-weighted magnetic resonance imaging. Stroke 1998;29:2268–76	Patients with acute stroke	Study of evolution of acute ischemic stroke and appearance of infarcts on DWI at different timepoints
Schaefer et al. 2000 [304]	Diffusion-weighted MR imaging of the brain. Radiology 2000;217:331–45	Ischemic and nonischemic brain disorders	Classic review article summarizing the principles and applications of DWI for imaging of ischemic and nonischemic brain disorders
Fiebach et al. 2002 [43]	Serial analysis of the apparent diffusion coefficient time course in human stroke. Neuroradiology 2002;44:294–8	Stroke	Analysis of the appearance of ischemic infarcts on DWI at different stages
Mullins et al. 2002 [34]	CT and conventional and diffusion-weighted MR imaging in acute stroke: study in 691 patients at presentation to the emergency department. Radiology 2002;224:353–60	691 acute stroke patients	Study comparing the diagnostic accuracy of CT, conventional MRI (without DWI), and MRI with DWI for the diagnosis of an acute ischemic stroke
Al-Okaili et al. 2006 [264]	Advanced MR imaging techniques in the diagnosis of intraaxial brain tumors in adults. Radiographics 2006;26 Suppl 1:S173–89	Intra-axial brain tumors	Review of advanced MR techniques, including DWI, for characterization of brain masses
Chalela et al. 2007 [30]	Magnetic resonance imaging and computed tomography in emergency assessment of patients with suspected acute stroke: a prospective comparison. Lancet 2007;369:293–8	Patients with suspected acute stroke	A prospective comparison of MRI (with DWI and susceptibility-sensitive images) with CT for the diagnosis of an acute stroke
Easton et al. 2009 [101]	Definition and evaluation of transient ischemic attack: a scientific statement for healthcare professionals from the American Heart Association/American Stroke Association Stroke Council; Council on Cardiovascular Surgery and Anesthesia; Council on Cardiovascular Radiology and Intervention; Council on Cardiovascular Nursing; and the Interdisciplinary Council on Peripheral Vascular Disease. The American Academy of Neurology affirms the value of this statement as an educational tool for neurologists. Stroke 2009;40:2276–93	Transient ischemic attack	Scientific statement reviewing and revising the definition of a transient ischemic attack
Olivot et al. 2009 [67]	Relationships between cerebral perfusion and reversibility of acute diffusion lesions in DEFUSE: insights from RADAR. Stroke 2009;40:1692–7	DEFUSE trial participants	Analysis of reversibility of DWI positive lesions based on perfusion status and recanalization in patients from the DEFUSE trial treated with IV thrombolysis
Yoo et al. 2010 [99]	Combining acute DWI and MTT lesion volumes with NIHSS score improves the prediction of acute stroke outcome. Stroke 2010;41(8):1728–35.	Acute DWI and MTT lesions	An evaluation of the use of DWI and mean transit time in conjunction with NIHSS for prediction of stroke outcome

positive shear lesions is similar to that seen on conventional sequences, most commonly affecting the corticomedullary junction, followed by central white matter and the junction of the midbrain and pons. In one study, the volume of lesions identified on DWI had a better correlation with the modified Rankin scale (mRS) at discharge than volume of lesions on FLAIR, T2, T2* or all images, including DWI, combined [302]. In another study, ADC maps were used to detect DAI lesions not visible on other sequences [303]. In this study, ADC values in normal-appearing brain parenchyma were shown to be predictive of outcome with significantly higher mean deep gray and white matter ADC values in patients with unfavorable outcomes, defined as Glasgow Outcome Scale scores 1–3, compared to those with favorable outcomes and controls.

Conclusion: Future Applications of Diffusion Imaging in the Brain

Over the past 10 years, DWI has become a standard sequence for MR evaluation of ischemic and nonischemic central nervous system (CNS) lesions (see Table 2.16 for a summary of some important diffusion studies). Currently, DWI is the gold standard for evaluation of acute ischemic infarction and provides the best estimate of the infarct core. In addition, DWI is an important adjunctive sequence for characterization of a wide range of infectious, inflammatory, neoplastic, and traumatic brain lesions. DWI and ADC maps are increasingly used in clinical research for quantification of the irreversible infarct core, prediction of infarct complications such as hemorrhagic transformation, and evaluation of pseudoprogression and other treatment-related changes in tumor imaging. Although currently in the research phase, these parameters are likely to be implemented in the clinical arena in the near future. In the future, computer-assisted analysis may be used for subsite analysis of DWI, perfusion images, and MR spectroscopy as part of complex algorithms for patient stratification and prognostication in stroke imaging and to distinguish treatment-related changes from tumor progression in the evaluation of CNS astrocytomas. These provide exciting opportunities for additional research and the potential to further expand the role of DWI in diagnostic imaging of brain disorders in the next decade.

References

1. Stejskal EO, Tanner JE. Spin diffusion measurements: spin echoes in the presence of a time-dependent field gradient. J Chem Phys. 1965;42:288–92.
2. James TL, McDonald GG. Measurement of the self-diffusion coefficient of each component in a complex system using pulsed-gradient fourier transform NMR. J Magn Reson. 1973;11:58–61.
3. Le Bihan D, Breton E, Lallemand D, Grenier P, Cabanis E, Laval-Jeantet M. MR imaging of intravoxel incoherent motions: application to diffusion and perfusion in neurologic disorders. Radiology. 1986;161:401–7.
4. Thomsen C, Henriksen O, Ring P. In vivo measurement of water self diffusion in the human brain by magnetic resonance imaging. Acta Radiol. 1987;28:353–61.
5. Le Bihan D, Breton E, Lallemand D, Aubin ML, Vignaud J, Laval-Jeantet M. Separation of diffusion and perfusion in intravoxel incoherent motion MR imaging. Radiology. 1988;168:497–505.
6. Brooks DJ, Luthert P, Gadian D, Marsden CD. Does signal-attenuation on high-field T2-weighted MRI of the brain reflect regional cerebral iron deposition? Observations on the relationship between regional cerebral water proton T2 values and iron levels. J Neurol Neurosurg Psychiatry. 1989;52:108–11.
7. Merboldt KD, Bruhn H, Frahm J, Gyngell ML, Hanicke W, Deimling M. MRI of "diffusion" in the human brain: new results using a modified CE-FAST sequence. Magn Reson Med. 1989;9:423–9.
8. Moseley ME, Cohen Y, Mintorovitch J, et al. Early detection of regional cerebral ischemia in cats: comparison of diffusion- and T2-weighted MRI and spectroscopy. Magn Reson Med. 1990;14:330–46.
9. Doran M, Hajnal JV, Van Bruggen N, King MD, Young IR, Bydder GM. Normal and abnormal white matter tracts shown by MR imaging using directional diffusion weighted sequences. J Comput Assist Tomogr. 1990;14:865–73.
10. Sevick RJ, Kucharczyk J, Mintorovitch J, Moseley ME, Derugin N, Norman D. Diffusion-weighted MR imaging and T2-weighted MR imaging in acute cerebral ischaemia: comparison and correlation with histopathology. Acta Neurochir Suppl (Wien). 1990;51:210–2.
11. Moseley ME, Cohen Y, Kucharczyk J, et al. Diffusion-weighted MR imaging of anisotropic water diffusion in cat central nervous system. Radiology. 1990;176:439–45.
12. Moseley ME, Kucharczyk J, Mintorovitch J, et al. Diffusion-weighted MR imaging of acute stroke: correlation with T2-weighted and magnetic susceptibility-enhanced MR imaging in cats. AJNR Am J Neuroradiol. 1990;11:423–9.
13. Tsuruda JS, Chew WM, Moseley ME, Norman D. Diffusion-weighted MR imaging of the brain: value of differentiating between extraaxial cysts and epidermoid tumors. AJNR Am J Neuroradiol. 1990;11:925–31. discussion 932–924.
14. Merboldt KD, Hanicke W, Gyngell ML, Frahm J, Bruhn H. The influence of flow and motion in MRI of diffusion using a modified CE-FAST sequence. Magn Reson Med. 1989;12:198–208.
15. Goodman JA, Kroenke CD, Bretthorst GL, Ackerman JJ, Neil JJ. Sodium ion apparent diffusion coefficient in living rat brain. Magn Reson Med. 2005;53:1040–5.
16. Mintorovitch J, Yang GY, Shimizu H, Kucharczyk J, Chan PH, Weinstein PR. Diffusion-weighted magnetic resonance imaging of acute focal cerebral ischemia: comparison of signal intensity with changes in brain water and Na+, K(+)-ATPase activity. J Cereb Blood Flow Metab. 1994;14:332–6.
17. Benveniste H, Hedlund LW, Johnson GA. Mechanism of detection of acute cerebral ischemia in rats by diffusion-weighted magnetic resonance microscopy. Stroke. 1992;23:746–54.
18. Veldhuis WB, van der Stelt M, Delmas F, et al. In vivo excitotoxicity induced by ouabain, a Na+/K+−ATPase inhibitor. J Cereb Blood Flow Metab. 2003;23:62–74.
19. Sevick RJ, Kanda F, Mintorovitch J, et al. Cytotoxic brain edema: assessment with diffusion-weighted MR imaging. Radiology. 1992;185:687–90.
20. Duong TQ, Ackerman JJ, Ying HS, Neil JJ. Evaluation of extra- and intracellular apparent diffusion in normal and globally ischemic rat brain via 19 F NMR. Magn Reson Med. 1998;40:1–13.

21. Babsky AM, Topper S, Zhang H, et al. Evaluation of extra- and intracellular apparent diffusion coefficient of sodium in rat skeletal muscle: effects of prolonged ischemia. Magn Reson Med. 2008;59:485–91.
22. Qiao M, Malisza KL, Del Bigio MR, Tuor UI. Transient hypoxia-ischemia in rats: changes in diffusion-sensitive MR imaging findings, extracellular space, and Na^+-K^+-adenosine triphosphatase and cytochrome oxidase activity. Radiology. 2002;223:65–75.
23. Anderson AW, Zhong J, Petroff OA, et al. Effects of osmotically driven cell volume changes on diffusion-weighted imaging of the rat optic nerve. Magn Reson Med. 1996;35:162–7.
24. van der Toorn A, Sykova E, Dijkhuizen RM, et al. Dynamic changes in water ADC, energy metabolism, extracellular space volume, and tortuosity in neonatal rat brain during global ischemia. Magn Reson Med. 1996;36:52–60.
25. van der Toorn A, Dijkhuizen RM, Tulleken CA, Nicolay K. Diffusion of metabolites in normal and ischemic rat brain measured by localized 1H MRS. Magn Reson Med. 1996;36:914–22.
26. Neil JJ, Duong TQ, Ackerman JJ. Evaluation of intracellular diffusion in normal and globally-ischemic rat brain via 133Cs NMR. Magn Reson Med. 1996;35:329–35.
27. Mastro AM, Babich MA, Taylor WD, Keith AD. Diffusion of a small molecule in the cytoplasm of mammalian cells. Proc Natl Acad Sci USA. 1984;81:3414–8.
28. Wojcieszyn JW, Schlegel RA, Wu ES, Jacobson KA. Diffusion of injected macromolecules within the cytoplasm of living cells. Proc Natl Acad Sci USA. 1981;78:4407–10.
29. Szafer A, Zhong J, Gore JC. Theoretical model for water diffusion in tissues. Magn Reson Med. 1995;33:697–712.
30. Chalela JA, Kidwell CS, Nentwich LM, et al. Magnetic resonance imaging and computed tomography in emergency assessment of patients with suspected acute stroke: a prospective comparison. Lancet. 2007;369:293–8.
31. Gonzalez RG, Schaefer PW, Buonanno FS, et al. Diffusion-weighted MR imaging: diagnostic accuracy in patients imaged within 6 hours of stroke symptom onset. Radiology. 1999;210:155–62.
32. Saur D, Kucinski T, Grzyska U, et al. Sensitivity and interrater agreement of CT and diffusion-weighted MR imaging in hyperacute stroke. AJNR Am J Neuroradiol. 2003;24:878–85.
33. Urbach H, Flacke S, Keller E, et al. Detectability and detection rate of acute cerebral hemisphere infarcts on CT and diffusion-weighted MRI. Neuroradiology. 2000;42:722–7.
34. Mullins ME, Schaefer PW, Sorensen AG, et al. CT and conventional and diffusion-weighted MR imaging in acute stroke: study in 691 patients at presentation to the emergency department. Radiology. 2002;224:353–60.
35. Hjort N, Christensen S, Solling C, et al. Ischemic injury detected by diffusion imaging 11 minutes after stroke. Ann Neurol. 2005;58:462–5.
36. Engelter ST, Wetzel SG, Radue EW, Rausch M, Steck AJ, Lyrer PA. The clinical significance of diffusion-weighted MR imaging in infratentorial strokes. Neurology. 2004;62:574–80.
37. Lutsep HL, Albers GW, DeCrespigny A, Kamat GN, Marks MP, Moseley ME. Clinical utility of diffusion-weighted magnetic resonance imaging in the assessment of ischemic stroke. Ann Neurol. 1997;41:574–80.
38. Welch KM, Windham J, Knight RA, et al. A model to predict the histopathology of human stroke using diffusion and T2-weighted magnetic resonance imaging. Stroke. 1995;26:1983–9.
39. Knight RA, Dereski MO, Helpern JA, Ordidge RJ, Chopp M. Magnetic resonance imaging assessment of evolving focal cerebral ischemia. Comparison with histopathology in rats. Stroke. 1994;25:1252–61. discussion 1261–1252.
40. Schlaug G, Siewert B, Benfield A, Edelman RR, Warach S. Time course of the apparent diffusion coefficient (ADC) abnormality in human stroke. Neurology. 1997;49:113–9.
41. Warach S, Chien D, Li W, Ronthal M, Edelman RR. Fast magnetic resonance diffusion-weighted imaging of acute human stroke. Neurology. 1992;42:1717–23.
42. Schwamm LH, Koroshetz WJ, Sorensen AG, et al. Time course of lesion development in patients with acute stroke: serial diffusion- and hemodynamic-weighted magnetic resonance imaging. Stroke. 1998;29:2268–76.
43. Fiebach JB, Jansen O, Schellinger PD, Heiland S, Hacke W, Sartor K. Serial analysis of the apparent diffusion coefficient time course in human stroke. Neuroradiology. 2002;44:294–8.
44. Warach S, Gaa J, Siewert B, Wielopolski P, Edelman RR. Acute human stroke studied by whole brain echo planar diffusion-weighted magnetic resonance imaging. Ann Neurol. 1995;37:231–41.
45. Copen WA, Schwamm LH, Gonzalez RG, et al. Ischemic stroke: effects of etiology and patient age on the time course of the core apparent diffusion coefficient. Radiology. 2001;221:27–34.
46. Kuker W, Weise J, Krapf H, Schmidt F, Friese S, Bahr M. MRI characteristics of acute and subacute brainstem and thalamic infarctions: value of T2- and diffusion-weighted sequences. J Neurol. 2002;249:33–42.
47. Oppenheim C, Stanescu R, Dormont D, et al. False-negative diffusion-weighted MR findings in acute ischemic stroke. AJNR Am J Neuroradiol. 2000;21:1434–40.
48. Ay H, Buonanno FS, Rordorf G, et al. Normal diffusion-weighted MRI during stroke-like deficits. Neurology. 1999;52:1784–92.
49. Narisawa A, Shamoto H, Shimizu H, Tominaga T, Yoshimoto T. Diffusion-weighted magnetic resonance imaging (MRI) in acute brain stem infarction. No To Shinkei. 2001;53:1021–6.
50. Etgen T, Grafin von Einsiedel H, Rottinger M, Winbeck K, Conrad B, Sander D. Detection of acute brainstem infarction by using DWI/MRI. Eur Neurol. 2004;52:145–50.
51. Fitzek S, Fitzek C, Urban PP, Marx J, Hopf HC, Stoeter P. Time course of lesion development in patients with acute brain stem infarction and correlation with NIHSS score. Eur J Radiol. 2001;39:180–5.
52. Linfante I, Llinas RH, Schlaug G, Chaves C, Warach S, Caplan LR. Diffusion-weighted imaging and National Institutes of Health Stroke Scale in the acute phase of posterior-circulation stroke. Arch Neurol. 2001;58:621–8.
53. Toi H, Uno M, Harada M, et al. Diagnosis of acute brain-stem infarcts using diffusion-weighed MRI. Neuroradiology. 2003;45:352–6.
54. Burdette JH, Elster AD. Diffusion-weighted imaging of cerebral infarctions: are higher B values better? J Comput Assist Tomogr. 2002;26:622–7.
55. Cihangiroglu M, Citci B, Kilickesmez O, et al. The utility of high b-value DWI in evaluation of ischemic stroke at 3T. Eur J Radiol. 2011;78:75–81.
56. Kim HJ, Choi CG, Lee DH, Lee JH, Kim SJ, Suh DC. High-b-value diffusion-weighted MR imaging of hyperacute ischemic stroke at 1.5T. AJNR Am J Neuroradiol. 2005;26:208–15.
57. Meyer JR, Gutierrez A, Mock B, et al. High-b-value diffusion-weighted MR imaging of suspected brain infarction. AJNR Am J Neuroradiol. 2000;21:1821–9.
58. Bertrand A, Oppenheim C, Lamy C, et al. Comparison of optimized and standard diffusion-weighted imaging at 1.5T for the detection of acute lesions in patients with transient ischemic attack. AJNR Am J Neuroradiol. 2008;29:363–5.
59. Kuhl CK, Textor J, Gieseke J, et al. Acute and subacute ischemic stroke at high-field-strength (3.0-T) diffusion-weighted MR imaging: intraindividual comparative study. Radiology. 2005;234:509–16.
60. Baird AE, Benfield A, Schlaug G, et al. Enlargement of human cerebral ischemic lesion volumes measured by diffusion-weighted magnetic resonance imaging. Ann Neurol. 1997;41:581–9.

61. van Everdingen KJ, van der Grond J, Kappelle LJ, Ramos LM, Mali WP. Diffusion-weighted magnetic resonance imaging in acute stroke. Stroke. 1998;29:1783–90.
62. Tong DC, Yenari MA, Albers GW, O'Brien M, Marks MP, Moseley ME. Correlation of perfusion- and diffusion-weighted MRI with NIHSS score in acute (<6.5 hour) ischemic stroke. Neurology. 1998;50:864–70.
63. Kidwell CS, Saver JL, Mattiello J, et al. Thrombolytic reversal of acute human cerebral ischemic injury shown by diffusion/perfusion magnetic resonance imaging. Ann Neurol. 2000;47:462–9.
64. Kidwell CS, Saver JL, Starkman S, et al. Late secondary ischemic injury in patients receiving intraarterial thrombolysis. Ann Neurol. 2002;52:698–703.
65. Schaefer PW, Hassankhani A, Putman C, et al. Characterization and evolution of diffusion MR imaging abnormalities in stroke patients undergoing intra-arterial thrombolysis. AJNR Am J Neuroradiol. 2004;25:951–7.
66. Miyasaka N, Nagaoka T, Kuroiwa T, et al. Histopathologic correlates of temporal diffusion changes in a rat model of cerebral hypoxia/ischemia. AJNR Am J Neuroradiol. 2000;21:60–6.
67. Olivot JM, Mlynash M, Thijs VN, et al. Relationships between cerebral perfusion and reversibility of acute diffusion lesions in DEFUSE: insights from RADAR. Stroke. 2009;40:1692–7.
68. Schaefer PW, Ozsunar Y, He J, et al. Assessing tissue viability with MR diffusion and perfusion imaging. AJNR Am J Neuroradiol. 2003;24:436–43.
69. Fiehler J, Knab R, Reichenbach JR, Fitzek C, Weiller C, Rother J. Apparent diffusion coefficient decreases and magnetic resonance imaging perfusion parameters are associated in ischemic tissue of acute stroke patients. J Cereb Blood Flow Metab. 2001;21:577–84.
70. Schlaug G, Benfield A, Baird AE, et al. The ischemic penumbra: operationally defined by diffusion and perfusion MRI. Neurology. 1999;53:1528–37.
71. Rohl L, Ostergaard L, Simonsen CZ, et al. Viability thresholds of ischemic penumbra of hyperacute stroke defined by perfusion-weighted MRI and apparent diffusion coefficient. Stroke. 2001;32:1140–6.
72. Gonen KA, Simsek MM. Diffusion weighted imaging and estimation of prognosis using apparent diffusion coefficient measurements in ischemic stroke. Eur J Radiol. 2010;76:157–61.
73. Fiehler J, Foth M, Kucinski T, et al. Severe ADC decreases do not predict irreversible tissue damage in humans. Stroke. 2002;33:79–86.
74. Jones TH, Morawetz RB, Crowell RM, et al. Thresholds of focal cerebral ischemia in awake monkeys. J Neurosurg. 1981;54:773–82.
75. Calandre L, Ortega JF, Bermejo F. Anticoagulation and hemorrhagic infarction in cerebral embolism secondary to rheumatic heart disease. Arch Neurol. 1984;41:1152–4.
76. Hakim AM, Ryder-Cooke A, Melanson D. Sequential computerized tomographic appearance of strokes. Stroke. 1983;14:893–7.
77. Hornig CR, Dorndorf W, Agnoli AL. Hemorrhagic cerebral infarction – a prospective study. Stroke. 1986;17:179–85.
78. Horowitz SH, Zito JL, Donnarumma R, Patel M, Alvir J. Computed tomographic-angiographic findings within the first five hours of cerebral infarction. Stroke. 1991;22:1245–53.
79. Furlan A, Higashida R, Wechsler L, et al. Intra-arterial prourokinase for acute ischemic stroke. The PROACT II study: a randomized controlled trial. Prolyse in Acute Cerebral Thromboembolism. JAMA. 1999;282:2003–11.
80. Hacke W, Kaste M, Bluhmki E, et al. Thrombolysis with alteplase 3 to 4.5 hours after acute ischemic stroke. N Engl J Med. 2008;359:1317–29.
81. Intracerebral hemorrhage after intravenous t-PA therapy for ischemic stroke. The NINDS t-PA Stroke Study Group. Stroke. 1997;28:2109–18.
82. Kim EY, Na DG, Kim SS, Lee KH, Ryoo JW, Kim HK. Prediction of hemorrhagic transformation in acute ischemic stroke: role of diffusion-weighted imaging and early parenchymal enhancement. AJNR Am J Neuroradiol. 2005;26:1050–5.
83. Derex L, Hermier M, Adeleine P, et al. Clinical and imaging predictors of intracerebral haemorrhage in stroke patients treated with intravenous tissue plasminogen activator. J Neurol Neurosurg Psychiatry. 2005;76:70–5.
84. Tong DC, Adami A, Moseley ME, Marks MP. Prediction of hemorrhagic transformation following acute stroke: role of diffusion- and perfusion-weighted magnetic resonance imaging. Arch Neurol. 2001;58:587–93.
85. Selim M, Fink JN, Kumar S, et al. Predictors of hemorrhagic transformation after intravenous recombinant tissue plasminogen activator: prognostic value of the initial apparent diffusion coefficient and diffusion-weighted lesion volume. Stroke. 2002;33:2047–52.
86. Oppenheim C, Samson Y, Dormont D, et al. DWI prediction of symptomatic hemorrhagic transformation in acute MCA infarct. J Neuroradiol. 2002;29:6–13.
87. Singer OC, Humpich MC, Fiehler J, et al. Risk for symptomatic intracerebral hemorrhage after thrombolysis assessed by diffusion-weighted magnetic resonance imaging. Ann Neurol. 2008;63:52–60.
88. Campbell BC, Christensen S, Butcher KS, et al. Regional very low cerebral blood volume predicts hemorrhagic transformation better than diffusion-weighted imaging volume and thresholded apparent diffusion coefficient in acute ischemic stroke. Stroke. 2010;41:82–8.
89. Kim JH, Bang OY, Liebeskind DS, et al. Impact of baseline tissue status (diffusion-weighted imaging lesion) versus perfusion status (severity of hypoperfusion) on hemorrhagic transformation. Stroke. 2010;41:e135–42.
90. Kassner A, Roberts T, Taylor K, Silver F, Mikulis D. Prediction of hemorrhage in acute ischemic stroke using permeability MR imaging. AJNR Am J Neuroradiol. 2005;26:2213–7.
91. Hjort N, Wu O, Ashkanian M, et al. MRI detection of early blood-brain barrier disruption: parenchymal enhancement predicts focal hemorrhagic transformation after thrombolysis. Stroke. 2008;39:1025–8.
92. Adams Jr HP, del Zoppo G, Alberts MJ, et al. Guidelines for the early management of adults with ischemic stroke: a guideline from the American Heart Association/American Stroke Association Stroke Council, Clinical Cardiology Council, Cardiovascular Radiology and Intervention Council, and the Atherosclerotic Peripheral Vascular Disease and Quality of Care Outcomes in Research Interdisciplinary Working Groups: the American Academy of Neurology affirms the value of this guideline as an educational tool for neurologists. Stroke. 2007;38:1655–711.
93. Lovblad KO, Baird AE, Schlaug G, et al. Ischemic lesion volumes in acute stroke by diffusion-weighted magnetic resonance imaging correlate with clinical outcome. Ann Neurol. 1997;42:164–70.
94. Nighoghossian N, Hermier M, Adeleine P, et al. Baseline magnetic resonance imaging parameters and stroke outcome in patients treated by intravenous tissue plasminogen activator. Stroke. 2003;34:458–63.
95. Engelter ST, Provenzale JM, Petrella JR, DeLong DM, Alberts MJ. Infarct volume on apparent diffusion coefficient maps correlates with length of stay and outcome after middle cerebral artery stroke. Cerebrovasc Dis. 2003;15:188–91.
96. Derex L, Nighoghossian N, Hermier M, et al. Influence of pretreatment MRI parameters on clinical outcome, recanalization and infarct size in 49 stroke patients treated by intravenous tissue plasminogen activator. J Neurol Sci. 2004;225:3–9.
97. Sanak D, Nosal V, Horak D, et al. Impact of diffusion-weighted MRI-measured initial cerebral infarction volume on clinical outcome in acute stroke patients with middle cerebral artery occlusion treated by thrombolysis. Neuroradiology. 2006;48:632–9.

98. Parsons MW, Christensen S, McElduff P, et al. Pretreatment diffusion- and perfusion-MR lesion volumes have a crucial influence on clinical response to stroke thrombolysis. J Cereb Blood Flow Metab. 2010;30(6):1214–25.
99. Yoo AJ, Barak ER, Copen WA, et al. Combining acute DWI and MTT lesion volumes with NIHSS score improves the prediction of acute stroke outcome. Stroke. 2010;41(8):1728–35.
100. Yoo AJ, Verduzco LA, Schaefer PW, Hirsch JA, Rabinov JD, Gonzalez RG. MRI-based selection for intra-arterial stroke therapy: value of pretreatment diffusion-weighted imaging lesion volume in selecting patients with acute stroke who will benefit from early recanalization. Stroke. 2009;40:2046–54.
101. Easton JD, Saver JL, Albers GW, et al. Definition and evaluation of transient ischemic attack: a scientific statement for healthcare professionals from the American Heart Association/American Stroke Association Stroke Council; Council on Cardiovascular Surgery and Anesthesia; Council on Cardiovascular Radiology and Intervention; Council on Cardiovascular Nursing; and the Interdisciplinary Council on Peripheral Vascular Disease. The American Academy of Neurology affirms the value of this statement as an educational tool for neurologists. Stroke. 2009;40:2276–93.
102. Albers GW, Caplan LR, Easton JD, et al. Transient ischemic attack – proposal for a new definition. N Engl J Med. 2002;347:1713–6.
103. Ay H, Oliveira-Filho J, Buonanno FS, et al. 'Footprints' of transient ischemic attacks: a diffusion-weighted MRI study. Cerebrovasc Dis. 2002;14:177–86.
104. Kidwell CS, Alger JR, Di Salle F, et al. Diffusion MRI in patients with transient ischemic attacks. Stroke. 1999;30:1174–80.
105. Crisostomo RA, Garcia MM, Tong DC. Detection of diffusion-weighted MRI abnormalities in patients with transient ischemic attack: correlation with clinical characteristics. Stroke. 2003;34:932–7.
106. Inatomi Y, Kimura K, Yonehara T, Fujioka S, Uchino M. DWI abnormalities and clinical characteristics in TIA patients. Neurology. 2004;62:376–80.
107. Purroy F, Montaner J, Rovira A, Delgado P, Quintana M, Alvarez-Sabin J. Higher risk of further vascular events among transient ischemic attack patients with diffusion-weighted imaging acute ischemic lesions. Stroke. 2004;35:2313–9.
108. Ay H, Koroshetz WJ, Benner T, et al. Transient ischemic attack with infarction: a unique syndrome? Ann Neurol. 2005;57:679–86.
109. Mullins ME, Grant PE, Wang B, Gonzalez RG, Schaefer PW. Parenchymal abnormalities associated with cerebral venous sinus thrombosis: assessment with diffusion-weighted MR imaging. AJNR Am J Neuroradiol. 2004;25:1666–75.
110. Keller E, Flacke S, Urbach H, Schild HH. Diffusion- and perfusion-weighted magnetic resonance imaging in deep cerebral venous thrombosis. Stroke. 1999;30:1144–6.
111. Ducreux D, Oppenheim C, Vandamme X, et al. Diffusion-weighted imaging patterns of brain damage associated with cerebral venous thrombosis. AJNR Am J Neuroradiol. 2001;22:261–8.
112. Sagduyu A, Sirin H, Mulayim S, et al. Cerebral cortical and deep venous thrombosis without sinus thrombosis: clinical MRI correlates. Acta Neurol Scand. 2006;114:254–60.
113. Schwartz RB, Mulkern RV, Gudbjartsson H, Jolesz F. Diffusion-weighted MR imaging in hypertensive encephalopathy: clues to pathogenesis. AJNR Am J Neuroradiol. 1998;19:859–62.
114. McKinney AM, Short J, Truwit CL, et al. Posterior reversible encephalopathy syndrome: incidence of atypical regions of involvement and imaging findings. AJR Am J Roentgenol. 2007;189:904–12.
115. Donmez FY, Basaran C, Kayahan Ulu EM, Yildirim M, Coskun M. MRI Features of posterior reversible encephalopathy syndrome in 33 patients. J Neuroimaging. 2010;20(1):22–8.
116. Crasto SG, Rizzo L, Sardo P, Davini O, De Lucchi R. Reversible encephalopathy syndrome: report of 12 cases with follow-up. Neuroradiology. 2004;46:795–804.
117. Ahn KJ, You WJ, Jeong SL, et al. Atypical manifestations of reversible posterior leukoencephalopathy syndrome: findings on diffusion imaging and ADC mapping. Neuroradiology. 2004;46:978–83.
118. Onder AM, Lopez R, Teomete U, et al. Posterior reversible encephalopathy syndrome in the pediatric renal population. Pediatr Nephrol. 2007;22:1921–9.
119. Chen TY, Lee HJ, Wu TC, Tsui YK. MR imaging findings of medulla oblongata involvement in posterior reversible encephalopathy syndrome secondary to hypertension. AJNR Am J Neuroradiol. 2009;30:755–7.
120. Pande AR, Ando K, Ishikura R, et al. Clinicoradiological factors influencing the reversibility of posterior reversible encephalopathy syndrome: a multicenter study. Radiat Med. 2006;24:659–68.
121. Kuroda H, Ogasawara K, Hirooka R, et al. Prediction of cerebral hyperperfusion after carotid endarterectomy using middle cerebral artery signal intensity in preoperative single-slab 3-dimensional time-of-flight magnetic resonance angiography. Neurosurgery. 2009;64:1065–71. discussion 1071–1072.
122. Karapanayiotides T, Meuli R, Devuyst G, et al. Postcarotid endarterectomy hyperperfusion or reperfusion syndrome. Stroke. 2005;36:21–6.
123. Scozzafava J, Hussain MS, Yeo T, Jeerakathil T, Brindley PG. Case report: aggressive blood pressure management for carotid endarterectomy hyperperfusion syndrome. Can J Anaesth. 2006;53:764–8.
124. Du Mesnil De Rochemont R, Schneider S, Yan B, Lehr A, Sitzer M, Berkefeld J. Diffusion-weighted MR imaging lesions after filter-protected stenting of high-grade symptomatic carotid artery stenoses. AJNR Am J Neuroradiol. 2006;27:1321–5.
125. Cho AH, Suh DC, Kim GE, et al. MRI evidence of reperfusion injury associated with neurological deficits after carotid revascularization procedures. Eur J Neurol. 2009;16:1066–9.
126. Hirooka R, Ogasawara K, Sasaki M, et al. Magnetic resonance imaging in patients with cerebral hyperperfusion and cognitive impairment after carotid endarterectomy. J Neurosurg. 2008;108:1178–83.
127. Shinno K, Ueda S, Uno M, Nishitani K, Nagahiro S, Harada M. Hyperperfusion syndrome following carotid endarterectomy: evaluation using diffusion-weighted magnetic resonance imaging – case report. Neurol Med Chir (Tokyo). 1998;38:557–61.
128. Sander K, Sander D. New insights into transient global amnesia: recent imaging and clinical findings. Lancet Neurol. 2005;4:437–44.
129. Sedlaczek O, Hirsch JG, Grips E, et al. Detection of delayed focal MR changes in the lateral hippocampus in transient global amnesia. Neurology. 2004;62:2165–70.
130. Toledo M, Pujadas F, Grive E, Alvarez-Sabin J, Quintana M, Rovira A. Lack of evidence for arterial ischemia in transient global amnesia. Stroke. 2008;39:476–9.
131. Lee HY, Kim JH, Weon YC, et al. Diffusion-weighted imaging in transient global amnesia exposes the CA1 region of the hippocampus. Neuroradiology. 2007;49:481–7.
132. Yang Y, Kim S, Kim JH. Ischemic evidence of transient global amnesia: location of the lesion in the hippocampus. J Clin Neurol. 2008;4:59–66.
133. Weon YC, Kim JH, Lee JS, Kim SY. Optimal diffusion-weighted imaging protocol for lesion detection in transient global amnesia. AJNR Am J Neuroradiol. 2008;29:1324–8.
134. Matsui M, Imamura T, Sakamoto S, Ishii K, Kazui H, Mori E. Transient global amnesia: increased signal intensity in the right hippocampus on diffusion-weighted magnetic resonance imaging. Neuroradiology. 2002;44:235–8.

135. Greer DM, Schaefer PW, Schwamm LH. Unilateral temporal lobe stroke causing ischemic transient global amnesia: role for diffusion-weighted imaging in the initial evaluation. J Neuroimaging. 2001;11:317–9.
136. Ay H, Furie KL, Yamada K, Koroshetz WJ. Diffusion-weighted MRI characterizes the ischemic lesion in transient global amnesia. Neurology. 1998;51:901–3.
137. Saito K, Kimura K, Minematsu K, Shiraishi A, Nakajima M. Transient global amnesia associated with an acute infarction in the retrosplenium of the corpus callosum. J Neurol Sci. 2003;210:95–7.
138. Lee SY, Kim WJ, Suh SH, Oh SH, Lee KY. Higher lesion detection by 3.0T MRI in patient with transient global amnesia. Yonsei Med J. 2009;50:211–4.
139. Chabriat H, Vahedi K, Clark CA, et al. Decreased hemispheric water mobility in hemiplegic migraine related to mutation of CACNA1A gene. Neurology. 2000;54:510–2.
140. Bhatia R, Desai S, Tripathi M, et al. Sporadic hemiplegic migraine: report of a case with clinical and radiological features. J Headache Pain. 2008;9:385–8.
141. Gutschalk A, Kollmar R, Mohr A, et al. Multimodal functional imaging of prolonged neurological deficits in a patient suffering from familial hemiplegic migraine. Neurosci Lett. 2002;332: 115–8.
142. Jacob A, Mahavish K, Bowden A, Smith ET, Enevoldson P, White RP. Imaging abnormalities in sporadic hemiplegic migraine on conventional MRI, diffusion and perfusion MRI and MRS. Cephalalgia. 2006;26:1004–9.
143. Oberndorfer S, Wober C, Nasel C, et al. Familial hemiplegic migraine: follow-up findings of diffusion-weighted magnetic resonance imaging (MRI), perfusion-MRI and [99mTc] HMPAO-SPECT in a patient with prolonged hemiplegic aura. Cephalalgia. 2004;24:533–9.
144. Gonzalez-Alegre P, Tippin J. Prolonged cortical electrical depression and diffuse vasospasm without ischemia in a case of severe hemiplegic migraine during pregnancy. Headache. 2003;43:72–5.
145. Butteriss DJ, Ramesh V, Birchall D. Serial MRI in a case of familial hemiplegic migraine. Neuroradiology. 2003;45:300–3.
146. Masuzaki M, Utsunomiya H, Yasumoto S, Mitsudome A. A case of hemiplegic migraine in childhood: transient unilateral hyperperfusion revealed by perfusion MR imaging and MR angiography. AJNR Am J Neuroradiol. 2001;22:1795–7.
147. Prodan CI, Holland NR, Lenaerts ME, Parke JT. Magnetic resonance angiogram evidence of vasospasm in familial hemiplegic migraine. J Child Neurol. 2002;17:470–2.
148. Grimaldi D, Tonon C, Cevoli S, et al. Clinical and neuroimaging evidence of interictal cerebellar dysfunction in FHM2. Cephalalgia. 2010;30(5):552–9.
149. Hasegawa D, Orima H, Fujita M, et al. Diffusion-weighted imaging in kainic acid-induced complex partial status epilepticus in dogs. Brain Res. 2003;983:115–27.
150. Righini A, Pierpaoli C, Alger JR, Di Chiro G. Brain parenchyma apparent diffusion coefficient alterations associated with experimental complex partial status epilepticus. Magn Reson Imaging. 1994;12:865–71.
151. Wieshmann UC, Symms MR, Shorvon SD. Diffusion changes in status epilepticus. Lancet. 1997;350:493–4.
152. Sagiuchi T, Ishii K, Asano Y, et al. Transient seizure activity demonstrated by Tc-99m HMPAO SPECT and diffusion-weighted MR imaging. Ann Nucl Med. 2001;15:267–70.
153. Lansberg MG, O'Brien MW, Norbash AM, Moseley ME, Morrell M, Albers GW. MRI abnormalities associated with partial status epilepticus. Neurology. 1999;52:1021–7.
154. Huang YC, Weng HH, Tsai YT, et al. Periictal magnetic resonance imaging in status epilepticus. Epilepsy Res. 2009;86:72–81.
155. Kim JA, Chung JI, Yoon PH, et al. Transient MR signal changes in patients with generalized tonicoclonic seizure or status epilepticus: periictal diffusion-weighted imaging. AJNR Am J Neuroradiol. 2001;22:1149–60.
156. Hong KS, Cho YJ, Lee SK, Jeong SW, Kim WK, Oh EJ. Diffusion changes suggesting predominant vasogenic oedema during partial status epilepticus. Seizure. 2004;13:317–21.
157. Milligan TA, Zamani A, Bromfield E. Frequency and patterns of MRI abnormalities due to status epilepticus. Seizure. 2009;18:104–8.
158. Okumura A, Abe S, Hara S, Aoyagi Y, Shimizu T, Watanabe K. Transiently reduced water diffusion in the corpus callosum in infants with benign partial epilepsy in infancy. Brain Dev. 2010;32:564–6.
159. Oster J, Doherty C, Grant PE, Simon M, Cole AJ. Diffusion-weighted imaging abnormalities in the splenium after seizures. Epilepsia. 2003;44:852–4.
160. Men S, Lee DH, Barron JR, Munoz DG. Selective neuronal necrosis associated with status epilepticus: MR findings. AJNR Am J Neuroradiol. 2000;21:1837–40.
161. Nakasu Y, Nakasu S, Morikawa S, Uemura S, Inubushi T, Handa J. Diffusion-weighted MR in experimental sustained seizures elicited with kainic acid. AJNR Am J Neuroradiol. 1995;16:1185–92.
162. Parmar H, Lim SH, Tan NC, Lim CC. Acute symptomatic seizures and hippocampus damage: DWI and MRS findings. Neurology. 2006;66:1732–5.
163. Londono A, Castillo M, Lee YZ, Smith JK. Apparent diffusion coefficient measurements in the hippocampi in patients with temporal lobe seizures. AJNR Am J Neuroradiol. 2003;24:1582–6.
164. Wieshmann UC, Clark CA, Symms MR, Barker GJ, Birnie KD, Shorvon SD. Water diffusion in the human hippocampus in epilepsy. Magn Reson Imaging. 1999;17:29–36.
165. Wehner T, Lapresto E, Tkach J, et al. The value of interictal diffusion-weighted imaging in lateralizing temporal lobe epilepsy. Neurology. 2007;68:122–7.
166. Lee JH, Chung CK, Song IC, Chang KH, Kim HJ. Limited utility of interictal apparent diffusion coefficient in the evaluation of hippocampal sclerosis. Acta Neurol Scand. 2004;110:53–8.
167. Luat AF, Chugani HT. Molecular and diffusion tensor imaging of epileptic networks. Epilepsia. 2008;49 Suppl 3:15–22.
168. Pillai JJ, Williams HT, Faro S. Functional imaging in temporal lobe epilepsy. Semin Ultrasound CT MR. 2007;28:437–50.
169. Lo L, Tan AC, Umapathi T, Lim CC. Diffusion-weighted MR imaging in early diagnosis and prognosis of hypoglycemia. AJNR Am J Neuroradiol. 2006;27:1222–4.
170. Cordonnier C, Oppenheim C, Lamy C, Meder JF, Mas JL. Serial diffusion and perfusion-weighted MR in transient hypoglycemia. Neurology. 2005;65:175.
171. Bottcher J, Kunze A, Kurrat C, et al. Localized reversible reduction of apparent diffusion coefficient in transient hypoglycemia-induced hemiparesis. Stroke. 2005;36:e20–2.
172. Okamoto K, Tokiguchi S, Furusawa T, et al. MR features of diseases involving bilateral middle cerebellar peduncles. AJNR Am J Neuroradiol. 2003;24:1946–54.
173. Finelli PF. Diffusion-weighted MR in hypoglycemic coma. Neurology. 2001;57:933.
174. Kim JH, Choi JY, Koh SB, Lee Y. Reversible splenial abnormality in hypoglycemic encephalopathy. Neuroradiology. 2007;49:217–22.
175. Chan R, Erbay S, Oljeski S, Thaler D, Bhadelia R. Case report: hypoglycemia and diffusion-weighted imaging. J Comput Assist Tomogr. 2003;27:420–3.
176. Fujioka M, Okuchi K, Hiramatsu KI, Sakaki T, Sakaguchi S, Ishii Y. Specific changes in human brain after hypoglycemic injury. Stroke. 1997;28:584–7.
177. Chen CY, Lee KW, Lee CC, Chin SC, Chung HW, Zimmerman RA. Heroin-induced spongiform leukoencephalopathy: value of diffusion MR imaging. J Comput Assist Tomogr. 2000;24:735–7.
178. Hagel J, Andrews G, Vertinsky T, Heran MK, Keogh C. "Chasing the dragon" – imaging of heroin inhalation leukoencephalopathy. Can Assoc Radiol J. 2005;56:199–203.

179. Ahmed A, Loes DJ, Bressler EL. Reversible magnetic resonance imaging findings in metronidazole-induced encephalopathy. Neurology. 1995;45:588–9.
180. Kim E, Na DG, Kim EY, Kim JH, Son KR, Chang KH. MR imaging of metronidazole-induced encephalopathy: lesion distribution and diffusion-weighted imaging findings. AJNR Am J Neuroradiol. 2007;28:1652–8.
181. Lee SS, Cha SH, Lee SY, Song CJ. Reversible inferior colliculus lesion in metronidazole-induced encephalopathy: magnetic resonance findings on diffusion-weighted and fluid attenuated inversion recovery imaging. J Comput Assist Tomogr. 2009;33:305–8.
182. Kim DW, Park JM, Yoon BW, Baek MJ, Kim JE, Kim S. Metronidazole-induced encephalopathy. J Neurol Sci. 2004;224: 107–11.
183. Seok JI, Yi H, Song YM, Lee WY. Metronidazole-induced encephalopathy and inferior olivary hypertrophy: lesion analysis with diffusion-weighted imaging and apparent diffusion coefficient maps. Arch Neurol. 2003;60:1796–800.
184. Kinoshita T, Sugihara S, Matsusue E, Fujii S, Ametani M, Ogawa T. Pallidoreticular damage in acute carbon monoxide poisoning: diffusion-weighted MR imaging findings. AJNR Am J Neuroradiol. 2005;26:1845–8.
185. Teksam M, Casey SO, Michel E, Liu H, Truwit CL. Diffusion-weighted MR imaging findings in carbon monoxide poisoning. Neuroradiology. 2002;44:109–13.
186. Kawanami T, Kato T, Kurita K, Sasaki H. The pallidoreticular pattern of brain damage on MRI in a patient with carbon monoxide poisoning. J Neurol Neurosurg Psychiatry. 1998;64:282.
187. Kim JH, Chang KH, Song IC, et al. Delayed encephalopathy of acute carbon monoxide intoxication: diffusivity of cerebral white matter lesions. AJNR Am J Neuroradiol. 2003;24:1592–7.
188. Chu K, Kang DW, Ko SB, Kim M. Diffusion-weighted MR findings of central pontine and extrapontine myelinolysis. Acta Neurol Scand. 2001;104:385–8.
189. Chua GC, Sitoh YY, Lim CC, Chua HC, Ng PY. MRI findings in osmotic myelinolysis. Clin Radiol. 2002;57:800–6.
190. Cramer SC, Stegbauer KC, Schneider A, Mukai J, Maravilla KR. Decreased diffusion in central pontine myelinolysis. AJNR Am J Neuroradiol. 2001;22:1476–9.
191. Chu K, Kang DW, Kim HJ, Lee YS, Park SH. Diffusion-weighted imaging abnormalities in wernicke encephalopathy: reversible cytotoxic edema? Arch Neurol. 2002;59:123–7.
192. Loh Y, Watson WD, Verma A, Krapiva P. Restricted diffusion of the splenium in acute Wernicke's encephalopathy. J Neuroimaging. 2005;15:373–5.
193. Johkura K, Naito M, Naka T. Cortical involvement in Marchiafava-Bignami disease. AJNR Am J Neuroradiol. 2005;26:670–3.
194. Hlaihel C, Gonnaud PM, Champin S, Rousset H, Tran-Minh VA, Cotton F. Diffusion-weighted magnetic resonance imaging in Marchiafava-Bignami disease: follow-up studies. Neuroradiology. 2005;47:520–4.
195. Menegon P, Sibon I, Pachai C, Orgogozo JM, Dousset V. Marchiafava-Bignami disease: diffusion-weighted MRI in corpus callosum and cortical lesions. Neurology. 2005;65:475–7.
196. Aggunlu L, Oner Y, Kocer B, Akpek S. The value of diffusion-weighted imaging in the diagnosis of Marchiafava-Bignami disease: apropos of a case. J Neuroimaging. 2008;18:188–90.
197. Gallucci M, Limbucci N, Paonessa A, Caranci F. Reversible focal splenial lesions. Neuroradiology. 2007;49:541–4.
198. Kim SS, Chang KH, Kim ST, et al. Focal lesion in the splenium of the corpus callosum in epileptic patients: antiepileptic drug toxicity? AJNR Am J Neuroradiol. 1999;20:125–9.
199. Maeda M, Shiroyama T, Tsukahara H, Shimono T, Aoki S, Takeda K. Transient splenial lesion of the corpus callosum associated with antiepileptic drugs: evaluation by diffusion-weighted MR imaging. Eur Radiol. 2003;13:1902–6.
200. Gurtler S, Ebner A, Tuxhorn I, Ollech I, Pohlmann-Eden B, Woermann FG. Transient lesion in the splenium of the corpus callosum and antiepileptic drug withdrawal. Neurology. 2005;65: 1032–6.
201. Honda K, Nishimiya J, Sato H, et al. Transient splenial lesion of the corpus callosum after acute withdrawal of antiepileptic drug: a case report. Magn Reson Med Sci. 2006;5:211–5.
202. Winslow H, Mickey B, Frohman EM. Sympathomimetic-induced kaleidoscopic visual illusion associated with a reversible splenium lesion. Arch Neurol. 2006;63:135–7.
203. Steinborn M, Leiz S, Rudisser K, Griebel M, Harder T, Hahn H. CT and MRI in haemolytic uraemic syndrome with central nervous system involvement: distribution of lesions and prognostic value of imaging findings. Pediatr Radiol. 2004;34:805–10.
204. Toldo I, Manara R, Cogo P, et al. Diffusion-weighted imaging findings in hemolytic uremic syndrome with central nervous system involvement. J Child Neurol. 2009;24:247–50.
205. Ogura H, Takaoka M, Kishi M, et al. Reversible MR findings of hemolytic uremic syndrome with mild encephalopathy. AJNR Am J Neuroradiol. 1998;19:1144–5.
206. Kallenberg K, Bailey DM, Christ S, et al. Magnetic resonance imaging evidence of cytotoxic cerebral edema in acute mountain sickness. J Cereb Blood Flow Metab. 2007;27:1064–71.
207. Wong SH, Turner N, Birchall D, Walls TJ, English P, Schmid ML. Reversible abnormalities of DWI in high-altitude cerebral edema. Neurology. 2004;62:335–6.
208. Rovira A, Pericot I, Alonso J, Rio J, Grive E, Montalban X. Serial diffusion-weighted MR imaging and proton MR spectroscopy of acute large demyelinating brain lesions: case report. AJNR Am J Neuroradiol. 2002;23:989–94.
209. Tievsky AL, Ptak T, Farkas J. Investigation of apparent diffusion coefficient and diffusion tensor anisotrophy in acute and chronic multiple sclerosis lesions. AJNR Am J Neuroradiol. 1999;20:1491–9.
210. Bernarding J, Braun J, Koennecke HC. Diffusion- and perfusion-weighted MR imaging in a patient with acute demyelinating encephalomyelitis (ADEM). J Magn Reson Imaging. 2002;15: 96–100.
211. Rovaris M, Gass A, Bammer R, et al. Diffusion MRI in multiple sclerosis. Neurology. 2005;65:1526–32.
212. Castriota-Scanderbeg A, Sabatini U, Fasano F, et al. Diffusion of water in large demyelinating lesions: a follow-up study. Neuroradiology. 2002;44:764–7.
213. Rossi A. Imaging of acute disseminated encephalomyelitis. Neuroimaging Clin N Am. 2008;18:149–61. ix.
214. Przeklasa-Auth M, Ovbiagele B, Yim C, Shewmon A. Multiple sclerosis with initial stroke-like clinicoradiologic features: case report and literature review. J Child Neurol. 2009.
215. Malhotra HS, Jain KK, Agarwal A, et al. Characterization of tumefactive demyelinating lesions using MR imaging and in-vivo proton MR spectroscopy. Mult Scler. 2009;15:193–203.
216. Castriota Scanderbeg A, Tomaiuolo F, Sabatini U, Nocentini U, Grasso MG, Caltagirone C. Demyelinating plaques in relapsing-remitting and secondary-progressive multiple sclerosis: assessment with diffusion MR imaging. AJNR Am J Neuroradiol. 2000;21:862–8.
217. Rovaris M, Filippi M. Diffusion tensor MRI in multiple sclerosis. J Neuroimaging. 2007;17 Suppl 1:27S–30.
218. Matthews PM. Brain imaging of multiple sclerosis: the next 10 years. Neuroimaging Clin N Am. 2009;19:101–12.
219. Rovaris M, Agosta F, Pagani E, Filippi M. Diffusion tensor MR imaging. Neuroimaging Clin N Am. 2009;19:37–43.
220. Lai PH, Ho JT, Chen WL, et al. Brain abscess and necrotic brain tumor: discrimination with proton MR spectroscopy and diffusion-weighted imaging. AJNR Am J Neuroradiol. 2002;23:1369–77.
221. Mueller-Mang C, Castillo M, Mang TG, Cartes-Zumelzu F, Weber M, Thurnher MM. Fungal versus bacterial brain abscesses: is

diffusion-weighted MR imaging a useful tool in the differential diagnosis? Neuroradiology. 2007;49:651–7.
222. Luthra G, Parihar A, Nath K, et al. Comparative evaluation of fungal, tubercular, and pyogenic brain abscesses with conventional and diffusion MR imaging and proton MR spectroscopy. AJNR Am J Neuroradiol. 2007;28:1332–8.
223. Bergui M, Zhong J, Bradac GB, Sales S. Diffusion-weighted images of intracranial cyst-like lesions. Neuroradiology. 2001;43:824–9.
224. Duprez TP, Cosnard G, Hernalsteen D. Diffusion-weighted monitoring of conservatively treated pyogenic brain abscesses: a marker for antibacterial treatment efficacy. AJNR Am J Neuroradiol. 2005;26:1296–8. author reply 1300–1291.
225. Cartes-Zumelzu FW, Stavrou I, Castillo M, Eisenhuber E, Knosp E, Thurnher MM. Diffusion-weighted imaging in the assessment of brain abscesses therapy. AJNR Am J Neuroradiol. 2004;25:1310–7.
226. Fanning NF, Laffan EE, Shroff MM. Serial diffusion-weighted MRI correlates with clinical course and treatment response in children with intracranial pus collections. Pediatr Radiol. 2006;36:26–37.
227. Gordon M, Parmar H, Ibrahim M. Spread of infection to Virchow-Robin spaces in a patient with *Streptococcus pneumoniae* meningitis. J Comput Assist Tomogr. 2009;33:562–4.
228. Gaviani P, Schwartz RB, Hedley-Whyte ET, et al. Diffusion-weighted imaging of fungal cerebral infection. AJNR Am J Neuroradiol. 2005;26:1115–21.
229. Chong-Han CH, Cortez SC, Tung GA. Diffusion-weighted MRI of cerebral toxoplasma abscess. AJR Am J Roentgenol. 2003;181:1711–4.
230. Camacho DL, Smith JK, Castillo M. Differentiation of toxoplasmosis and lymphoma in AIDS patients by using apparent diffusion coefficients. AJNR Am J Neuroradiol. 2003;24:633–7.
231. Schroeder PC, Post MJ, Oschatz E, Stadler A, Bruce-Gregorios J, Thurnher MM. Analysis of the utility of diffusion-weighted MRI and apparent diffusion coefficient values in distinguishing central nervous system toxoplasmosis from lymphoma. Neuroradiology. 2006;48:715–20.
232. Fujikawa A, Tsuchiya K, Honya K, Nitatori T. Comparison of MRI sequences to detect ventriculitis. AJR Am J Roentgenol. 2006;187:1048–53.
233. Fukui MB, Williams RL, Mudigonda S. CT and MR imaging features of pyogenic ventriculitis. AJNR Am J Neuroradiol. 2001;22:1510–6.
234. Pezzullo JA, Tung GA, Mudigonda S, Rogg JM. Diffusion-weighted MR imaging of pyogenic ventriculitis. AJR Am J Roentgenol. 2003;180:71–5.
235. Han KT, Choi DS, Ryoo JW, et al. Diffusion-weighted MR imaging of pyogenic intraventricular empyema. Neuroradiology. 2007;49:813–8.
236. Heiner L, Demaerel P. Diffusion-weighted MR imaging findings in a patient with herpes simplex encephalitis. Eur J Radiol. 2003;45:195–8.
237. Bulakbasi N, Kocaoglu M. Central nervous system infections of herpesvirus family. Neuroimaging Clin N Am. 2008;18:53–84. viii.
238. Tsuchiya K, Katase S, Yoshino A, Hachiya J. Diffusion-weighted MR imaging of encephalitis. AJR Am J Roentgenol. 1999;173:1097–9.
239. Dhawan A, Kecskes Z, Jyoti R, Kent AL. Early diffusion-weighted magnetic resonance imaging findings in neonatal herpes encephalitis. J Paediatr Child Health. 2006;42:824–6.
240. Kiroglu Y, Calli C, Yunten N, et al. Diffusion-weighted MR imaging of viral encephalitis. Neuroradiology. 2006;48:875–80.
241. Sener RN. Herpes simplex encephalitis: diffusion MR imaging findings. Comput Med Imaging Graph. 2001;25:391–7.
242. McCabe K, Tyler K, Tanabe J. Diffusion-weighted MRI abnormalities as a clue to the diagnosis of herpes simplex encephalitis. Neurology. 2003;61:1015–6.
243. Gupta RK, Jain KK, Kumar S. Imaging of nonspecific (nonherpetic) acute viral infections. Neuroimaging Clin N Am. 2008;18:41–52. vii.
244. Hatipoglu HG, Gurbuz MO, Sakman B, Yuksel E. Diffusion-weighted magnetic resonance imaging in rhombencephalitis due to *Listeria monocytogenes*. Acta Radiol. 2007;48:464–7.
245. Lo CP, Chen CY. Neuroimaging of viral infections in infants and young children. Neuroimaging Clin N Am. 2008;18:119–32. viii.
246. Rumboldt Z. Imaging of topographic viral CNS infections. Neuroimaging Clin N Am. 2008;18:85–92. viii.
247. Hagemann G, Mentzel HJ, Weisser H, Kunze A, Terborg C. Multiple reversible MR signal changes caused by Epstein-Barr virus encephalitis. AJNR Am J Neuroradiol. 2006;27:1447–9.
248. Vrancken AF, Frijns CJ, Ramos LM. FLAIR MRI in sporadic Creutzfeldt-Jakob disease. Neurology. 2000;55:147–8.
249. Wada R, Kucharczyk W. Prion infections of the brain. Neuroimaging Clin N Am. 2008;18:183–91. ix.
250. Finkenstaedt M, Szudra A, Zerr I, et al. MR imaging of Creutzfeldt-Jakob disease. Radiology. 1996;199:793–8.
251. Mittal S, Farmer P, Kalina P, Kingsley PB, Halperin J. Correlation of diffusion-weighted magnetic resonance imaging with neuropathology in Creutzfeldt-Jakob disease. Arch Neurol. 2002;59:128–34.
252. Kallenberg K, Schulz-Schaeffer WJ, Jastrow U, et al. Creutzfeldt-Jakob disease: comparative analysis of MR imaging sequences. AJNR Am J Neuroradiol. 2006;27:1459–62.
253. Collie DA, Summers DM, Sellar RJ, et al. Diagnosing variant Creutzfeldt-Jakob disease with the pulvinar sign: MR imaging findings in 86 neuropathologically confirmed cases. AJNR Am J Neuroradiol. 2003;24:1560–9.
254. Zeidler M, Sellar RJ, Collie DA, et al. The pulvinar sign on magnetic resonance imaging in variant Creutzfeldt-Jakob disease. Lancet. 2000;355:1412–8.
255. Hyare H, Thornton J, Stevens J, et al. High-b-value diffusion MR imaging and basal nuclei apparent diffusion coefficient measurements in variant and sporadic Creutzfeldt-Jakob disease. AJNR Am J Neuroradiol. 2010;31:521–6.
256. Murata T, Shiga Y, Higano S, Takahashi S, Mugikura S. Conspicuity and evolution of lesions in Creutzfeldt-Jakob disease at diffusion-weighted imaging. AJNR Am J Neuroradiol. 2002;23:1164–72.
257. Young GS, Geschwind MD, Fischbein NJ, et al. Diffusion-weighted and fluid-attenuated inversion recovery imaging in Creutzfeldt-Jakob disease: high sensitivity and specificity for diagnosis. AJNR Am J Neuroradiol. 2005;26:1551–62.
258. Bahn MM, Parchi P. Abnormal diffusion-weighted magnetic resonance images in Creutzfeldt-Jakob disease. Arch Neurol. 1999;56:577–83.
259. Manners DN, Parchi P, Tonon C, et al. Pathologic correlates of diffusion MRI changes in Creutzfeldt-Jakob disease. Neurology. 2009;72:1425–31.
260. Haik S, Dormont D, Faucheux BA, Marsault C, Hauw JJ. Prion protein deposits match magnetic resonance imaging signal abnormalities in Creutzfeldt-Jakob disease. Ann Neurol. 2002;51:797–9.
261. Shiga Y, Miyazawa K, Sato S, et al. Diffusion-weighted MRI abnormalities as an early diagnostic marker for Creutzfeldt-Jakob disease. Neurology. 2004;63:443–9.
262. Matoba M, Tonami H, Miyaji H, Yokota H, Yamamoto I. Creutzfeldt-Jakob disease: serial changes on diffusion-weighted MRI. J Comput Assist Tomogr. 2001;25:274–7.
263. Ukisu R, Kushihashi T, Kitanosono T, et al. Serial diffusion-weighted MRI of Creutzfeldt-Jakob disease. AJR Am J Roentgenol. 2005;184:560–6.
264. Al-Okaili RN, Krejza J, Wang S, Woo JH, Melhem ER. Advanced MR imaging techniques in the diagnosis of intraaxial brain tumors in adults. Radiographics. 2006;26 Suppl 1:S173–89.
265. Gupta RK, Sinha U, Cloughesy TF, Alger JR. Inverse correlation between choline magnetic resonance spectroscopy signal intensity

and the apparent diffusion coefficient in human glioma. Magn Reson Med. 1999;41:2–7.
266. Chenevert TL, Stegman LD, Taylor JM, et al. Diffusion magnetic resonance imaging: an early surrogate marker of therapeutic efficacy in brain tumors. J Natl Cancer Inst. 2000;92:2029–36.
267. Yang D, Korogi Y, Sugahara T, et al. Cerebral gliomas: prospective comparison of multivoxel 2D chemical-shift imaging proton MR spectroscopy, echoplanar perfusion and diffusion-weighted MRI. Neuroradiology. 2002;44:656–66.
268. Lam WW, Poon WS, Metreweli C. Diffusion MR imaging in glioma: does it have any role in the pre-operation determination of grading of glioma? Clin Radiol. 2002;57:219–25.
269. Bulakbasi N, Kocaoglu M, Ors F, Tayfun C, Ucoz T. Combination of single-voxel proton MR spectroscopy and apparent diffusion coefficient calculation in the evaluation of common brain tumors. AJNR Am J Neuroradiol. 2003;24:225–33.
270. Arvinda HR, Kesavadas C, Sarma PS, et al. Glioma grading: sensitivity, specificity, positive and negative predictive values of diffusion and perfusion imaging. J Neurooncol. 2009;94:87–96.
271. Fan GG, Deng QL, Wu ZH, Guo QY. Usefulness of diffusion/perfusion-weighted MRI in patients with non-enhancing supratentorial brain gliomas: a valuable tool to predict tumour grading? Br J Radiol. 2006;79:652–8.
272. Rizzo L, Crasto SG, Moruno PG, et al. Role of diffusion- and perfusion-weighted MR imaging for brain tumour characterisation. Radiol Med. 2009;114:645–59.
273. Kan P, Liu JK, Hedlund G, Brockmeyer DL, Walker ML, Kestle JR. The role of diffusion-weighted magnetic resonance imaging in pediatric brain tumors. Childs Nerv Syst. 2006;22:1435–9.
274. Hayashida Y, Hirai T, Morishita S, et al. Diffusion-weighted imaging of metastatic brain tumors: comparison with histologic type and tumor cellularity. AJNR Am J Neuroradiol. 2006;27:1419–25.
275. Lu S, Ahn D, Johnson G, Cha S. Peritumoral diffusion tensor imaging of high-grade gliomas and metastatic brain tumors. AJNR Am J Neuroradiol. 2003;24:937–41.
276. Hall DE, Moffat BA, Stojanovska J, et al. Therapeutic efficacy of DTI-015 using diffusion magnetic resonance imaging as an early surrogate marker. Clin Cancer Res. 2004;10:7852–9.
277. Schubert MI, Wilke M, Muller-Weihrich S, Auer DP. Diffusion-weighted magnetic resonance imaging of treatment-associated changes in recurrent and residual medulloblastoma: preliminary observations in three children. Acta Radiol. 2006;47:1100–4.
278. Mardor Y, Pfeffer R, Spiegelmann R, et al. Early detection of response to radiation therapy in patients with brain malignancies using conventional and high b-value diffusion-weighted magnetic resonance imaging. J Clin Oncol. 2003;21:1094–100.
279. Tomura N, Narita K, Izumi J, et al. Diffusion changes in a tumor and peritumoral tissue after stereotactic irradiation for brain tumors: possible prediction of treatment response. J Comput Assist Tomogr. 2006;30:496–500.
280. Hamstra DA, Chenevert TL, Moffat BA, et al. Evaluation of the functional diffusion map as an early biomarker of time-to-progression and overall survival in high-grade glioma. Proc Natl Acad Sci USA. 2005;102:16759–64.
281. Moffat BA, Chenevert TL, Lawrence TS, et al. Functional diffusion map: a noninvasive MRI biomarker for early stratification of clinical brain tumor response. Proc Natl Acad Sci USA. 2005;102:5524–9.
282. Chenevert TL, Ross BD. Diffusion imaging for therapy response assessment of brain tumor. Neuroimaging Clin N Am. 2009;19:559–71.
283. Hein PA, Eskey CJ, Dunn JF, Hug EB. Diffusion-weighted imaging in the follow-up of treated high-grade gliomas: tumor recurrence versus radiation injury. AJNR Am J Neuroradiol. 2004;25:201–9.
284. Kwee TC, Galban CJ, Tsien C, et al. Intravoxel water diffusion heterogeneity imaging of human high-grade gliomas. NMR Biomed. 2010;23:179–87.
285. Zeng QS, Li CF, Liu H, Zhen JH, Feng DC. Distinction between recurrent glioma and radiation injury using magnetic resonance spectroscopy in combination with diffusion-weighted imaging. Int J Radiat Oncol Biol Phys. 2007;68:151–8.
286. Asao C, Korogi Y, Kitajima M, et al. Diffusion-weighted imaging of radiation-induced brain injury for differentiation from tumor recurrence. AJNR Am J Neuroradiol. 2005;26:1455–60.
287. Pruzincova L, Steno J, Srbecky M, et al. MR imaging of late radiation therapy- and chemotherapy-induced injury: a pictorial essay. Eur Radiol. 2009;19:2716–27.
288. Tung GA, Evangelista P, Rogg JM, Duncan 3rd JA. Diffusion-weighted MR imaging of rim-enhancing brain masses: is markedly decreased water diffusion specific for brain abscess? AJR Am J Roentgenol. 2001;177:709–12.
289. Jain R, Scarpace LM, Ellika S, et al. Imaging response criteria for recurrent gliomas treated with bevacizumab: role of diffusion weighted imaging as an imaging biomarker. J Neurooncol. 2010;96:423–31.
290. Sundgren PC, Fan X, Weybright P, et al. Differentiation of recurrent brain tumor versus radiation injury using diffusion tensor imaging in patients with new contrast-enhancing lesions. Magn Reson Imaging. 2006;24:1131–42.
291. Sundgren PC, Cao Y. Brain irradiation: effects on normal brain parenchyma and radiation injury. Neuroimaging Clin N Am. 2009;19:657–68.
292. Stadnik TW, Chaskis C, Michotte A, et al. Diffusion-weighted MR imaging of intracerebral masses: comparison with conventional MR imaging and histologic findings. AJNR Am J Neuroradiol. 2001;22:969–76.
293. Horger M, Fenchel M, Nagele T, et al. Water diffusivity: comparison of primary CNS lymphoma and astrocytic tumor infiltrating the corpus callosum. AJR Am J Roentgenol. 2009;193:1384–7.
294. Barajas Jr RF, Rubenstein JL, Chang JS, Hwang J, Cha S. Diffusion-weighted MR imaging derived apparent diffusion coefficient is predictive of clinical outcome in primary central nervous system lymphoma. AJNR Am J Neuroradiol. 2010;31:60–6.
295. Forghani R, Farb RI, Kiehl TR, Bernstein M. Fourth ventricle epidermoid tumor: radiologic, intraoperative, and pathologic findings. Radiographics. 2007;27:1489–94.
296. Bukte Y, Paksoy Y, Genc E, Uca AU. Role of diffusion-weighted MR in differential diagnosis of intracranial cystic lesions. Clin Radiol. 2005;60:375–83.
297. Hakyemez B, Yildirim N, Gokalp G, Erdogan C, Parlak M. The contribution of diffusion-weighted MR imaging to distinguishing typical from atypical meningiomas. Neuroradiology. 2006;48:513–20.
298. Nagar VA, Ye JR, Ng WH, et al. Diffusion-weighted MR imaging: diagnosing atypical or malignant meningiomas and detecting tumor dedifferentiation. AJNR Am J Neuroradiol. 2008;29:1147–52.
299. Filippi CG, Edgar MA, Ulug AM, Prowda JC, Heier LA, Zimmerman RD. Appearance of meningiomas on diffusion-weighted images: correlating diffusion constants with histopathologic findings. AJNR Am J Neuroradiol. 2001;22:65–72.
300. Huisman TA, Sorensen AG, Hergan K, Gonzalez RG, Schaefer PW. Diffusion-weighted imaging for the evaluation of diffuse axonal injury in closed head injury. J Comput Assist Tomogr. 2003;27:5–11.
301. Kinoshita T, Moritani T, Hiwatashi A, et al. Conspicuity of diffuse axonal injury lesions on diffusion-weighted MR imaging. Eur J Radiol. 2005;56:5–11.
302. Schaefer PW, Huisman TA, Sorensen AG, Gonzalez RG, Schwamm LH. Diffusion-weighted MR imaging in closed head injury: high correlation with initial glasgow coma scale score and score on modified Rankin scale at discharge. Radiology. 2004;233:58–66.
303. Hou DJ, Tong KA, Ashwal S, et al. Diffusion-weighted magnetic resonance imaging improves outcome prediction in adult traumatic brain injury. J Neurotrauma. 2007;24:1558–69.
304. Schaefer et al. Diffusion-weighted MR imaging of the brain. Radiology 2000;217:331–45.

http://www.springer.com/978-1-4419-0343-3

Functional Neuroradiology
Principles and Clinical Applications
(Eds.)S.H. Faro; F.B. Mohamed; M. Law; J.T. Ulmer
2012, XXI, 1029 p. 897 illus., 476 in color. With online files/update., Hardcover
ISBN: 978-1-4419-0343-3